

**Structural and Functional Characterization of the p62 Complex,  
a Subcomplex of the Nuclear Pore Complex**

**Inauguraldissertation**

zur  
Erlangung der Würde eines Doktors der Philosophie  
vorgelegt der  
Philosophisch-Naturwissenschaftlichen Fakultät  
der Universität Basel

von

Kyrill Schwarz-Herion

aus Ettlingen, Deutschland

Basel, 2008

Genehmigt von der Philosophischen-Naturwissenschaftlichen Fakultät

auf Antrag von

Prof. Dr. Dr. h.c. Ueli Aebi, PD Dr. Ralph Kehlenbach und

PD Dr. Birthe Fahrenkrog

Basel, den 19.02.2008

Prof. Dr. Hans-Peter Hauri

Dekan der Philosophisch

Naturwissenschaftlichen Fakultät

*Wir meinen die Natur zu beherrschen, aber  
wahrscheinlich hat sie sich nur an uns gewöhnt*

(Karl Heinrich Waggerl)

**To Odile and my parents**



<b>LIST OF ABBREVIATIONS .....</b>	<b>X</b>
<b>LIST OF FIGURES .....</b>	<b>XII</b>
<b>LIST OF TABLES .....</b>	<b>XIV</b>
<b>CHAPTER 1. INTRODUCTION: NUCLEOPORINS OF THE CENTRAL REGION OF THE NUCLEAR PORE COMPLEX AND REGULATION OF NUCLEOCYTOPLASMIC TRANSPORT: AN INVENTORY .....</b>	<b>15</b>
<b>SUMMARY .....</b>	<b>17</b>
<b>1.1 INTRODUCTION .....</b>	<b>18</b>
<b>1.2. p62: IDENTIFICATION AND FUNCTION.....</b>	<b>20</b>
<b>1.3. THE NUP93 COMPLEX .....</b>	<b>23</b>
<b>1.4. NUP155 .....</b>	<b>25</b>
<b>1.5. THE NUP107-160 SUBCOMPLEX .....</b>	<b>26</b>
<b>1.6. NUCLEOCYTOPLASMIC TRANSPORT .....</b>	<b>27</b>
1.6.1. NUCLEAR PROTEIN IMPORT.....	27
1.6.1.1. NUCLEAR LOCALIZATION SIGNAL .....	28
1.6.1.2. NUCLEAR IMPORT RECEPTORS .....	28
1.6.1.3. REGULATION OF NUCLEAR IMPORT: THE RAN CYCLE .....	30
1.6.2. NUCLEAR EXPORT .....	33
1.6.2.1. EXPORTINS AND OTHER NUCLEAR EXPORT FACTORS .....	33
1.6.2.2. mRNA NUCLEAR EXPORT .....	34
1.6.2.3. tRNA EXPORT .....	36
1.6.2.4. EXPORT OF RIBOSOMAL SUBUNITS .....	37

1.6.2.5. EXPORT OF U SNRNAs .....	38
1.6.3. CARGO TRANSLOCATION THROUGH THE NPC .....	38
<b>1.7. FUNCTION OF NUCLEOPORINS BEYOND THE NUCLEOCYTOPLASMIC TRANSPORT .....</b>	<b>40</b>
<b>1.8. REFERENCES .....</b>	<b>42</b>
<b>CHAPTER 2: DOMAIN TOPOLOGY OF THE p62 COMPLEX WITHIN THE 3-D ARCHITECTURE OF THE NUCLEAR PORE COMPLEX .....</b>	<b>61</b>
<b>SUMMARY .....</b>	<b>63</b>
<b>2.1. INTRODUCTION .....</b>	<b>64</b>
<b>2.2. RESULTS .....</b>	<b>66</b>
2.2.1 PRODUCTION AND CHARACTERIZATION OF AN ANTIBODY AGAINST THE C-TERMINUS OF p62 .....	66
2.2.2 p62 HAS A DISTINCT DOMAIN TOPOLOGY IN THE NPC .....	68
2.2.3 RECOMBINANT EXPRESSION OF EPIOTOPE-TAGGED p62 IN XENOPUS NPCs .....	70
2.2.4 LOCALIZATION OF EPIOTOPE-TAGGED p54 AND p58 WITHIN THE NPC .....	73
<b>2.3. DISCUSSION .....</b>	<b>75</b>
2.3.1 THE COILED-COIL DOMAINS MEDIATE THE ANCHORING OF THE p62 COMPLEX TO THE CYTOPLASMIC SIDE OF THE NPC .....	75
2.3.2 DOMAIN TOPOLOGY OF THE FG-REPEAT DOMAIN OF p62, p54 AND p58 .....	76
2.3.3 THE NUCLEOPORINS OF THE p62 COMPLEX ARE ASYMMETRIC NUCLEOPORINS .....	78
<b>2.4. MATERIALS AND METHODS .....</b>	<b>79</b>
2.4.1 ANTIBODY PRODUCTION AND PURIFICATION .....	79
2.4.2 ISOLATION OF XENOPUS OOCYTE NUCLEI .....	79
2.4.3 DIRECT CONJUGATION OF ANTIBODIES TO COLLOIDAL GOLD .....	79
2.4.4 LABELING OF ISOLATED NUCLEI FROM XENOPUS OOCYTES .....	80
2.4.5 QUANTIFICATION OF GOLD LABELING AT THE NPCs AND CALCULATION OF LOCATION CLOUDS .....	80

2.4.6 MICROINJECTION OF TAGGED p62, p54 AND p58 .....	80
<b>2.5. ACKNOWLEDGEMENTS .....</b>	<b>81</b>
<b>2.6. REFERENCES .....</b>	<b>82</b>
<b>CHAPTER 3: INFLUENCE OF ANTIBODIES AGAINST THE p62 COMPLEX ON NUCLEOCYTOPLASMIC TRANSPORT .....</b>	<b>85</b>
<b>SUMMARY .....</b>	<b>87</b>
<b>3.1. INTRODUCTION .....</b>	<b>88</b>
<b>3.2. RESULTS .....</b>	<b>91</b>
3.2.1. ULTRASTRUCTURAL NUCLEAR IMPORT ASSAY .....	91
3.2.2 TRANSPORT OF NUCLEOPORINS IS DELAYED BY ANTIBODIES AGAINST THE C-TERMINAL DOMAIN OF p62 .....	94
3.2.3 ANTIBODIES AGAINST THE NUCLEOPORINS p54 AND p58 HAVE DIFFERENT IMPACT ON THE NUCLEAR IMPORT OF GFP-NUCLEOPLASMIN.....	95
3.2.4. A COMBINATION OF ANTIBODIES AGAINST THE p62 COMPLEX INHIBITS NUCLEOCYTOPLASMIC TRANSPORT .....	97
<b>3.3. DISCUSSION .....</b>	<b>99</b>
3.3.1. INTERPRETATION OF THE RESULTS FROM THE FLUORESCENCE AND ULTRASTRUCTURAL ASSAY .....	100
3.3.2. DOCKING SITES OF THE IMPORT COMPLEX DURING TRANSPORT .....	101
3.3.3. THE EFFECTS OF ANTIBODIES AGAINST FULL LENGTH p62 AND ITS C-TERMINAL DOMAIN .....	102
3.3.4. ANTIBODIES AGAINST FULL LENGTH RAT p54 AND p58 AFFECT TRANSPORT IN DIFFERENT WAYS ..	103
3.3.5. A COMBINATION OF THE ANTIBODIES AGAINST THE p62 COMPLEX INHIBITS TRANSPORT .....	104
<b>3.4. MATERIAL AND METHODS .....</b>	<b>106</b>
3.4.1.RECOMBINANT PROTEIN EXPRESSION .....	106
3.4.2. ISOLATION OF XENOPUS OOCYTE NUCLEI .....	106
3.4.3. DIRECT CONJUGATION OF NUCLEOPLASMIN-GFP TO COLLOIDAL GOLD .....	106

3.4.4. ANTIBODIES .....	106
3.4.5. ULTRASTRUCTURAL NUCLEAR IMPORT ASSAY IN ISOLATED XENOPUS OOCYTES NUCLEI .....	106
3.4.6. QUANTIFICATION OF GOLD LABELING AT THE NPCS AND CALCULATION OF LOCATION CLOUDS ....	107
3.4.7. FLUORESCENCE MICROSCOPY IMPORT ASSAY IN HeLa CELLS .....	107
<b>3.5. ACKNOWLEDGEMENTS .....</b>	<b>109</b>
<b>3.6. REFERENCES .....</b>	<b>110</b>

**CHAPTER 4: DEPLETION OF COMPONENTS OF THE p62 COMPLEX BY RNAi  
LEADS TO MITOTIC ARREST AND INCREASED APOPTOSIS .....** **117**

<b>SUMMARY .....</b>	<b>119</b>
<b>4.1. INTRODUCTION .....</b>	<b>120</b>
<b>4.2. RESULTS .....</b>	<b>122</b>
4.2.1. DEPLETION OF p62, p54, AND p58 .....	122
4.2.2. IMMUNOFUORESCENCE ANALYSIS OF p62- AND p54-DEPLETED CELLS .....	122
4.2.3. ANALYSIS OF CELL GROWTH WITH FLUORESCENCE ACTIVATED CELL SORTING (FACS) ASSAY .....	122
4.2.4. ANALYSIS OF VIABILITY .....	124
4.2.5. CELL CYCLE ANALYSIS .....	126
4.2.6. IN VITRO TRANSPORT STUDIES WITH NUCLEOPORIN-DEPLETED CELLS .....	128
<b>4.3. DISCUSSION .....</b>	<b>129</b>
4.3.1. CELL GROWTH OF p62/p54-DEPLETED CELLS .....	129
4.3.2. p54-DEPLETED CELLS SHOW AN ARREST IN G0/G1 STATE .....	130
4.3.3. THE p62 COMPLEX AND NUCLEOCYTOPLASMIC TRANSPORT .....	130
<b>4.4. MATERIALS AND METHODS .....</b>	<b>132</b>
4.4.1. PLASMIDS .....	132



4.4.2. RECOMBINANT PROTEIN EXPRESSION .....	132
4.4.3. CELL CULTURE AND TRANSFECTION OF CELLS .....	132
4.4.4. RNA INTERFERENCE .....	132
4.4.5. CELL CYCLE ANALYSIS .....	133
4.4.6. IMMUNOFLUORESCENCE .....	133
4.4.7. APOPTOSIS FACS ASSAY .....	133
4.4.8. CARBOXYFLUORESCHEIN SUCCINIMIDYL ESTER (CFSE) STAINING .....	134
4.4.9. SDS-PAGE AND IMMUNOBLOTTING .....	134
4.4.10. ANTIBODIES .....	134
4.4.11. FLUORESCENCE MICROSCOPY IMPORT ASSAY IN HELA CELLS .....	134
<b>4.5. ACKNOWLEDGEMENTS .....</b>	<b>136</b>
<b>4.6. REFERENCES .....</b>	<b>137</b>
<b>Chapter 5: Conclusion and Outlook .....</b>	<b>141</b>
<b>5.1. Summary and outlook .....</b>	<b>143</b>
5.1.1 DOMAIN TOPOLOGY OF THE P62 COMPLEX WITHIN THE 3D ARCHITECTURE OF THE NPC.....	143
5.1.2. THE ROLE OF THE P62 COMPLEX IN NUCLEAR PROTEIN IMPORT.....	144
5.1.3. DEPLETION OF P62 AND P54 CAUSES DEFECTS IN CELL GROWTH AND NUCLEAR IMPORT .....	144
5.1.4. FURTHER BIOCHEMICAL EXPERIMENTS REGARDING THE P62 COMPLEX AND COMPLEXES, WHICH INTERACT WITH THE P62 COMPLEX.....	145
5.1.5. OUTLOOK .....	148
<b>5.2. REFERENCES .....</b>	<b>149</b>
<b>APPENDIX 1: CURRICULUM VITAE .....</b>	<b>153</b>
<b>APPENDIX 2: ACKNOWLEDGEMENTS .....</b>	<b>157</b>

## List of Abbreviations

AFM	atomic force microscope
ARM repeat	armadillo repeat
ATP	adenosine triphosphat
CAS	cellular apoptosis susceptibility (gene)
CFSE	carboxyfluoresceinsuccinimidylester
CRM1	chromosome region maintenance 1 protein
cryo-EM	cryo-electron microscopy
CTE	constitutive transport element
Da	Dalton
DAPI	4',6-Diamidino-2-phenylindol
DEAD	Asp(D)-Glu(E)-Ala(A)-Asp(D)
DMEM	Dulbecco's Modified Eagles's Medium
DNA	deoxyribonucleic acid
DRAQ	deep red anthraquinone
DTT	dithiothreitol
EDTA	ethylenediaminetetraacetic acid
EGTA	ethylen glycol tetraacetic acid
EJC	exon junction complex
EM	electron microscope
EXP	exportin
FCS	fetal calf serum
FG	phenylalanine-glycine
GFP	green fluorescent protein
GlcNac	N-acetylglucosamine
GTP	guanosine triphosphate
HEAT	huntingtin elongation factor 3 alpha regulatory subunit of protein phosphatase 2A TOR
HeLa	Henrietta lacks' cervical cancer cell
HEPES	[4-(2-hydroxyethyl)-1-piperazinyl]-ethansulfonic acid
His	histidine
hnRNP	heterogenous ribonucleoprotein
IBB	importin $\beta$ -binding

## LIST OF ABBREVIATIONS

---

IgG	immunoglobulin G
Immuno-EM	immuno-electron microscopy
Imp	importin
IPTG	isopropyl- $\beta$ -thiogalactopyrasonide
KCl	potassium chloride
LSB	low salt buffer
MgCl <sub>2</sub>	magnesium chloride
MPMV	Mason-Pfizer monkey virus
NE	nuclear envelope
NEBD	nuclear envelope breakdown
NES	nuclear export signal
NLS	nuclear localization signal
NPC	nuclear pore complex
NTF2	nuclear transport factor 2
Nup	nucleoporin
O-GlcNac	O-linked beta-N-acetylglucosamine
PHAX	phosphorylated adaptor for RNA export
PMSF	phenylmethanesulphonylfluoride
RanBP	Ran binding protein
RanGAP	Ran GTPase activating protein
RanGDP	Ran guanosine diphosphate (GDP)-bound form
RanGEF	Ran guanine nucleotide exchange factor
RanGTP	Ran guanosine triphosphate (GTP)-bound form
RCC1	regulator of chromosome condensation
RNA	ribonucleic acid
RNAi	ribonucleic acid interference
RNP	ribonucleoprotein
SDS-PAGE	sodium dodecyl sulfate polyacrylamide gel electrophoresis
siRNA	small interfering ribonucleic acid
snRNP	small nuclear ribonucleic acid-binding protein
SR	small subunit ribonucleic acid
TMH	transmembrane helices
WGA	wheat germ agglutinin

## List of Figures

<b>Figure</b>	<b>Page</b>
1.1. Schematic representation of the 3-D architecture of the nuclear pore complex	<b>19</b>
1.2 Schematic representation of nucleoporins and nucleoporin subcomplexes localization within the vertebrate NPC	<b>21</b>
1.3. Schematic overview of the physical interactions between the nucleoporins in the central region of the NPC	<b>24</b>
1.4. Schematic representation of the nuclear import and export cycles	<b>29</b>
1.5. 3 D structures of transport receptors	<b>31</b>
1.6. RanGTPase Cycle	<b>35</b>
2.1. Domain-specific antibodies against p62	<b>66</b>
2.2. Domain topology of p62 within the nuclear pore complex	<b>67</b>
2.3. Domain topology of epitope-tagged nucleoporin Xenopus p62 within the nuclear pore complex	<b>69</b>
2.4. Domain topology of epitope-tagged rat p54 within the NPC	<b>71</b>
2.5. Domain topology of epitope-tagged nucleoporin rat p58 within the NPC	<b>72</b>
2.6. Localization of the p62 domains at the cytoplasmic and the nuclear face of the NPC	<b>73</b>
2.7. Schematic representation of the epitope distribution of the different domains of the p62 complex within the 3-D architecture of the NPC	<b>77</b>

<b>Figure</b>	<b>Page</b>
3.1. The nuclear import of gold-labeled nucleoplasmin-GFP	93
3.2. Influence of antibodies against different domains of the mammalian nucleoporin p62 on nuclear transport	96
3.3. Influence of antibodies against the full length mammalian nucleoporins on nuclear transport	98
3.4. The nuclear import of gold-labeled nucleoplasmin-GFP	100
4.1. Depletion of the nucleoporins p62, p54, and p58 by siRNA	123
4.2. Immunofluorescence analysis of p62 and p54 depletion	124
4.3. Proliferation assay using CFSE-staining	125
4.4. Apoptosis assay and cell cycle distribution	126
4.5. p62 and p54 are required for nuclear protein import	127
5.1. Domain topology of the epitope-tagged nucleoporin human Nup35 within the nuclear pore complex	146
5.2. Model of the Nsp1p complex	147

## List of Tables

<b>Table</b>	<b>Page</b>
1.1. Summary of NLS and NE sequences	<b>32</b>

**Nucleoporins of the the central region of the nuclear pore  
complex and regulation of nucleocytoplasmic transport:  
An inventory**

CHAPTER 1: INTRODUCTION: NUCLEOPORINS OF THE CENTRAL REGION OF THE NPC



## **Summary**

The nuclear pore complex (NPC) is a highly conserved eukaryotic protein complex, which perforates the nuclear envelope and regulates nucleocytoplasmic transport of cargos between the cytoplasm and nucleus. The structure and function of NPCs were examined in recent years by different molecular and structural biology techniques, such as immunoprecipitation, RNA interference, or electron- and fluorescence microscopy, allowing deeper insights into the molecular mechanisms underlying nucleocytoplasmic transport. In this introduction, I will highlight recent developments in understanding the organization of four subcomplexes of the central region of the NPC, namely, the p62 complex, the Nup93 complex, the Nup107-160 complex, and the Nup155 complex as well as their impact on nucleocytoplasmic transport. In addition, I will discuss the role of these subcomplexes in cell cycle regulation and their impact on human diseases. Furthermore, the molecular interactions between different transport receptors, cargos, and components of the NPC are described.

## 1.1. Introduction

The nuclear envelope (NE) is perforated by huge protein complexes, called nuclear pore complexes (NPCs), which mediate the exchange of proteins and RNAs between the cytoplasm and nucleus of eukaryotic cells (Fahrenkrog and Aebi 2003; Fahrenkrog, Koser et al. 2004). The NPC is composed of about 30 different proteins, called nucleoporins (Rout, Aitchison et al. 2000; Cronshaw, Krutchinsky et al. 2002). Due to the highly symmetric organization of the NPC, nucleoporins are present in 8 copies or multiples thereof per NPC, and they are typically organized in distinct subcomplexes, which are arranged to form an eightfold symmetric structure (Jarnik and Aebi 1991; Schwartz 2005; Beck, Lucic et al. 2007). The total mass of the NPC is estimated to be ~125 MDa in vertebrates and its structure is divided into three parts (Reichelt, Holzenburg et al. 1990). As shown in Figure 1.1., the center of these huge complexes is formed by a central framework built of eight multidomain spokes (Hinshaw, Carragher et al. 1992; Yang, Rout et al. 1998; Stoffler, Feja et al. 2003; Beck, Forster et al. 2004). This central framework, which encloses the central pore of the NPC (Devos, Dokudovskaya et al. 2004), has a height of ~50 nm and is sandwiched between cytoplasmic and nuclear ring moieties. The functional diameter of the central pore was determined to be ~39 nm (Pante and Kann 2002), which is close to its physical diameter of 40-50 nm (Feldherr and Akin 1997; Stoffler, Feja et al. 2003). Flexible cytoplasmic filaments, ~50 nm in length, extend from the cytoplasmic ring moiety, whereas thin ~70 nm filaments are anchored to the nuclear ring moiety, which join to a 30-50 nm diameter distal ring. This fishtrap-like nuclear structure of the NPC is named nuclear basket (Stoffler, Feja et al. 2003; Beck, Forster et al. 2004). Earlier 3D reconstruction studies of the NPC provided evidence for the existence of a central plug or transporter, located in the center of the NPC as bona fide substructure of the NPC (Hinshaw, Carragher et al. 1992; Akey and Radermacher 1993). More recent atomic force microscopy (AFM) and cryo-electron microscopy (cryo-EM) studies, however, have shown that the central plug most likely corresponds to cargo caught in transit and/or the distal ring of the nuclear basket (Bustamante, Michelette et al. 2000; Oberleithner, Schillers et al. 2000; Stoffler, Feja et al. 2003; Beck, Forster et al. 2004; Beck, Lucic et al. 2007).

The overall 3D structure of the NPC seems to be conserved among species, from yeast over *C. elegans* to higher eukaryotes (Fahrenkrog, Hurt et al. 1998; Stoffler, Fahrenkrog et al. 1999; Cronshaw, Krutchinsky et al. 2002; Galy, Mattaj et al. 2003). Nevertheless, the NPCs of different species vary significantly in their total mass, their linear dimensions, and the composition of nucleoporins. No homologue of vertebrate Nup358/RanBP2 is known in yeast, while the number of the nucleoporins always appears to be ~30.

Recent homologue modeling studies for NPC components of the Rout lab and X-ray crystallography of nucleoporin domains revealed that only a few structural features like transmembrane helices-fold (TMH-fold),  $\beta$ -propeller,  $\alpha$ -solenoid folds, coiled-coil domains, and largely unstructured phenylalanine-glycine repeat (FG-repeat) domains appear present in nucleoporins (Hodel, Hodel et al. 2002; Devos, Dokudovskaya et al. 2004; Weirich, Erzberger et al. 2004). These FG-repeat domains, which are anchored to the cytoplasmic and the nuclear side of the NPC, act as docking sites for nuclear transport receptors like importin  $\beta$  and other importins or exportins (see 1.6 and Fig. 1.3. and 1.4.), and they facilitate the transport of macromolecular cargos through the NPC (Pante, Bastos et al. 1994; Fahrenkrog, Hurt et al. 1998; Rout, Aitchison et al. 2000). At the same time, they function as an entropic barrier to inert mole-

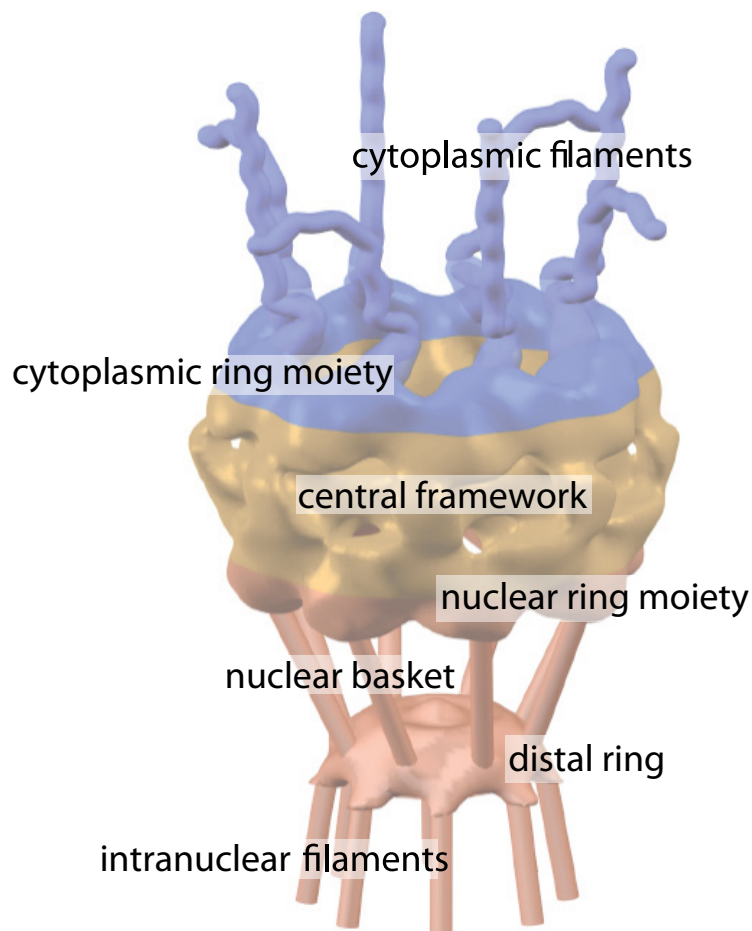


**Figure 1.1:** Schematic representation of the 3-D architecture of the nuclear pore complex. This figure was modeled and prepared by D. Stoffler using ViPER, a Visual Programming Environment, that was developed by D. Stoffler and M. Sanner at the Scripps Research Institute, La Jolla, California, USA. The model is based on a reconstruction of native NPCs embedded in thick amorphous ice (Stoffler, Feja et al. 2003).

cules, most likely due to a polymer brush-like conformation (Rout, Aitchison et al. 2003; Lim, Huang et al. 2006; Lim, Fahrenkrog et al. 2007).

Biochemical fractionation of NPCs has shown that many nucleoporins associate with one another to build subcomplexes. The best characterized subcomplexes are the p62 complex, the Nup93 complex, the Nup107-160 complex, and the Nup155 complex (Finlay, Meier et al. 1991; Grandi, Dang et al. 1997; Lutzmann, Kunze et al. 2002; Mansfeld, Guttinger et al. 2006). A summary of the characterized subcomplexes and the localization data based on immuno-EM is shown in Fig. 1.2. In the following, I will first introduce the four major subcomplexes of the central pore and then give an overview of nucleocytoplasmic transport and its regulation.

### 1.2. p62: identification and function

p62 was the first nucleoporin, which had been discovered and is probably one of the best characterized ones (Davis and Blobel 1986; Davis and Blobel 1987). Based on its amino acid sequence, vertebrate p62 is organized into three distinct domains: an N-terminal domain, which contains several FG-repeats (rat; residues 1-190), a central threonine-rich linker (rat; residues 190-330), and a C-terminal domain containing heptad repeats, characteristic for  $\alpha$ -helical coiled-coil proteins (rat; residues 331-547) (Hu, Guan et al. 1996). p62 belongs to a subset of nucleoporins, which possess O-linked N-acetylglucosamine residues (Davis and Blobel 1987; Hanover, Cohen et al. 1987; Finlay, Meier et al. 1991; Cordes and Krohne 1993). These modifications seem to have no function in nucleocytoplasmic transport or NPC assembly (Finlay, Meier et al. 1991), but, however, might play a role during cell cycle, thereby preventing hypophosphorylation of p62 and p54, a nucleoporin, which has a similar domain organization like p62 and is a known binding partner (Bodoor, Shaikh et al. 1999).

Extensive biochemical studies have shown that p62 stably interacts with two other nucleoporins, p54 and p58/p45, whereby p45 is a splice variant of p58, building a NPC subcomplex, which can be isolated by immunoprecipitation with antibodies against any of its components (Finlay, Meier et al. 1991; Hu, Guan et al. 1996). Blot overlay assays further revealed a direct interaction between the C-terminal domains of p62 and p54 (Buss and Stewart 1995). Biochemical isolation from rat liver NEs and structural characterization by EM revealed a donut-like structure of the p62 complex with an average mass of 210 kDa, corresponding to a complex containing one copy of each nucleoporin (Guan, Muller et al. 1995). Immunodepletion of the p62 complex from highspeed *Xenopus* egg extracts led to the assembly of nuclei,

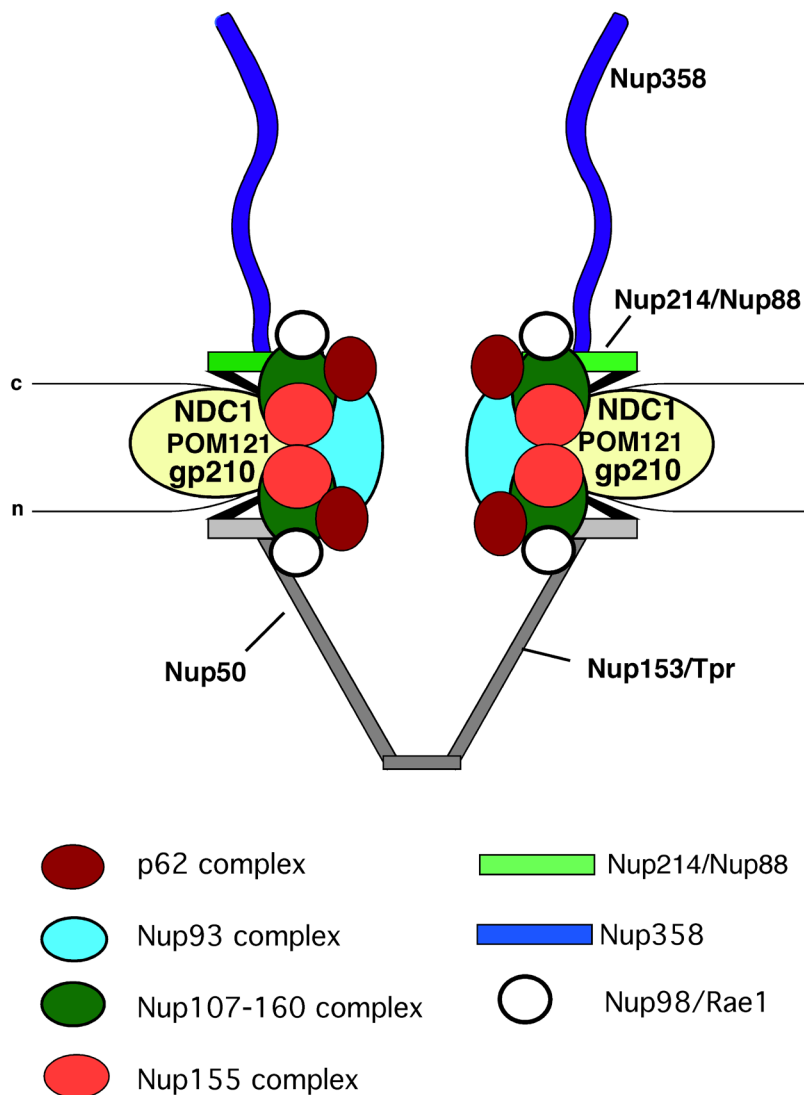


**Figure 1.2:** Schematic representation of nucleoporins and nucleoporin subcomplexes localization within the vertebrate NPC. Nup107-160 complex: Nup107, Nup160, Nup133, Nup96, Nup75, Nup43, Nup37, Seh1, Sec13; Nup155 complex: Nup155, Nup35, NDC1, Nup93; Nup93 complex: Nup93, Nup205, Nup188; p62 complex: p62, p54, p58, p45. c, cytoplasm; n, nucleus.

which were deficient for nucleocytoplasmic transport (Finlay, Meier et al. 1991). Moreover, depletion of any member of the p62 complex leads to co-depletion of import factor importin  $\beta$  from a cytosolic extract (Hu, Guan et al. 1996), indicating that p62 plays a critical role in nuclear import.

The crystal structure of the  $\alpha$ -helical region of rat p58/p45 revealed that p58 forms distinct tetramers, each consisting of two anti-parallel hairpin dimers (Melcak, Hoelz et al. 2007). The dimer-dimer association at the intradimeric interface occurs via large hydrophilic residues, which are laterally displaced in various tetramer conformations. The authors propose an intermolecular sliding mechanism for the p58/p45 tetramer conformation, which could play a role in adjusting the diameter of the central pore

of the NPC during cargo translocation.

Attempts to determine the localization of the p62 complex on the ultrastructural level have led to controversial results, locating this complex to either the cytoplasmic face or both sides of the NPC (Dabauvalle, Benavente et al. 1988; Cordes and Krohne 1993; Guan, Muller et al. 1995; Hu, Guan et al. 1996). Nevertheless, transport studies with gold-coupled nucleoplasmin indicated that the region, where the p62 complex might be located at the cytoplasmic face of the NPC, functions as a docking site for transport complexes during the multistage import process of cargos (Pante and Aebi 1996). A recent paper, focused on the localization of the vertebrate p62 complex domains with domain-specific antibodies by immunocytochemistry (EM), showed that the p62 complex is exclusively anchored to the cytoplasmic face of the NPC (Schwarz-Herion, Maco et al. 2007).

Comparison of the amino acid sequence between vertebrate p62 and yeast Nsp1p showed partial sequence similarity between both proteins, whereby the sequence of the C-terminal part of Nsp1p bearing heptad repeats showed higher sequence similarity than the N-terminal half of the protein (Carmo-Fonseca, Kern et al. 1991). The N-terminal FG-repeat-domain of Nsp1p contains 32 FG-repeats, which are distributed over 600 residues, whereas vertebrate p62 contains 6 FG-repeats over a length of about 180 residues. Nsp1p interacts with the nucleoporin Nic96p (Grandi, Dang et al. 1997); similarly, the p62 complex interacts with Nup93, which resembles the mammalian homologue of Nic96p and forms itself another NPC subcomplex in association with Nup205 and Nup188 (Grandi, Dang et al. 1997; Miller, Powers et al. 2000). By a yeast two-hybrid assay it was shown that the *C. elegans* homologues of p62, p54, p58/p45, Nup93 and Nup205 physically interact with one another (Schetter, Askjaer et al. 2006). In addition, p62 interacts with Nup214 and Nup88 during interphase (Stochaj, Banski et al. 2006), and two studies could confirm an interaction between Nup214 and p62 also during mitosis (Matsuoka, Takagi et al. 1999; Stochaj, Banski et al. 2006).

Sequence analysis identified the essential *C. elegans* glue Npp-11 as homologue of vertebrate p62 (Schetter, Askjaer et al. 2006). Deletion of Npp-11 in *C. elegans* leads to an embryonic lethality of 99% (Galy, Mattaj et al. 2003). Silencing of the p62-complex members p54 (Npp-1) and p45 (Npp-4) lead also to a high lethality among the *C. elegans* embryos (Galy, Mattaj et al. 2003). Transport studies in Npp-1 (p54)-depleted *C. elegans* embryos revealed some defects of the permeability barrier, i.e. tubulin-GFP is not excluded from the nucleus and some cargos are not imported any more (Schetter, Askjaer et al.

2006). Similar effects, such as the leakage of a reporter gene from the nucleus into the cytoplasm, could be observed in Nsp1p mutants in yeast (Nehrbass and Blobel 1996). In contrast, a recent comprehensive RNAi-knock-down of nucleoporin genes in *Drosophila melanogaster* showed that depletion of the p54-homologue leads to an nuclear protein import defect (Sabri, Roth et al. 2007) as shown by GFP-reporter cargos in p54-depleted *Drosophila* cells .

The main feature of the depletion of the p62, p54 and p45 homologues in *C. elegans* was a defect in spindle orientation of early embryos. In addition, cell cycle progression was slower and embryos showed a reduced size compared to mock-transfected embryos (Galy, Mattaj et al. 2003; Schetter, Askjaer et al. 2006). Consistently, a recent study using monoclonal antibodies against the central and C-terminal part of p62 revealed cell division defects in HeLa cells as well when these antibodies are microinjected into the cytoplasm (Fukuhara, Sakaguchi et al. 2006). Besides of its function in nuclear protein import and in mitosis, there are several reports implicating p62 in human diseases, such as primary biliary cirrhosis and autosomal recessive infantile bilateral striatal necrosis (Wesierska-Gadek, Hohenuer et al. 1996; Enarson, Rattner et al. 2004; Basel-Vanagaite, Muncher et al. 2006).

### **1.3. The Nup93 complex**

The nucleoporin Nup93 forms another NPC subcomplex with its interacting partners Nup205 and Nup188 (Grandi, Dang et al. 1997; Miller, Powers et al. 2000). The Nup93 complex furthermore physically interacts with several other nucleoporins and it appears to anchor the p62 complex to the NPC (Miller, Powers et al. 2000; Galy, Mattaj et al. 2003; Krull, Thyberg et al. 2004; Hawryluk-Gara, Shibuya et al. 2005).

RNAi in *C. elegans* revealed that Nup93 and Nup205 depleted embryos show clustered NPCs and a failure in nuclear exclusion of macromolecules, which do not possess NLSs, of ~70 kDa without preventing active nuclear protein import or assembly of the nuclear envelope (Galy, Mattaj et al. 2003). Recent RNAi studies furthermore revealed the interaction of the Nup93 complex with further nucleoporins like Nup35, Nup155, and Ndc1. A loss of Nup93 ,e.g., could be detected in Nup35-depleted mammalian cells, which were treated with siRNAs specific for Nup35 (Hawryluk-Gara, Shibuya et al. 2005). In a corresponding experiment using siRNAs specific for Nup93, the cellular levels of Nup35, Nup155 and Nup205 were significantly reduced, indicating an interaction between these four proteins. In addition, cells, which were transfected with siRNAs specific against Nup93 and Nup35, show misshaped nuclei, which often

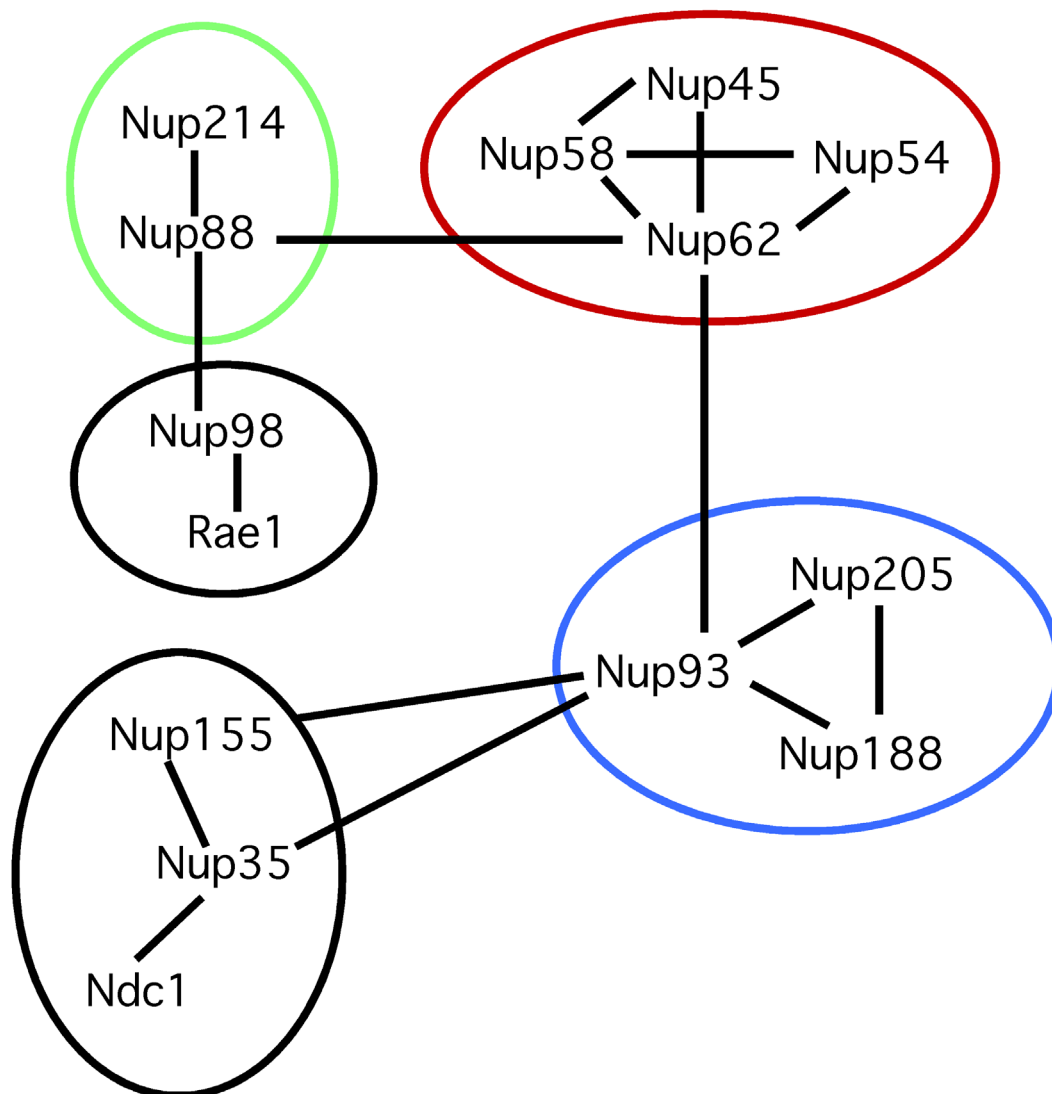


**Figure 1.3** Schematic overview of the physical interactions between the nucleoporins in the central region of the NPC. Scheme is based on data obtained from immunoprecipitation, pull-downs, yeast two-hybrid assays, and RNAi-studies.

appear elongated or kidney-shaped (Krull, Thyberg et al. 2004). A fifth interaction partner of Nup93 was revealed by using siRNAs specific to the transmembrane nucleoporin Ndc1: Downregulation of Ndc1 in HeLa cells caused a reduced NPC association of Nup35, Nup93, and Nup205 (Hawryluk-Gara, Shibuya et al. 2005). Biochemical data confirmed the finding that Nup93 anchors the Nup93 complex to the NE via interaction with the transmembran protein Ndc1 (Hawryluk-Gara, Shibuya et al. 2005). Previously, it was already shown that Nup93-depleted nuclei showed an NPC assembly defect and reduced nuclear rim staining with the monoclonal antibody mAb414, indicating a loss of FG-repeat bearing nucleoporins (Grandi, Dang et al. 1997).

During mitosis, the Nup93 complex may be associated with the p62 complex (Bodoor, Shaikh et al. 1999; Schetter, Askjaer et al. 2006) as both complexes show similar dynamics at the end of mitosis being



recruited at the same time to the reforming NPCs (Bodoor, Shaikh et al. 1999; Rabut, Doye et al. 2004; Rabut, Lenart et al. 2004).

### **1.4. Nup155**

The mammalian nucleoporin Nup155 was first identified and characterized in a fraction with other structural nucleoporins after depleting WGA-binding nucleoporins from a purified NPC fraction (Radu et al. 1993). Immuno-EM showed that Nup155 is localized to the nucleoplasmic and cytoplasmic face of the NPC (Radu, Blobel et al. 1993; Krull, Thyberg et al. 2004).

A recent study using RNAi in *C. elegans* revealed that depletion of Nup155 causes defects in nuclear morphology and segregation of sister chromatids as well as impaired viability of *C. elegans* embryos (Franz, Askjaer et al. 2005). Moreover, a strong defect in recruitment of Nup35 and mAb414 nucleoporins (i.e. Nup358/RanBP2, Nup214/CAN, Nup153, and p62) to the NPC was detected in Nup155 depleted cells (Franz, Askjaer et al. 2005). Furthermore, in *Xenopus* egg extracts and in *C. elegans*, the absence of Nup155 leads to a block in nuclear membrane fusion (Franz, Askjaer et al. 2005). Analysis of the Nup155 dynamics revealed that GFP-Nup155 was recruited to chromatin one minute after anaphase onset, similar to Nup35 and the p62 complex (Franz, Askjaer et al. 2005), indicating that Nup155 has an intermediate position during NPC assembly as compared to nucleoporins, which are recruited early after mitosis to the growing NPC, such as the Nup107-160 complex, and nucleoporins, that are recruited at the end of mitosis, such as gp210 and Tpr.

Nup155 is not only a structural nucleoporin, but also acts in the export of mRNA due to a direct interaction with the mRNA export factor Gle1 via a domain in the C-terminal half of Nup155 (Rayala, Kendirgi et al. 2004). In human cells, shuttling of Gle1 between nucleus and cytoplasm is essential for bulk mRNA export (Alcazar-Roman, Tran et al. 2006).

During mitosis, Nup155 has - like several other nucleoporins - a diffuse cytoplasmic distribution, that reverses back to a punctate nuclear rim localization at the end of mitosis. Depletion of Nup155 causes two distinct mitotic defects in *C. elegans* (Franz, Askjaer et al. 2005). First, chromatin was positioned between the two centrosomes, and microtubules connecting the centrosomes to chromatin were visible, indicating a strong anaphase segregation phenotype. In a second class of mitotic defects, no chromatin was detected between centrosomes, and a mitotic spindle was not formed.

Two yeast homologues of Nup155 have been identified, namely Nup170p and Nup157p (Aitchison, Rout et al. 1995). Nucleotide sequence comparison of *Nup155*, *Nup170p*, and *Nup157p* revealed highly conserved features like high sequence homology in certain regions of the primary sequence, that are common for all three proteins. Structural analysis of the Nup157p by single particle analysis revealed a structure of a gripping hand (Lutzmann, Kunze et al. 2005). In addition, biochemical analysis of Nup157p and the yeast Nup84p complex indicated that Nup157p might function as a bridge between the Nup84p complex and other structural nucleoporins (Lutzmann, Kunze et al. 2005). Taking the high homology of *Nup157p* and *Nup155* into consideration, this suggests that Nup155 may possess a similar structure and function similar to Nup157p.

A synthetic lethal screen showed that *Nup170p* and *Nup157p* are genetically interacting with the pore-membrane protein Pom152p and the nucleoporin Nup188p (Aitchison, Rout et al. 1995). Deletion mutants of *Nup170p* and *Nup157p* are viable, whereas double deletion mutants (*Nup157pΔNup170pΔ*) showed synthetic lethality (Aitchison, Rout et al. 1995). Depletion and overexpression of Nup170p leads to structural abnormalities of the NE, such as loss of its regular shape, massive extensions, and intra-nuclear annulate lamellae (Aitchison, Rout et al. 1995). These structural alterations in nuclear shape in Nup170p/Nup157p-depleted cells correspond well with the results of Nup155-depleted cells of Franz et al. as described above (Franz, Askjaer et al. 2005).

### 1.5. The Nup107-160 subcomplex

The Nup107-160 complex is a major building block of the central framework of the NPC and comprises the nucleoporins Nup160, Nup133, Nup107, Nup96, Nup85, Nup43, Nup37, Seh1, and Sec13 (Radu, Blobel et al. 1994; Vasu, Shah et al. 2001; Boehmer, Enninga et al. 2003; Walther, Alves et al. 2003; Loiodice, Alves et al. 2004; Zuccolo, Alves et al. 2007). The Nup107-160 complex is evolutionary conserved and it localizes to both sides of the NPC (Vasu, Shah et al. 2001; Devos, Dokudovskaya et al. 2004). Depletion of this complex in nuclear reconstitution assays or by RNAi in HeLa cells results in an NE devoid of NPCs, indicating that this complex is critical for NPCs' assembly (Harel, Orjalo et al. 2003; Walther, Alves et al. 2003; Boehmer, Enninga et al. 2003). In addition, RNA export defects were observed in cells, in which the Nup107-160 complex was depleted by RNAi (Boehmer, Enninga et al. 2003).

The Nup107-160 complex does not only play a crucial role as scaffold of the NPC, but also as component of the kinetochores during mitosis and as an important structural component for NPC reassembly

after mitosis (Devos, Dokudovskaya et al. 2004; Loiodice, Alves et al. 2004). The constituents of the Nup107-160 complex, which remain associated with each other throughout mitosis, are among the earliest nucleoporins recruited on the chromatin surface in anaphase (Belgareh, Rabut et al. 2001). Depletion of the Nup107-160 complex fails to establish proper microtubule attachments to the kinetochore, thus inducing a checkpoint-dependent mitotic delay in the G2 phase of the cell cycle (Loiodice, Alves et al. 2004; Orjalo, Arnaoutov et al. 2006; Zuccolo, Alves et al. 2007). In a recent study, it was demonstrated that efficient targeting of the Nup107–160 complex to kinetochores requires the Ndc80 complex (i.e. Ndc80, Nuf2, Spc24 and Spc25) and CENP-F, both of which were previously localized to the kinetochore outer plate. Depletion of the Nup107-160 complex component Seh1 in HeLa cells alone induces a mitotic delay, probably caused by chromosome congression, reduced chromosome tension, and kinetochore-microtubule attachment defects (Zuccolo, Alves et al. 2007). Furthermore, the presence of the Nup107-160 complex at the kinetochores seems to be required for the recruitment of CRM1 and RanGAP1-RanBP2 (see 1.6.1.3. and 1.6.2.) to the kinetochores (Zuccolo, Alves et al. 2007).

### **1.6. Nucleocytoplasmic transport**

Bidirectional traffic occurs continuously between the cytosol and nucleus of eukaryotic cells. The many proteins, that act in the nucleus are selectively imported into the nucleus from the cytosol where they are made. At the same time, tRNAs and mRNAs are synthesized in the nuclear compartment and then exported to the cytosol. Since each of the transport events can be crucial for cell fate, the transport across the nuclear envelope is selective and strongly regulated.

#### **1.6.1. Nuclear Protein Import**

Different cargos require distinct nuclear import receptors for their translocation into the nucleus. Despite the usage of different receptors, distinct nuclear import pathways share many common features (Conti, Muller et al. 2006). The best characterized nuclear import pathway is the importin  $\beta$  pathway (Fig.1.4.(a); see 1.6.1.2.). Importin  $\beta$  does not bind directly to a nuclear localization sequence (NLS; see 1.6.1.1), but only via importin  $\alpha$ , which recognizes basic NLSs, and, in turn, binds importin  $\beta$  via its N-terminal importin- $\beta$ -binding (IBB) domain (Cingolani, Petosa et al. 1999). After assembly in the cytoplasm, the importin  $\alpha$ /importin  $\beta$ /NLS-cargo complex first accumulates at the cytoplasmic filaments of the NPC (Fig. 1.4. (a)). Next, the cargo-receptor complex is translocated to the central pore of the NPC, most likely by bending of the cytoplasmic filaments towards the cytoplasmic periphery of the central

pore, which represents the second docking site of the cargo receptor complex at the NPC (Pante and Aebi 1996; Beck, Forster et al. 2004). The cargo-receptor complex is further transported to the nuclear side of the NPC by interaction of importin  $\beta$  with FG-repeat domains of nucleoporins. After translocation through the central pore, the cargo-receptor complex binds to the nuclear face of the NPC, where the complex is dissociated by binding of the small GTPase RanGTP to importin  $\beta$  (see 1.6.1.3.; Lee, Matsuura et al. 2005). Importin  $\alpha$  is exported by the importin- $\beta$ -like protein CAS in complex with RanGTP, and the importin  $\alpha$ -RanGTP complex is recycled to the cytoplasm to start another import cycle (Fig. 1.4. (a)) (Kutay, Izaurralde et al. 1997).

### ***1.6.1.1. Nuclear Localization Signal***

Nuclear import is mediated by a group of transport receptors, which are called importins or karyopherins, and it is energy-driven (Fried and Kutay 2003; Pemberton and Paschal 2005; Stewart 2007). The importins recognize specific amino acid sequences, called nuclear localization sequence (NLS), of proteins, which are destined to the nucleus (Conti, Uy et al. 1998). A so-called classical NLS, which was first identified in the simian virus 40 large T antigen, contains a stretch of basic amino acids (Table 1.1.). Such classical NLS is recognized by the adapter protein importin  $\alpha$ , which interacts with the receptor importin  $\beta$  (see 1.6.1.2.). Alternatively, the importin  $\alpha/\beta$  heterodimer can recognize bipartite NLS sequences as first described in nucleoplasmin or arginine-glycine rich sequences, which are characteristic of RNA binding proteins (Table 1.1.) (Dingwall, Sharnick et al. 1982; Robbins, Dilworth et al. 1991). Transportin, another importin, recognizes so-called M9 NLS sequences, which are 38 amino acids long and devoid of basic amino acids (Table 1.1.) (Rosenblum, Pemberton et al. 1998). Non-classical NLSs-like M9 domains play also a role in the import of small nuclear RNA-binding proteins (snRNPs) or of heterogenous nuclear ribonucleotide particles (hnRNPs) (Lee, Cansizoglu et al. 2006).

### ***1.6.1.2. Nuclear import receptors***

Importin  $\alpha$  forms a helix consisting of 10 armadillo (ARM) repeats as determined by sequence analysis and X-ray crystallography (Conti, Uy et al. 1998; Fig. 1.5.(a)). Each ARM repeat consists of about 40 residues, which are arranged into three helices, thereby generating a banana-shaped molecule with the NLS-binding site being located in a groove on the inner concave surface (Conti, Uy et al. 1998). The N-terminus of importin  $\alpha$  binds to importin  $\beta$  through a domain, named importin- $\beta$ -binding (IBB) domain.

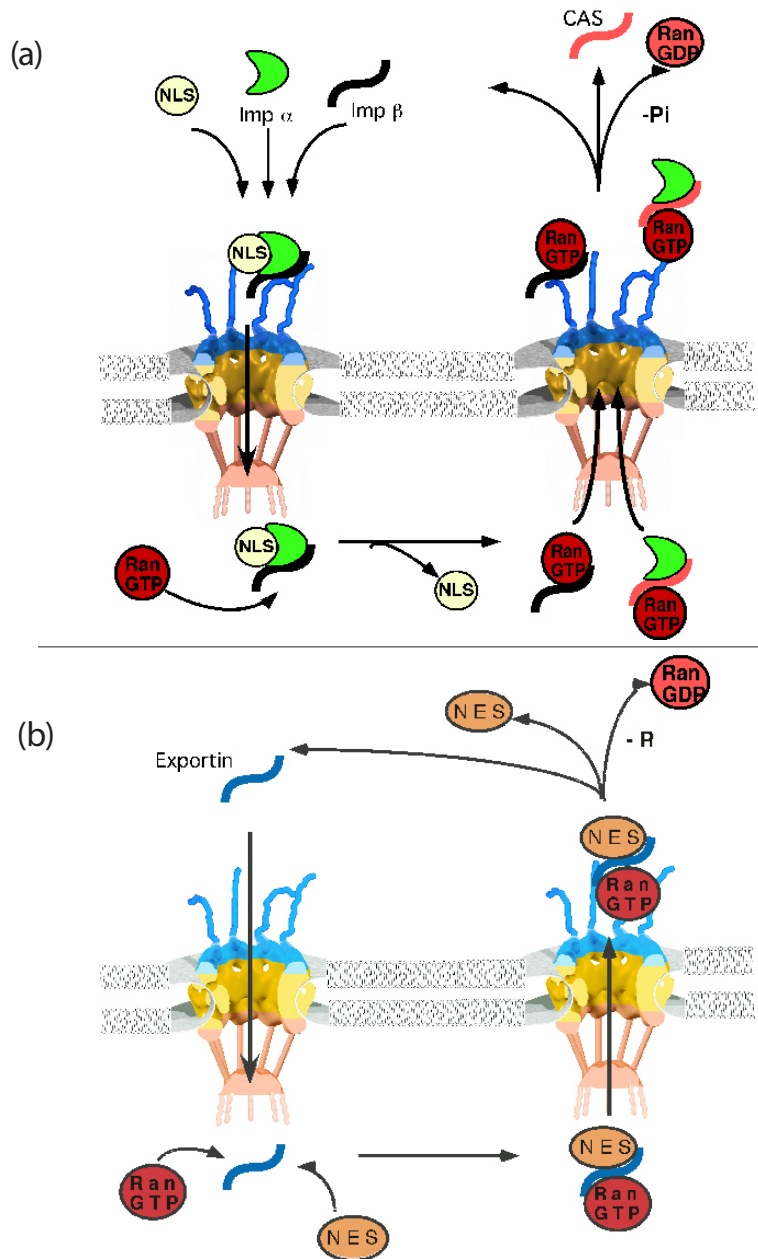


**Figure 1.4.** Schematic representation of the nuclear import and export cycles. (a) A cargo bearing a NLS (yellow) is recognized by importin  $\beta$  (green), which forms a nuclear import complex together with importin  $\alpha$  (black). The cargo-receptor complexes can interact with FG-repeat nucleoporins at the cytoplasmic filaments or at the periphery of the central pore. From here, the cargo-receptor complex is transferred to the extended FG-repeat domains of a nucleoplasmic nucleoporin, for example, Nup153, in the center of the NPC. RanGTP (red) biases the direction of transport into the nucleus by sequestering importin  $\beta$ , which, in turn, leads to the dissociation of the cargo from the receptor. Importin  $\alpha$  is actively transported back to the cytoplasm via interaction with the transport receptor CAS (orange) and RanGTP. Importin  $\alpha$  shuttles back to the cytoplasm without the help of another transport receptor. At the cytoplasmic filaments, RanGTP is hydrolysed to RanGDP, which leads to a dissociation of the cargo-receptor complex. Importin  $\beta$  and Importin  $\alpha$  are now ready to start a new nuclear import cycle. (b) At the nuclear side of the NPC, a nuclear export complex is formed by an exportin (blue), an NES-cargo (yellow) and RanGTP (red). The cargo-receptor complex is translocated through the NPC via specific interactions with the FG-repeat domains of nucleoporins. The nuclear export complex is disassembled at the cytoplasmic filaments of the NPC where RanGAP hydrolyses RanGTP to RanGDP and the NES-cargo is released into the cytoplasm.

Importin  $\beta$  is composed of 19 HEAT repeats, each of which is made up from two  $\alpha$ -helices connected by a short turn (Cingolani, Petosa et al. 1999; Chook and Blobel 1999; 1.5.(b)). Importins appear to fold into a right-handed spirale-like helical structure, which forms two C-shaped arches (Chook and Blobel 1999; Cingolani, Petosa et al. 1999). A crystal structure of importin  $\beta$  co-crystallized with FG-repeats of the yeast nucleoporin Nsp1p revealed that one interaction side between importin  $\beta$  and the FxFG motif occurs at the N-terminal domain of importin  $\beta$  (Bayliss, Littlewood et al. 2000). Recent Molecular Dynamics (MD) simulation studies with the X-ray structure of importin  $\beta$  and the FG-repeat domain of Nsp1 revealed 10 predicted and 4 confirmed sites for the interaction between importin  $\beta$  and the FG-repeat domain (Isgro and Schulten, 2005). The transport receptors of the importin  $\beta$  family are highly flexible molecules, which help to adapt the shape to encircle the cargo (Conti, Muller et al. 2006).

A common feature of all members of the importin  $\beta$  family is an N-terminal binding domain for the small GTPase Ran, a protein, which regulates the directionality of the nucleocytoplasmic transport (see 1.6.1.3.; Chook and Blobel 1999; 1.5. (d)).

Besides importin  $\beta$ , 21 other importin  $\beta$ -like human proteins have been identified, which mediate nuclear import (Fried and Kutay 2003). Transportin 1, for example, mediates nuclear import of mRNA binding proteins and ribosomal proteins (Siomi, Eder et al. 1997). Ribosomal proteins are also imported by importins 4, 5, 7, and 11 (Jakel and Gorlich 1998; Plafker and Macara 2000; Jakel, Mingot et al. 2002). The importins 5 and 9 are involved in the import of core histones (Deane, Schafer et al. 1997; Muhlhassser, Muller et al. 2001). Specialized importins, namely importin 5, transportin or importin 13 for ribonucleoproteins, splicing factors and transcription factors have been described (Fried and Kutay 2003). The variety of importins is most likely due to their dual function as nuclear import receptors as well as cytoplasmic chaperones for exposed basic domains (Jakel, Mingot et al. 2002).

### **1.6.1.3. Regulation of nuclear import: The Ran Cycle**

Ran, a member of the Ras-related GTPase superfamily, regulates the directionality of nucleocytoplasmic transport and mediates the assembly and disassembly of cargo-receptor complexes (Rexach and Blobel 1995; Gorlich, Pante et al. 1996). The RanGTPase system is regulated by several co-factors, which catalyze the hydrolysis of RanGTP to RanGDP or the conversion of RanGDP to RanGTP (Fig. 1.6.)

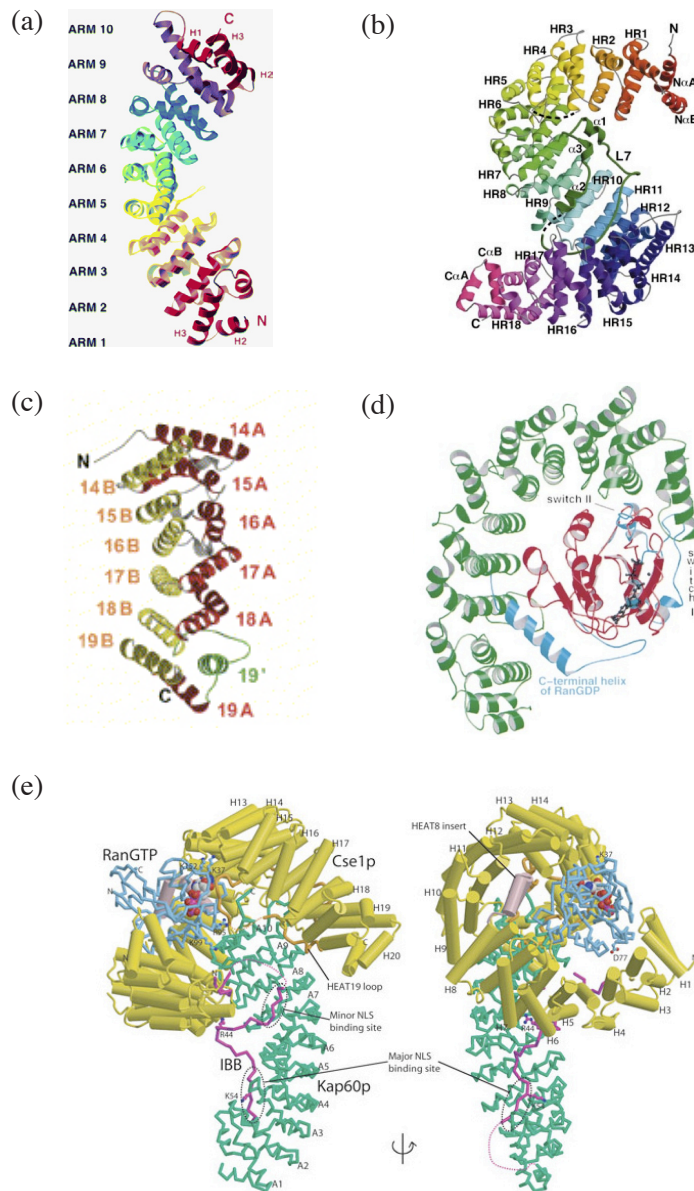


**Figure 1.5.** (a) 3D-structure of Kap $\alpha$ 50 (yeast importin  $\alpha$ ). The molecule contains ten tandem repeats, which are shown in different colors (Conti, Uy et al. 1998). (b) Ribbon diagram of human Kap- $\beta$ 2 (importin  $\beta$ ), which contains eighteen HEAT repeats. Each HEAT repeat is presented in a different colour and labeled HR1-HR18 (Chook and Blobel, 1999). (c) CRM1 is shown with the A and B helices in red and yellow, respectively; the insertion containing helix 19' is in green (Petosa, Schoehn et al. 2004). (d) Ribbon representation of the Ran-Importin  $\beta$  complex with Ran in red, Importin  $\beta$  in green, superimposed with RanGDP in blue to highlight the potential clashes in switch I and the C-terminal end. GppNHp (a nonhydrolyzable GTP analog) and Mg $^{2+}$  are shown as ball- and stick models (Vetter, Arndt et al. 1999). (e) Two orthogonal views showing an overview of the structure of the Cse1p:Kap60p:RanGTP complex. The structure illustrates how Cse1p (yellow), envelopes RanGTP (blue), and the C-terminal region of Kap60p (green) and its IBB domain (magenta). GTP is shown as spacefilling spheres (Matsuura and Stewart 2004).

**Table 1.1.** : Summary of NLS and NE sequences. Table was adapted from Fried et al. (Fried and Kutay 2003).

Transport signal	Example substrates	Sequence	References	Transport receptors
Classical monopartite NLS	SV40 T antigen	PKKKRKVE	(Kalderon, Richardson et al. 1984)	Imp $\alpha$ /Imp $\beta$
Classical bipartite NLS	nucleoplasmin	KRPAATKKAGQAKKKKLD	(Dingwall, Sharnick et al. 1982; Robbins, Dilworth et al. 1991)	Imp $\alpha$ /Imp $\beta$
M9 domain	hnRNPA1	YNDFGNYNQSSNFGPMKGGN FGGRSSGPY	(Siomi and Dreyfuss 1995)	transportin
BIB domain	rpL23a	VHSHKKKKIRTSPTRRPKTLR LRRQPKYPRKSAPRRNKLDHY	(Jakel and Gorlich 1998)	transportin, Imp5, Imp7, Imp $\beta$
RS domain	SR proteins	Phosphorylated RS domains	(Kataoka, Bachorik et al. 1999)	Transportin SR2
Leucine-rich NES	HIV Rev, PKI	Consensus: L-X <sub>2,3</sub> -(L,I,M,F,M)-X <sub>2,3</sub> -L-X-(L,I,V)	(Bogerd, Fridell et al. 1996)	CRM1

Ran itself has low GTPase activity and requires a Ran-specific GTPase activating protein, RanGAP1, which increases Ran's rate of GTP hydrolysis by five orders of magnitude (Bischoff, Klebe et al. 1994; Klebe, Bischoff et al. 1995). To ensure an asymmetric distribution of RanGTP, RanGAP is restricted to the cytoplasmic periphery of the NPC. Dissociation of RanGTP from nuclear import receptors is mediated by the Ran-binding proteins RanBP1, Ran GAP and RanBP2/Nup358, which are located to the cytoplasmic filaments of the NPC (Gorlich, Pante et al. 1996; Delphin, Guan et al. 1997; Kehlenbach, Dickmanns et al. 1999; Yaseen and Blobel 1999). The Ran nucleotide state on the nuclear side of the NPC is controlled by its guanine nucleotide exchange factor (RanGEF), which catalyses reloading of RanGDP with GTP (Klebe, Bischoff et al. 1995). As required for maintenance of the nuclear RanGTP level, RanGEF (RCC1 in metazoans) is restricted to the nucleus and bound to chromatin (Ohtsubo, Okazaki et al. 1989).

The ratio of concentration between free nuclear and cytoplasmic RanGTP is at least 200-fold (Kalab, Weis et al. 2002; Smith, Slepchenko et al. 2002). To maintain the RanGTP gradient, cytoplasmic RanGDP is transported to the nucleus by its specific carrier, nuclear transport factor 2 (NTF2), to enable its reloading with GTP (Ribbeck, Lipowsky et al. 1998).



### 1.6.2. Nuclear export

Typical nuclear export cargos, such as transcription factors or ribosomal sequences are shuttling proteins or distinct classes of RNAs (Fried and Kutay 2003; Pemberton and Paschal 2005). Nuclear export is mediated by export receptors, which recognize cargos with special nuclear export signals (NES) as summarized in Table 1.1. (Wen, Meinkoth et al. 1995).

Several types of NESs have been described, from which the NES of the HIV-1 protein Rev is the best characterized signal consisting of a short leucine-rich amino acid stretch (Table 1.1.) (Fischer, Huber et al. 1995). The second type of NES was identified in the C-terminus of hnRNP A1 (Table 1.1.). It consists of a 38 amino acid sequence, that serves as a combined signal for both import and export of A1 (Michael, Choi et al. 1995; Siomi and Dreyfuss 1995; Siomi, Eder et al. 1997). Most RNAs are associated with proteins and transported as RNPs through the NPC, whereas some RNAs also bind directly to their export receptors (Stewart 2007). Therefore, the proteins, which bind to the RNA and also the RNAs themselves, possess NESs. On the nuclear side of the NPC, a nuclear export complex is formed by an exportin, a NES-cargo, and RanGTP. This export complex is translocated through the NPC via specific interactions with the FG-repeat domains of nucleoporins. The nuclear export complex is disassembled at the cytoplasmic filaments of the NPC, where RanGAP hydrolyses RanGTP to RanGDP, which, in turn, dissociates the NES-cargo from the exportin. The export cycle is illustrated in Fig.1.4. (b).

#### 1.6.2.1. Exportins and other nuclear export factors

The first nuclear export receptor identified was CRM1/exportin 1 (1.5.(c)), which belongs to the importin- $\beta$ -family and directly binds to certain nucleoporins, such as Nup214, Nup88, and Nup558/RanBP2 (Fornerod, Ohno et al. 1997). The cytotoxin leptomycin B was found to interact with CRM1, thereby blocking the export of the Rev protein and U snRNAs (Fornerod, Ohno et al. 1997; Kutay, Bischoff et al. 1997). The export complex consisting of a cargo bearing a NES is exclusively formed in the presence of RanGTP.

The nuclear export receptor, required to transport importin  $\alpha$  back to the cytoplasm, is the exportin CAS (Kutay, Bischoff et al. 1997). The formation of the export complex of Cse1p, the yeast homologue

of CAS, with importin  $\alpha$  and RanGTP was studied in molecular detail (Matsuura and Stewart 2004; Fig. 1.5.(e)). Cse1p forms a super helix and C-terminal arches, that clamp around RanGTP. Simultaneously, Cse1p binds RanGTP with a high affinity and locks importin  $\alpha$  in a conformation, in which it cannot interact with other cargos. Cse1p possesses two Ran-binding sites. In the presence of a cargo like importin  $\alpha$ , Cse1p wraps around RanGTP so that both Ran-binding sites are engaged. These conformational changes in exportins couple cargo binding to high affinity for RanGTP, generating a spring-loaded molecule to facilitate disassembly of the export complex following GTP hydrolysis in the cytoplasm (Matsuura and Stewart 2004).

Analysis of the Mason–Pfizer monkey virus (MPMV) genome identified the constitutive transport element (CTE), a structured RNA element, that is required for the expression of viral structural proteins (Pasquinelli, Powers et al. 1997). Based on the finding that an excess of a CTE competitor inhibited nuclear export of mRNA, CTE was proposed to act as the target for a cellular nuclear RNA-export factor (Pasquinelli, Powers et al. 1997; Saavedra, Hammell et al. 1997).

Using biochemical approaches, Gruter et al. identified TAP/NXF1 as the cellular target of the MPMV CTE (Gruter, Tabernero et al. 1998). TAP differs from CRM1 in not being a member of the importin- $\beta$ -family of nucleocytoplasmic transport factors and not requiring the Ran GTPase as a cofactor (Clouse, Luo et al. 2001). TAP forms a heterodimer with a small cofactor, termed p15/TAP, and this interaction is essential for the high-affinity interaction of TAP with components of the NPC (Levesque, Guzik et al. 2001). TAP interacts directly with the FG-repeat nucleoporins Nup214, p62, and RanBP2 (Guzik, Levesque et al. 2001; Levesque, Guzik et al. 2001).

### ***1.6.2.2. mRNA nuclear export***

mRNA export is a highly regulated process, coupling the nuclear export of mRNA with its transcription, splicing, and processing (Cole and Scarcelli 2006; Stewart 2007). After transcription of mRNAs, dozens of factors participate in pre-RNA processing and packaging. mRNA export requires proper 3' processing, including addition of an poly(A) tail to the 3' end (Hammell, Gross et al. 2002; Brune, Munchel et al. 2005). The assembly of mRNA and proteins to form a major mRNP is not completely understood. Many proteins, e.g. the exon junction complex (EJC) or the poly(A) binding protein, Pab1, associate to mRNA during transcription, splicing, and polyadenylation (Dunn, Hammell et al. 2005; Bono, Ebert et al. 2006). Some of the mRNP proteins are removed before nuclear export, others accompany the

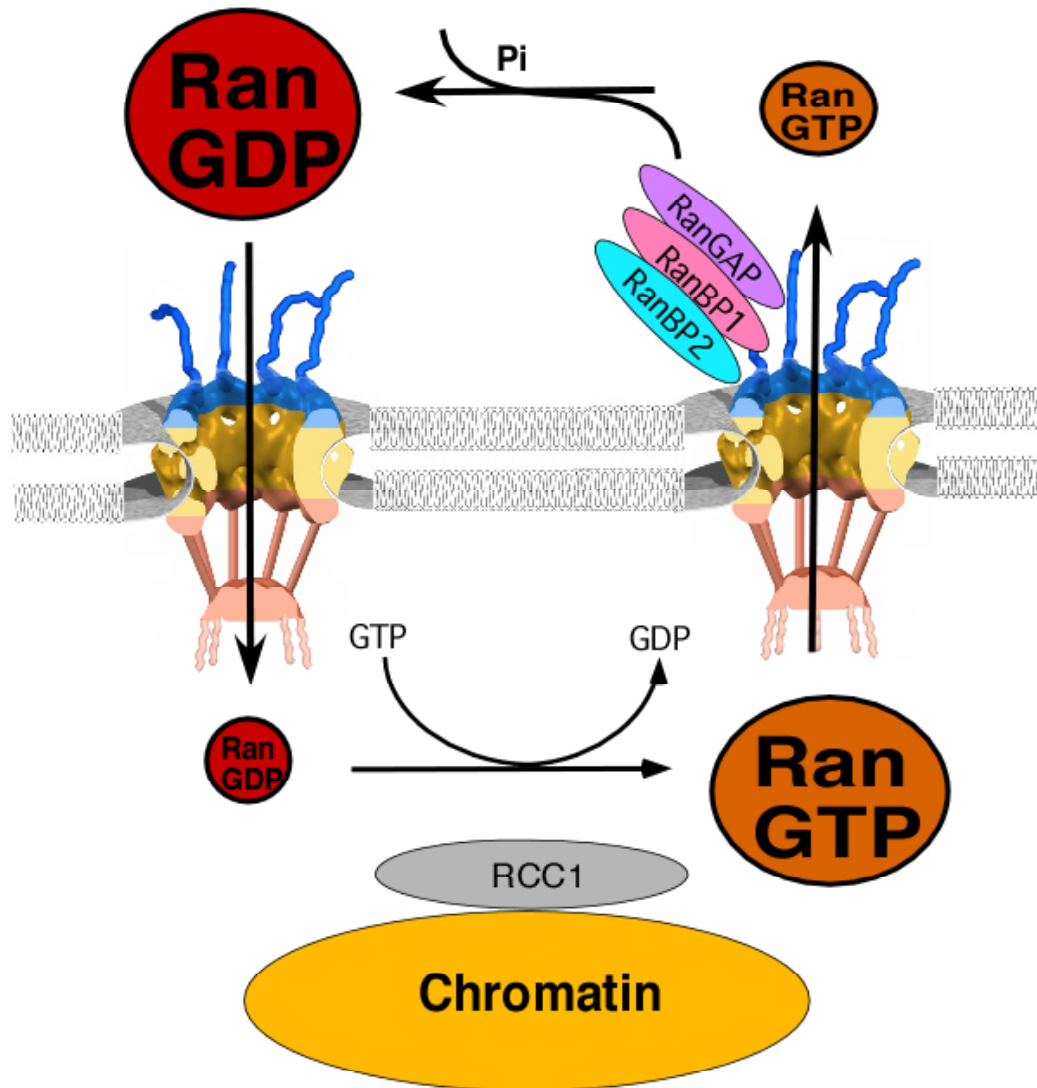


**Figure 1.6.** The RanGTPase cycle regulates the directionality of nucleocytoplasmic transport by binding and release of signal-bearing cargos from transport receptors. When RanGTP binds to an import cargo-receptor complex at the nuclear sphere of the NPC, the affinity between the cargo and the receptor is significantly lowered so that the cargo is released into the nucleus. The Ran gradient at the nuclear envelope is maintained by the asymmetric distribution of the Ran regulator across the nuclear double membrane. The Ran guanine-nucleotide exchange factor (RCC1) is bound to chromatin in the nucleus and initiates the dissociation of GDP from Ran and allows the binding of GTP. If RanGTP is exported from the nucleus, the Ran GTPase-activating protein (RanGAP) induces GTP hydrolysis by Ran in cooperation with the RanGTP-binding proteins (RanBP1 and RanBP2) at the cytoplasmic filaments of the NPC. Pi, inorganic phosphate.

mRNPs to the cytoplasm.

Transport of mRNP differs significantly from other karyopherin-mediated transports by the size of the cargo. One of the largest mRNPs are the Balbiani ring granules with a size of about 50 MD. It was determined that these large mRNPs pass through the central pore of the NPC with their 5' end entering the central pore of the NPC first (Daneshmandi 2001; Cheng, Dufu et al. 2006). Necessary for export of mRNPs is the heterodimer TAP/p15, which directly binds to the mRNA (Guzik, Levesque et al. 2001). It is

suggested that export of mRNP through the NPC is mediated by weak interaction between the TAP/p15 heterodimer and FG-repeat nucleoporins (Braun, Herold et al. 2002). Directionality of the translocation process is guaranteed by the disassembly of the mRNP export complex at the cytoplasmic side of the NPC.

Studies in yeast revealed the mechanism, how Mex67p, the yeast homologue of TAP, is removed from the mRNP. A central role in this context plays the DEAD-Box protein Dbp5p (Lund and Guthrie 2005). Dbp5p shuttles between the nucleus and cytoplasm and is recruited to the mRNPs during transcription. Nup159p, the yeast homologue of Nup214, a nucleoporin located on the cytoplasmic face of the NPC, possesses a  $\beta$ -propeller fold, which is able to bind Dbp5p (Weirich, Erzberger et al. 2004). Recent work showed that the ATPase activity of Dbp5p is stimulated by Gle1p and IP6 (Alcazar-Roman, Tran et al. 2006). Gle1p and IP6 are both anchored to the NPC through interactions with Nup100p and Nup42p/Rip1p (Strahm, Fahrenkrog et al. 1999). Therefore, all the proteins involved in remodeling the mRNP export complex are locally restricted to the cytoplasmic side of the NPC. Although the Dbp5p/Gle1p/IP6 interaction is important in mRNA export, the function of this complex is not well understood. Dbp5p may dissociate Mex67p from mRNPs by competing directly for a binding site on the mRNA or on the mRNP. Alternatively, the Dbp5p helicase activity of Dbp5p could alter the mRNA structure locally, thereby changing the conformation of the RNA, to which Mex67p is bound (Stewart 2007).

### ***1.6.2.3. tRNA export***

A unique feature among RNA export receptors is the ability of exportin-t (Exp-t) (Los1p in yeast) to bind directly to tRNA. Exp-t, a member of the importin- $\beta$ -family, is able to bind to a cargo and RanGTP cooperatively (Arts, Kuersten et al. 1998; Kutay, Lipowsky et al. 1998). Exp-t binds to the peripheral nucleoporins Nup153 and Nup358 in a RanGTP-dependent manner, whereas it does not require RanGTP to bind Nup214 (Kuersten, Arts et al. 2002). To ensure that only mature tRNA is exported, Exp-t binds much stronger to tRNA, which is base modified at its 5' and 3' ends, than to unmodified tRNA (Arts, Kuersten et al. 1998; Lund and Dahlberg 1998; Lipowsky, Bischoff et al. 1999). While Exp-t is the major tRNA export receptor, another important exportin, which mediates export of tRNA is Exportin 5 (Exp5) (Cole and Scarcelli 2006). Exp5 also binds directly to tRNAs in a RanGTP-dependent manner, but appears to bind different subsets of tRNAs as compared to Exp-t (Calado, Treichel et al. 2002). Exp 5 may not only export tRNAs but also other RNAs, which contain stable mini-helices (Gwizdek, Ossareh-Nazari et al. 2003; Lund, Guttinger et al. 2004). tRNAs are small and may also diffuse through the NPC,

although diffusion is expected to be slower than directed export.

### ***1.6.2.4. Export of ribosomal subunits***

Export of ribosomal subunits is also an energy-dependent, receptor-mediated process. Export of both 40S and 60S subunits has been shown to depend on functional Xpo1p and an intact RanGTPase system (Bataille, Helsner et al. 1990). An export adaptor for the export of 60S subunits is the yeast protein Nmd3p, a trans-acting factor associated with the late pre-60S particles. Nmd3p is a shuttling protein that has a C-terminal domain, which contains a leucine-rich NES. Deletion of the NES from Nmd3p leads to nuclear accumulation of the mutant protein and inhibition of the nuclear export of 60S subunits (Gadal, Strauss et al. 2001). Nmd3p shuttling and 60S export is also blocked by the CRM1p-specific inhibitor leptomycin B. This suggests that export of the 60S subunit is mediated by the adapter protein Nmd3p in a CRM1p-dependent pathway (Ho, Kallstrom et al. 2000). NMD3, the human homologue of Nmd3p, is also a shuttling protein, which binds to CRM1 via its C-terminal NES (Trotta, Lund et al. 2003). Another mediator of nuclear export implicated in pre-60S export is Mtr2p, a protein known for its essential role in mRNA export. Mtr2p was detected in late pre-60S particles in proteomic analysis of pre-ribosomes (Zemp and Kutay 2007). Recently, a new shuttling transport receptor, called Arx1p, was found, which is involved in the interaction with FG repeat nucleoporins and 60S subunit export (Bradatsch, Katahira et al. 2007). As NPC components required for the export of 60S particles, Nup214-Nup88 subcomplex in mammalian cells and the Nup84 subcomplex in yeast had been described (Bernad, Engelsma et al. 2006; Yao, Lutzmann et al. 2008)

Less is known about the export of the 40S subunit, but there are indications that 40S export is mediated by CRM1, too (Moy and Silver 1999; Moy and Silver 2002). A recent publication showed that maturation of the 18S rRNA is necessary for the proper export of 40S subunits (Rouquette, Choismel et al. 2005). Knock-down of Rps15 in HeLa cells by RNAi leads to nuclear accumulation of precursors of the 18S rRNA, thus Rps15 was suggested to act in nuclear export of pre-40S particles (Leger-Silvestre, Milkereit et al. 2004).

### ***1.6.2.5. Export of U snRNAs***

U snRNAs, such as U1, U2, and U5, are transcribed in the nucleus and acquire a monomethylated cap structure. U snRNAs are exported from the nucleus and bind to Sm proteins in the cytoplasm. After hypermethylation of the cap structure, the RNA-protein complexes are imported back into the nucleus, where they take part in pre-mRNA splicing (Mattaj, Dathan et al. 1988; Luhrmann 1990). The methylated cap structure is necessary for the export of the snRNPs via the CRM1/Xpo1p pathway (Hamm and Mattaj 1990; Fornerod, Ohno et al. 1997). The interaction between Xpo1p and U snRNA is mediated by two adaptor proteins. The nuclear cap binding complex (CBC) is a heterodimeric protein complex (Izaurrealde, Lewis et al. 1994; Izaurrealde, Lewis et al. 1995), which binds specifically to the monomethyl cap structure of nascent RNA polymerase II transcripts and promotes U snRNA export as well as pre-mRNA processing (Izaurrealde, Lewis et al. 1994; Izaurrealde, Lewis et al. 1995; Flaherty, Fortes et al. 1997).

The second adaptor protein is the recently identified phosphoprotein PHAX (Ohno, Segref et al. 2000). PHAX binds to both CBC and U snRNA, forming a trimeric complex, called the precomplex. The precomplex interacts with Xpo1p in a Ran-GTP dependent manner, forming the U snRNA export complex. For the formation of the export complex, phosphorylation of PHAX is required. After translocation of the complex to the cytoplasm, the U snRNA complex disassembles in a manner, that involves both hydrolysis of RanGTP and dephosphorylation of PHAX (Ohno, Segref et al. 2000).

### **1.6.3. Cargo translocation through the NPC**

Recently, it has been shown by Yang et al. by using single molecule fluorescence microscopy that transport cargo spends the majority of its 10 ms interaction time with the NPC associated with the central pore (Yang, Gelles et al. 2004). This suggests that the central pore might play a critical role during the transport process but in addition also in the control of the transport process. Therefore it is important to understand how the nucleoporins at the entry sides of the central pore work together to facilitate regulated transport. FG-repeat nucleoporins, which are known to interact directly with transport receptors via their FG-repeats, might play a critical role in this context (Hu, Guan et al. 1996; Bayliss, Littlewood et al. 2000; Matsuura, Lange et al. 2003).

One model, which explains cargo translocation through the nucleus and takes the localization of the FG-repeat nucleoporins at the entry sites of the central pore into consideration, is the virtual gating the-

ory (Rout, Aitchison et al. 2003). The virtual gating model describes the NPC as a translocation catalyst with an entropic barrier of FG-repeats on each entry side of the nuclear pore. Only cargo-complexes, which are able to specifically interact with FG-repeats, are able to overcome this barrier, whereas molecules ( $> 30\text{kDa}$ ), which do not specifically bind to FG-repeats, are hindered to enter the central pore. Directionality of nucleocytoplasmic transport is warranted by the Ran GTP/RanGDP gradient (Rout, Aitchison et al. 2003).

The experimental data of Lim et al. support the virtual gating model by showing that FG-repeat domains behave like polymer brushes on the nanomechanical scale and that the interaction of the FG-repeat domains with transport factors, such as importin  $\beta$ , affect the height of the brush, whereas unspecific cargos, such as bovine serum albumin, do not bind to the FG-repeat domain and cannot cause a collapse of the polymer brushes (Lim, Huang et al. 2006; Lim, Fahrenkrog et al. 2007). The collapse of the FG-repeat domains are reversed by the addition of RanGTP: RanGTP binds to importin  $\beta$ , importin  $\beta$  is removed from the FG-repeats, and the polymer brush is recovered. Nucleocytoplasmic transport might occur by continuously collapsing and recovery of the FG-repeat polymer brushes in the central pore, leading to a slow seeping of transport receptors, which specifically bind to the FG-repeat domains, through the central pore (Lim, Fahrenkrog et al. 2007).

A second model for cargo translocation through the NPC is the selective phase model, which predicts that FG-repeat nucleoporins residing in the central pore form a gel-like meshwork, which acts as a barrier for unspecific macromolecules and allows selectively passage of nuclear transport receptors (Ribbeck and Gorlich 2001). Experimentally, the formation of the gel from FG-repeat domains of the yeast nucleoporin Nsp1p could be demonstrated and calculated. Transport rates to the macroscopic gel were similar to those observed in NPCs of cells, but transport of transport receptors through the saturated gels consisting of FG-repeat domains was irreversible (Frey, Richter et al. 2006; Frey and Gorlich 2007).

In contrast to the demonstrated importance of FG-repeat domains for nucleocytoplasmic transport, some recent studies in yeast (Strawn, Shen et al. 2004; Zeitler and Weis 2004) showed that depletion of some FG-repeats does not significantly affect the nucleocytoplasmic transport or the viability of cells and that „asymmetric“ FG-repeats can be inversed with no effect on the nuclear import or export. In addition, Strawn et al. described after combinative depletion of several FG-repeat nucleoporins a minimal NPC pore, which enables yeast cells to survive (Strawn, Shen et al. 2004). All these papers, focused on the function of FG-repeat nucleoporins at the NPC, show the importance of these components for the function of the NPC.

## 1.7. Function of nucleoporins beyond the nucleocytoplasmic transport

In recent years, it became obvious that nucleoporins are not only involved in nucleocytoplasmic transport, but additionally play an important role in other fundamental cellular processes, such as the nuclear envelope breakdown (NEBD), mitosis, apoptosis, viral infection, and mitotic remodeling of the NE (Cronshaw and Matunis 2004; Greber and Fornerod 2005; Hetzer, Walther et al. 2005; Fahrenkrog 2006; Tran and Wentz 2006).

A number of nucleoporins interact with the mitotic machinery. The nucleoporin Nup358, for instance, is attached to the kinetochores during mitosis (Salina, Enarson et al. 2003), and the Nup107-160 complex is critical for correct bipolar spindle assembly (Zuccolo, Alves et al. 2007). Depletion of Nup155 results in a block of nuclear reformation after mitosis (Franz, Askjaer et al. 2005). Blower et al. demonstrated that Rael, a protein, which has been implicated in mRNA nuclear export, is required for spindle assembly (Blower, Nachury et al. 2005). Additionally, van Deusen and coworkers found that the Rael-Nup98 complex is a temporal regulator of the anaphase promoting complex and maintains euploidy by preventing unscheduled degradation of securin (Jeganathan, Malureanu et al. 2005). Therefore, nucleoporins may more generally have regulatory functions during mitosis but the function of most nucleoporins during mitosis remains obscure.

Recently, it was reported that the expression of certain subtypes of importin  $\alpha$ , a transport receptor, is strictly regulated in embryonic stem cells triggering neuronal differentiation (Yasuhara, Shibasaki et al. 2007). Thus, importin  $\alpha$  subtype switching may have an impact on cell differentiation due to regulated nuclear import of a specific set of transcription factors, suggesting that regulation of the transport machinery might more generally play a role in cell differentiation and development.

Several chromosomal alterations of nucleoporin genes, which produce oncogenic fusion proteins, were observed in different cancers. The gene encoding Nup98, for example, is associated with leukemic transformations (Lam and Aplan 2001). Fusion partners of many Nup98 translocations are genes of the homeobox (HOX) family of transcription factors (Suzuki, Ito et al. 2002). As described above, the nucleoporin Rael, which interacts with Nup98 is a regulator of mitotic checkpoint activation (Babu, Jeganathan et al. 2003). Rael deficiency results in a defective mitotic checkpoint, an increased rate of chromosome misaggregation and increased susceptibility to tumor formation in mice (Jeganathan, Malureanu et



al. 2005). Alterations of the Nup214 gene associated with myeloid leukemia, were found in two different chromosomal translocations, that fuse it to genes, encoding the DNA- associated proteins DEK and SET (von Lindern, van Baal et al. 1992). In addition, overexpression of Nup88 was found in malignant tumors of many types and its association with human tumors might be related to aberrant control of specific signal transduction pathways (Martinez, Alonso et al. 1999).

Autoantibodies against the nucleoporins p62 and gp210 are involved in the autoimmune disease primary biliary cirrhosis (PBC) and appear to be correlated with more advanced stages of PBC (Enarson, Rattner et al. 2004; Worman and Courvalin 2003).

Nucleoporin-associated diseases and diseases linked to nucleocytoplasmic transport might become a major research focus of the NPC research. Moreover, examination of the cell growth and the epigenetic regulation linked to the NPC is an expanding issue in the nucleocytoplasmic transport research (Schneider and Grosschedl 2007).

## 1.8. References

- Aitchison, J. D., M. P. Rout, et al. (1995). „Two novel related yeast nucleoporins Nup170p and Nup157p: complementation with the vertebrate homologue Nup155p and functional interactions with the yeast nuclear pore-membrane protein Pom152p.“ J Cell Biol 131(5): 1133-48.
- Akey, C. W. and M. Radermacher (1993). “Architecture of the *Xenopus* nuclear pore complex revealed by three-dimensional cryo-electron microscopy.” J Cell Biol 122(1): 1-19.
- Alcazar-Roman, A. R., E. J. Tran, et al. (2006). „Inositol hexakisphosphate and Gle1 activate the DEAD-box protein Dbp5 for nuclear mRNA export.“ Nat Cell Biol 8(7): 711-6.
- Arts, G. J., S. Kuersten, et al. (1998). „The role of exportin-t in selective nuclear export of mature tRNAs.“ Embo J 17(24): 7430-41.
- Babu, J. R., K. B. Jeganathan, et al. (2003). “Rae1 is an essential mitotic checkpoint regulator that cooperates with Bub3 to prevent chromosome missegregation.” J Cell Biol 160(3): 341-53.
- Basel-Vanagaite, L., L. Muncher, et al. (2006). „Mutated nup62 causes autosomal recessive infantile bilateral striatal necrosis.“ Ann Neurol 60(2): 214-22.
- Bataille, N., T. Helser, et al. (1990). „Cytoplasmic transport of ribosomal subunits microinjected into the *Xenopus laevis* oocyte nucleus: a generalized, facilitated process.“ J Cell Biol 111(4): 1571-82.
- Bayliss, R., T. Littlewood, et al. (2000). „Structural basis for the interaction between FxFG nucleoporin repeats and importin-beta in nuclear trafficking.“ Cell 102(1): 99-108.
- Beck, M., F. Forster, et al. (2004). „Nuclear pore complex structure and dynamics revealed by cryoelectron tomography.“ Science 306(5700): 1387-90.
- Beck, M., V. Lucic, et al. (2007). „Snapshots of nuclear pore complexes in action captured by cryo-electron tomography.“ Nature 449(7162): 611-5.

## CHAPTER 1: INTRODUCTION: NUCLEOPORINS OF THE CENTRAL REGION OF THE NPC

- Belgareh, N., G. Rabut, et al. (2001). „An evolutionarily conserved NPC subcomplex, which redistributes in part to kinetochores in mammalian cells.“ *J Cell Biol* 154(6): 1147-60.
- Bernad, R., D. Engelsma, et al. (2006). “Nup214-Nup88 nucleoporin subcomplex is required for CRM1-mediated 60 S preribosomal nuclear export.” *J Biol Chem* 281(28): 19378-86.
- Bischoff, F. R., C. Klebe, et al. (1994). „RanGAP1 induces GTPase activity of nuclear Ras-related Ran.“ *Proc Natl Acad Sci U S A* 91(7): 2587-91.
- Blower, M. D., M. Nachury, et al. (2005). “A Rae1-containing ribonucleoprotein complex is required for mitotic spindle assembly.” *Cell* 121(2): 223-234.
- Bodoor, K., S. Shaikh, et al. (1999). „Sequential recruitment of NPC proteins to the nuclear periphery at the end of mitosis.“ *J Cell Sci* 112 ( Pt 13): 2253-64.
- Boehmer, T., J. Enninga, et al. (2003). „Depletion of a single nucleoporin, Nup107, prevents the assembly of a subset of nucleoporins into the nuclear pore complex.“ *Proc Natl Acad Sci U S A* 100(3): 981-5.
- Bogerd, H. P., R. A. Fridell, et al. (1996). „Protein sequence requirements for function of the human T-cell leukemia virus type 1 Rex nuclear export signal delineated by a novel in vivo randomization-selection assay.“ *Mol Cell Biol* 16(8): 4207-14.
- Bono, F., J. Ebert, et al. (2006). „The crystal structure of the exon junction complex reveals how it maintains a stable grip on mRNA.“ *Cell* 126(4): 713-25.
- Bradatsch, B., J. Katahira, et al. (2007). “Arx1 functions as an unorthodox nuclear export receptor for the 60S preribosomal subunit.” *Mol Cell* 27(5): 767-79.
- Braun, I. C., A. Herold, et al. (2002). „Nuclear export of mRNA by TAP/NXF1 requires two nucleoporin-binding sites but not p15.“ *Mol Cell Biol* 22(15): 5405-18.

## CHAPTER 1: INTRODUCTION: NUCLEOPORINS OF THE CENTRAL REGION OF THE NPC

- Brune, C., S. E. Munchel, et al. (2005). „Yeast poly(A)-binding protein Pab1 shuttles between the nucleus and the cytoplasm and functions in mRNA export.“ *Rna* 11(4): 517-31.
- Buss, F. and M. Stewart (1995). „Macromolecular interactions in the nucleoporin p62 complex of rat nuclear pores: binding of nucleoporin p54 to the rod domain of p62.“ *J Cell Biol* 128(3): 251-61.
- Bustamante, J. O., E. R. Michelette, et al. (2000). „Calcium, ATP and nuclear pore channel gating.“ *Pflugers Arch* 439(4): 433-44.
- Calado, A., N. Treichel, et al. (2002). „Exportin-5-mediated nuclear export of eukaryotic elongation factor 1A and tRNA.“ *Embo J* 21(22): 6216-24.
- Carmo-Fonseca, M., H. Kern, et al. (1991). „Human nucleoporin p62 and the essential yeast nuclear pore protein NSP1 show sequence homology and a similar domain organization.“ *Eur J Cell Biol* 55(1): 17-30.
- Cheng, H., K. Dufu, et al. (2006). „Human mRNA export machinery recruited to the 5' end of mRNA.“ *Cell* 127(7): 1389-400.
- Chook, Y. M. and G. Blobel (1999). „Structure of the nuclear transport complex karyopherin-beta2-Ran x GppNHp.“ *Nature* 399(6733): 230-7.
- Cingolani, G., C. Petosa, et al. (1999). „Structure of importin-beta bound to the IBB domain of importin-alpha.“ *Nature* 399(6733): 221-9.
- Clouse, K. N., M. J. Luo, et al. (2001). „A Ran-independent pathway for export of spliced mRNA.“ *Nat Cell Biol* 3(1): 97-9.
- Cole, C. N. and J. J. Scarcelli (2006). „Transport of messenger RNA from the nucleus to the cytoplasm.“ *Curr Opin Cell Biol* 18(3): 299-306.

## CHAPTER 1: INTRODUCTION: NUCLEOPORINS OF THE CENTRAL REGION OF THE NPC

- Conti, E., C. W. Muller, et al. (2006). „Karyopherin flexibility in nucleocytoplasmic transport.“  
Curr Opin Struct Biol 16(2): 237-44.
- Conti, E., M. Uy, et al. (1998). „Crystallographic analysis of the recognition of a nuclear localization signal by the nuclear import factor karyopherin alpha.“ Cell 94(2): 193-204.
- Cordes, V. C. and G. Krohne (1993). „Sequential O-glycosylation of nuclear pore complex protein gp62 in vitro.“ Eur J Cell Biol 60(1): 185-95.
- Cronshaw, J. M., A. N. Krutchinsky, et al. (2002). „Proteomic analysis of the mammalian nuclear pore complex.“ J Cell Biol 158(5): 915-27.
- Cronshaw, J. M. and M. J. Matunis (2004). „The nuclear pore complex: disease associations and functional correlations.“ Trends Endocrinol Metab 15(1): 34-9.
- Dabauvalle, M. C., R. Benavente, et al. (1988). „Monoclonal antibodies to a Mr 68,000 pore complex glycoprotein interfere with nuclear protein uptake in *Xenopus* oocytes.“  
Chromosoma 97(3): 193-7.
- Daneholt, B. (2001). „Assembly and transport of a premessenger RNP particle.“ Proc Natl Acad Sci U S A 98(13): 7012-7.
- Davis, L. I. and G. Blobel (1986). „Identification and characterization of a nuclear pore complex protein.“ Cell 45(5): 699-709.
- Davis, L. I. and G. Blobel (1987). „Nuclear pore complex contains a family of glycoproteins that includes p62: glycosylation through a previously unidentified cellular pathway.“  
Proc Natl Acad Sci U S A 84(21): 7552-6.
- Deane, R., W. Schafer, et al. (1997). „Ran-binding protein 5 (RanBP5) is related to the nuclear transport factor importin-beta but interacts differently with RanBP1.“ Mol Cell Biol 17(9): 5087-96.

## CHAPTER 1: INTRODUCTION: NUCLEOPORINS OF THE CENTRAL REGION OF THE NPC

- Delphin, C., T. Guan, et al. (1997). „RanGTP targets p97 to RanBP2, a filamentous protein localized at the cytoplasmic periphery of the nuclear pore complex.“ *Mol Biol Cell* 8(12): 2379-90.
- Devos, D., S. Dokudovskaya, et al. (2004). „Components of coated vesicles and nuclear pore complexes share a common molecular architecture.“ *PLoS Biol* 2(12): e380.
- Dingwall, C., S. V. Sharnick, et al. (1982). „A polypeptide domain that specifies migration of nucleoplasmin into the nucleus.“ *Cell* 30(2): 449-58.
- Dunn, E. F., C. M. Hammell, et al. (2005). „Yeast poly(A)-binding protein, Pab1, and PAN, a poly(A) nuclease complex recruited by Pab1, connect mRNA biogenesis to export.“ *Genes Dev* 19(1): 90-103.
- Enarson, P., J. B. Rattner, et al. (2004). „Autoantigens of the nuclear pore complex.“ *J Mol Med* 82(7): 423-33.
- Fahrenkrog, B. (2006). „The nuclear pore complex, nuclear transport, and apoptosis.“ *Can J Physiol Pharmacol* 84(3-4): 279-86.
- Fahrenkrog, B. and U. Aebi (2003). „The nuclear pore complex: nucleocytoplasmic transport and beyond.“ *Nat Rev Mol Cell Biol* 4(10): 757-66.
- Fahrenkrog, B., E. C. Hurt, et al. (1998). „Molecular architecture of the yeast nuclear pore complex: localization of Nsp1p subcomplexes.“ *J Cell Biol* 143(3): 577-88.
- Fahrenkrog, B., J. Koser, et al. (2004). „The nuclear pore complex: a jack of all trades?“ *Trends Biochem Sci* 29(4): 175-82.
- Feldherr, C. M. and D. Akin (1997). „The location of the transport gate in the nuclear pore complex.“ *J Cell Sci* 110 ( Pt 24): 3065-70.
- Finlay, D. R., E. Meier, et al. (1991). „A complex of nuclear pore proteins required for pore function.“ *J Cell Biol* 114(1): 169-83.

## CHAPTER 1: INTRODUCTION: NUCLEOPORINS OF THE CENTRAL REGION OF THE NPC

- Fischer, U., J. Huber, et al. (1995). „The HIV-1 Rev activation domain is a nuclear export signal that accesses an export pathway used by specific cellular RNAs.“ *Cell* 82(3): 475-83.
- Flaherty, S. M., P. Fortes, et al. (1997). „Participation of the nuclear cap binding complex in pre-mRNA 3' processing.“ *Proc Natl Acad Sci U S A* 94(22): 11893-8.
- Fornerod, M., M. Ohno, et al. (1997). „CRM1 is an export receptor for leucine-rich nuclear export signals.“ *Cell* 90(6): 1051-60.
- Franz, C., P. Askjaer, et al. (2005). „Nup155 regulates nuclear envelope and nuclear pore complex formation in nematodes and vertebrates.“ *Embo J* 24(20): 3519-31.
- Frey, S. and D. Gorlich (2007). „A saturated FG-repeat hydrogel can reproduce the permeability properties of nuclear pore complexes.“ *Cell* 130(3): 512-23.
- Frey, S., R. P. Richter, et al. (2006). „FG-rich repeats of nuclear pore proteins form a three-dimensional meshwork with hydrogel-like properties.“ *Science* 314(5800): 815-7.
- Fried, H. and U. Kutay (2003). „Nucleocytoplasmic transport: taking an inventory.“ *Cell Mol Life Sci* 60(8): 1659-88.
- Fukuhara, T., N. Sakaguchi, et al. (2006). „Functional analysis of nuclear pore complex protein Nup62/p62 using monoclonal antibodies.“ *Hybridoma (Larchmt)* 25(2): 51-9.
- Gadal, O., D. Strauss, et al. (2001). „Nuclear export of 60s ribosomal subunits depends on Xpolp and requires a nuclear export sequence-containing factor, Nmd3p, that associates with the large subunit protein Rpl10p.“ *Mol Cell Biol* 21(10): 3405-15.
- Galy, V., I. W. Mattaj, et al. (2003). „Caenorhabditis elegans nucleoporins Nup93 and Nup205 determine the limit of nuclear pore complex size exclusion in vivo.“ *Mol Biol Cell* 14(12): 5104-15.
- Gorlich, D., N. Pante, et al. (1996). „Identification of different roles for RanGDP and RanGTP in nuclear protein import.“ *Embo J* 15(20): 5584-94.

## CHAPTER 1: INTRODUCTION: NUCLEOPORINS OF THE CENTRAL REGION OF THE NPC

- Gorlich, D., S. Prehn, et al. (1994). „Isolation of a protein that is essential for the first step of nuclear protein import.“ *Cell* 79(5): 767-78.
- Grandi, P., T. Dang, et al. (1997). „Nup93, a vertebrate homologue of yeast Nic96p, forms a complex with a novel 205-kDa protein and is required for correct nuclear pore assembly.“ *Mol Biol Cell* 8(10): 2017-38.
- Greber, U. F. and M. Fornerod (2005). „Nuclear import in viral infections.“ *Curr Top Microbiol Immunol* 285: 109-38.
- Gruter, P., C. Taberner, et al. (1998). „TAP, the human homolog of Mex67p, mediates CTE-dependent RNA export from the nucleus.“ *Mol Cell* 1(5): 649-59.
- Guan, T., S. Muller, et al. (1995). „Structural analysis of the p62 complex, an assembly of O-linked glycoproteins that localizes near the central gated channel of the nuclear pore complex.“ *Mol Biol Cell* 6(11): 1591-603.
- Gustin, K. E. and P. Sarnow (2002). „Inhibition of nuclear import and alteration of nuclear pore complex composition by rhinovirus.“ *J Virol* 76(17): 8787-96.
- Guzik, B. W., L. Levesque, et al. (2001). „NXT1 (p15) is a crucial cellular cofactor in TAP-dependent export of intron-containing RNA in mammalian cells.“ *Mol Cell Biol* 21(7): 2545-54.
- Gwizdek, C., B. Ossareh-Nazari, et al. (2003). „Exportin-5 mediates nuclear export of minihelix-containing RNAs.“ *J Biol Chem* 278(8): 5505-8.
- Hamm, J. and I. W. Mattaj (1990). „Monomethylated cap structures facilitate RNA export from the nucleus.“ *Cell* 63(1): 109-18.
- Hammell, C. M., S. Gross, et al. (2002). „Coupling of termination, 3' processing, and mRNA export.“ *Mol Cell Biol* 22(18): 6441-57.



## CHAPTER 1: INTRODUCTION: NUCLEOPORINS OF THE CENTRAL REGION OF THE NPC

Hanover, J. A., C. K. Cohen, et al. (1987). „O-linked N-acetylglucosamine is attached to proteins of the nuclear pore. Evidence for cytoplasmic and nucleoplasmic glycoproteins.“

J Biol Chem 262(20): 9887-94.

Harel, A., A. V. Orjalo, et al. (2003). „Removal of a single pore subcomplex results in vertebrate nuclei devoid of nuclear pores.“ Mol Cell 11(4): 853-64.

Hawryluk-Gara, L. A., E. K. Shibuya, et al. (2005). „Vertebrate Nup53 interacts with the nuclear lamina and is required for the assembly of a Nup93-containing complex.“

Mol Biol Cell 16(5): 2382-94.

Hetzer, M. W., T. C. Walther, et al. (2005). „Pushing the envelope: structure, function, and dynamics of the nuclear periphery.“ Annu Rev Cell Dev Biol 21: 347-80.

Hinshaw, J. E., B. O. Carragher, et al. (1992). „Architecture and design of the nuclear pore complex.“

Cell 69(7): 1133-41.

Ho, J. H., G. Kallstrom, et al. (2000). „Nmd3p is a Crm1p-dependent adapter protein for nuclear export of the large ribosomal subunit.“ J Cell Biol 151(5): 1057-66.

Hodel, A. E., M. R. Hodel, et al. (2002). „The three-dimensional structure of the autoproteolytic, nuclear pore-targeting domain of the human nucleoporin Nup98.“ Mol Cell 10(2): 347-58.

Hu, T., T. Guan, et al. (1996). „Molecular and functional characterization of the p62 complex, an assembly of nuclear pore complex glycoproteins.“ J Cell Biol 134(3): 589-601.

Izaurralde, E., J. Lewis, et al. (1995). „A cap-binding protein complex mediating U snRNA export.“ Nature 376(6542): 709-12.

Izaurralde, E., J. Lewis, et al. (1994). „A nuclear cap binding protein complex involved in pre-mRNA splicing.“ Cell 78(4): 657-68.

## CHAPTER 1: INTRODUCTION: NUCLEOPORINS OF THE CENTRAL REGION OF THE NPC

- Jakel, S. and D. Gorlich (1998). „Importin beta, transportin, RanBP5 and RanBP7 mediate nuclear import of ribosomal proteins in mammalian cells.“ *Embo J* 17(15): 4491-502.
- Jakel, S., J. M. Mingot, et al. (2002). „Importins fulfil a dual function as nuclear import receptors and cytoplasmic chaperones for exposed basic domains.“ *Embo J* 21(3): 377-86.
- Jarnik, M. and U. Aebi (1991). „Toward a more complete 3-D structure of the nuclear pore complex.“ *J Struct Biol* 107(3): 291-308.
- Jeganathan, K. B., L. Malureanu, et al. (2005). “The Rae1-Nup98 complex prevents aneuploidy by inhibiting securin degradation.” *Nature* 438(7070): 1036-9.
- Kalab, P., K. Weis, et al. (2002). „Visualization of a Ran-GTP gradient in interphase and mitotic *Xenopus* egg extracts.“ *Science* 295(5564): 2452-6.
- Kalderon, D., W. D. Richardson, et al. (1984). „Sequence requirements for nuclear location of simian virus 40 large-T antigen.“ *Nature* 311(5981): 33-8.
- Kataoka, N., J. L. Bachorik, et al. (1999). „Transportin-SR, a nuclear import receptor for SR proteins.“ *J Cell Biol* 145(6): 1145-52.
- Kehlenbach, R. H., A. Dickmanns, et al. (1999). „A role for RanBP1 in the release of CRM1 from the nuclear pore complex in a terminal step of nuclear export.“ *J Cell Biol* 145(4): 645-57.
- Klebe, C., F. R. Bischoff, et al. (1995). „Interaction of the nuclear GTP-binding protein Ran with its regulatory proteins RCC1 and RanGAP1.“ *Biochemistry* 34(2): 639-47.
- Kobe, B. (1999). „Autoinhibition by an internal nuclear localization signal revealed by the crystal structure of mammalian importin alpha.“ *Nat Struct Biol* 6(4): 388-97.
- Krull, S., J. Thyberg, et al. (2004). „Nucleoporins as components of the nuclear pore complex core structure and Tpr as the architectural element of the nuclear basket.“ *Mol Biol Cell* 15(9): 4261-77.

## CHAPTER 1: INTRODUCTION: NUCLEOPORINS OF THE CENTRAL REGION OF THE NPC

- Kuersten, S., G. J. Arts, et al. (2002). „Steady-state nuclear localization of exportin-t involves RanGTP binding and two distinct nuclear pore complex interaction domains.“  
Mol Cell Biol 22(16): 5708-20.
- Kutay, U., F. R. Bischoff, et al. (1997). „Export of importin alpha from the nucleus is mediated by a specific nuclear transport factor.“ Cell 90(6): 1061-71.
- Kutay, U., E. Izaurralde, et al. (1997). „Dominant-negative mutants of importin-beta block multiple pathways of import and export through the nuclear pore complex.“ Embo J 16(6): 1153-63.
- Kutay, U., G. Lipowsky, et al. (1998). „Identification of a tRNA-specific nuclear export receptor.“  
Mol Cell 1(3): 359-69.
- Lam, D. H. and P. D. Aplan (2001). “NUP98 gene fusions in hematologic malignancies.”  
Leukemia 15(11): 1689-95.
- Lee, B. J., A. E. Cansizoglu, et al. (2006). „Rules for nuclear localization sequence recognition by karyopherin beta 2.“ Cell 126(3): 543-58.
- Lee, S. J., Y. Matsuura, et al. (2005). „Structural basis for nuclear import complex dissociation by RanGTP.“ Nature 435(7042): 693-6.
- Leger-Silvestre, I., P. Milkereit, et al. (2004). “The ribosomal protein Rps15p is required for nuclear exit of the 40S subunit precursors in yeast.” Embo J 23(12): 2336-47.
- Levesque, L., B. Guzik, et al. (2001). „RNA export mediated by tap involves NXT1-dependent interactions with the nuclear pore complex.“ J Biol Chem 276(48): 44953-62.
- Lim, R. Y., B. Fahrenkrog, et al. (2007). „Nanomechanical Basis of Selective Gating by the Nuclear Pore Complex.“ Science 318(5850): 640-643
- Lim, R. Y., N. P. Huang, et al. (2006). „Flexible phenylalanine-glycine nucleoporins as entropic barriers to nucleocytoplasmic transport.“ Proc Natl Acad Sci U S A 103(25): 9512-7

## CHAPTER 1: INTRODUCTION: NUCLEOPORINS OF THE CENTRAL REGION OF THE NPC

- Lipowsky, G., F. R. Bischoff, et al. (1999). „Coordination of tRNA nuclear export with processing of tRNA.“ *Rna* 5(4): 539-49.
- Liodice, I., A. Alves, et al. (2004). „The entire Nup107-160 complex, including three new members, is targeted as one entity to kinetochores in mitosis.“ *Mol Biol Cell* 15(7): 3333-44.
- Luhrmann, R. (1990). „Functions of U-snRNPs.“ *Mol Biol Rep* 14(2-3): 183-92.
- Lund, E. and J. E. Dahlberg (1998). „Proofreading and aminoacylation of tRNAs before export from the nucleus.“ *Science* 282(5396): 2082-5.
- Lund, M. K. and C. Guthrie (2005). „The DEAD-box protein Dbp5p is required to dissociate Mex67p from exported mRNPs at the nuclear rim.“ *Mol Cell* 20(4): 645-51.
- Lund, E., S. Guttinger, et al. (2004). „Nuclear export of microRNA precursors.“ *Science* 303(5654): 95-8.
- Lutzmann, M., R. Kunze, et al. (2002). „Modular self-assembly of a Y-shaped multiprotein complex from seven nucleoporins.“ *Embo J* 21(3): 387-97.
- Lutzmann, M., R. Kunze, et al. (2005). „Reconstitution of Nup157 and Nup145N into the Nup84 complex.“ *J Biol Chem* 280(18): 18442-51.
- Makhnevych, T., C. P. Lusk, et al. (2003). „Cell cycle regulated transport controlled by alterations in the nuclear pore complex.“ *Cell* 115(7): 813-23.
- Mansfeld, J., S. Guttinger, et al. (2006). „The conserved transmembrane nucleoporin NDC1 is required for nuclear pore complex assembly in vertebrate cells.“ *Mol Cell* 22(1): 93-103.
- Martinez, N., A. Alonso, et al. (1999). “The nuclear pore complex protein Nup88 is overexpressed in tumor cells.” *Cancer Res* 59(21): 5408-11.

## CHAPTER 1: INTRODUCTION: NUCLEOPORINS OF THE CENTRAL REGION OF THE NPC

- Matsuoka, Y., M. Takagi, et al. (1999). „Identification and characterization of nuclear pore subcomplexes in mitotic extract of human somatic cells.“  
Biochem Biophys Res Commun 254(2): 417-23.
- Matsuura, Y., A. Lange, et al. (2003). „Structural basis for Nup2p function in cargo release and karyopherin recycling in nuclear import.“ Embo J 22(20): 5358-69.
- Matsuura, Y. and M. Stewart (2004). „Structural basis for the assembly of a nuclear export complex.“  
Nature 432(7019): 872-7.
- Mattaj, I. W., N. A. Dathan, et al. (1988). „Changing the RNA polymerase specificity of U snRNA gene promoters.“ Cell 55(3): 435-42.
- Melcak, I., A. Hoelz, et al. (2007). „Structure of Nup58/45 suggests flexible nuclear pore diameter by intermolecular sliding.“ Science 315(5819): 1729-32.
- Michael, W. M., M. Choi, et al. (1995). „A nuclear export signal in hnRNP A1: a signal-mediated, temperature-dependent nuclear protein export pathway.“ Cell 83(3): 415-22.
- Miller, B. R., M. Powers, et al. (2000). „Identification of a new vertebrate nucleoporin, Nup188, with the use of a novel organelle trap assay.“ Mol Biol Cell 11(10): 3381-96.
- Moy, T. I. and P. A. Silver (1999). „Nuclear export of the small ribosomal subunit requires the ran-GTPase cycle and certain nucleoporins.“ Genes Dev 13(16): 2118-33.
- Moy, T. I. and P. A. Silver (2002). „Requirements for the nuclear export of the small ribosomal subunit.“  
J Cell Sci 115(Pt 14): 2985-95.
- Muhlhausser, P., E. C. Muller, et al. (2001). „Multiple pathways contribute to nuclear import of core histones.“ EMBO Rep 2(8): 690-6.
- Nehrbass, U. and G. Blobel (1996). „Role of the nuclear transport factor p10 in nuclear import.“  
Science 272(5258): 120-2

## CHAPTER 1: INTRODUCTION: NUCLEOPORINS OF THE CENTRAL REGION OF THE NPC

- Oberleithner, H., H. Schillers, et al. (2000). „Nuclear pores collapse in response to CO<sub>2</sub> imaged with atomic force microscopy.“ *Pflugers Arch* 439(3): 251-5.
- Ohno, M., A. Segref, et al. (2000). „PHAX, a mediator of U snRNA nuclear export whose activity is regulated by phosphorylation.“ *Cell* 101(2): 187-98.
- Ohtsubo, M., H. Okazaki, et al. (1989). „The RCC1 protein, a regulator for the onset of chromosome condensation locates in the nucleus and binds to DNA.“ *J Cell Biol* 109(4 Pt 1): 1389-97.
- Orjalo, A. V., A. Arnautov, et al. (2006). „The Nup107-160 nucleoporin complex is required for correct bipolar spindle assembly.“ *Mol Biol Cell* 17(9): 3806-18.
- Pante, N. and U. Aebi (1996). „Sequential binding of import ligands to distinct nucleopore regions during their nuclear import.“ *Science* 273(5282): 1729-32.
- Pante, N., R. Bastos, et al. (1994). „Interactions and three-dimensional localization of a group of nuclear pore complex proteins.“ *J Cell Biol* 126(3): 603-17.
- Pante, N. and M. Kann (2002). „Nuclear pore complex is able to transport macromolecules with diameters of about 39 nm.“ *Mol Biol Cell* 13(2): 425-34.
- Pasquinelli, A. E., M. A. Powers, et al. (1997). „Inhibition of mRNA export in vertebrate cells by nuclear export signal conjugates.“ *Proc Natl Acad Sci U S A* 94(26): 14394-9.
- Patre, M., A. Tabbert, et al. (2006). „Caspases target only two architectural components within the core structure of the nuclear pore complex.“ *J Biol Chem* 281(2): 1296-304.
- Pemberton, L. F. and B. M. Paschal (2005). „Mechanisms of receptor-mediated nuclear import and nuclear export.“ *Traffic* 6(3): 187-98.
- Plafker, S. M. and I. G. Macara (2000). „Importin-11, a nuclear import receptor for the ubiquitin-conjugating enzyme, UbcM2.“ *Embo J* 19(20): 5502-13.

## CHAPTER 1: INTRODUCTION: NUCLEOPORINS OF THE CENTRAL REGION OF THE NPC

- Rabut, G., V. Doye, et al. (2004). „Mapping the dynamic organization of the nuclear pore complex inside single living cells.“ *Nat Cell Biol* 6(11): 1114-21.
- Rabut, G., P. Lenart, et al. (2004). „Dynamics of nuclear pore complex organization through the cell cycle.“ *Curr Opin Cell Biol* 16(3): 314-21.
- Radu, A., G. Blobel, et al. (1993). „Nup155 is a novel nuclear pore complex protein that contains neither repetitive sequence motifs nor reacts with WGA.“ *J Cell Biol* 121(1): 1-9.
- Radu, A., G. Blobel, et al. (1994). „Nup107 is a novel nuclear pore complex protein that contains a leucine zipper.“ *J Biol Chem* 269(26): 17600-5.
- Rayala, H. J., F. Kendirgi, et al. (2004). „The mRNA export factor human Gle1 interacts with the nuclear pore complex protein Nup155.“ *Mol Cell Proteomics* 3(2): 145-55.
- Reichelt, R., A. Holzenburg, et al. (1990). „Correlation between structure and mass distribution of the nuclear pore complex and of distinct pore complex components.“ *J Cell Biol* 110(4): 883-94.
- Rexach, M. and G. Blobel (1995). „Protein import into nuclei: association and dissociation reactions involving transport substrate, transport factors, and nucleoporins.“ *Cell* 83(5): 683-92.
- Ribbeck, K. and D. Gorlich (2001). „Kinetic analysis of translocation through nuclear pore complexes.“ *Embo J* 20(6): 1320-30.
- Ribbeck, K., G. Lipowsky, et al. (1998). „NTF2 mediates nuclear import of Ran.“ *Embo J* 17(22): 6587-98.
- Riddick, G. and I. G. Macara (2005). „A systems analysis of importin- $\alpha$ - $\beta$  mediated nuclear protein import.“ *J Cell Biol* 168(7): 1027-38.
- Robbins, J., S. M. Dilworth, et al. (1991). „Two interdependent basic domains in nucleoplasmin nuclear targeting sequence: identification of a class of bipartite nuclear targeting sequence.“ *Cell* 64(3): 61-73.

## CHAPTER 1: INTRODUCTION: NUCLEOPORINS OF THE CENTRAL REGION OF THE NPC

- Rosenblum, J. S., L. F. Pemberton, et al. (1998). „Nuclear import and the evolution of a multifunctional RNA-binding protein.“ *J Cell Biol* 143(4): 887-99.
- Rouquette, J., V. Choismel, et al. (2005). „Nuclear export and cytoplasmic processing of precursors to the 40S ribosomal subunits in mammalian cells.“ *Embo J* 24(16): 2862-72.
- Rout, M. P., J. D. Aitchison, et al. (2003). „Virtual gating and nuclear transport: the hole picture.“ *Trends Cell Biol* 13(12): 622-8.
- Rout, M. P., J. D. Aitchison, et al. (2000). „The yeast nuclear pore complex: composition, architecture, and transport mechanism.“ *J Cell Biol* 148(4): 635-51.
- Saavedra, C. A., C. M. Hammell, et al. (1997). „Yeast heat shock mRNAs are exported through a distinct pathway defined by Rip1p.“ *Genes Dev* 11(21): 2845-56.
- Sabri, N., P. Roth, et al. (2007). „Distinct functions of the Drosophila Nup153 and Nup214 FG domains in nuclear protein transport.“ *J Cell Biol* 178(4): 557-65.
- Salina, D., P. Enarson, et al. (2003). „Nup358 integrates nuclear envelope breakdown with kinetochore assembly.“ *J Cell Biol* 162(6): 991-1001.
- Schetter, A., P. Askjaer, et al. (2006). „Nucleoporins NPP-1, NPP-3, NPP-4, NPP-11 and NPP-13 are required for proper spindle orientation in *C. elegans*.“ *Dev Biol* 289(2): 360-71.
- Schneider, R. and R. Grosschedl (2007). „Dynamics and interplay of nuclear architecture, genome organization, and gene expression.“ *Genes Dev* 21(23): 3027-43.
- Schwartz, T. U. (2005). „Modularity within the architecture of the nuclear pore complex.“ *Curr Opin Struct Biol* 15(2): 221-6.
- Schwarz-Herion, K., B. Maco, et al. (2007). „Domain Topology of the p62 Complex Within the 3-D Architecture of the Nuclear Pore Complex.“ *J Mol Biol* 370(4): 796-806



## CHAPTER 1: INTRODUCTION: NUCLEOPORINS OF THE CENTRAL REGION OF THE NPC

- Segref, A., K. Sharma, et al. (1997). „Mex67p, a novel factor for nuclear mRNA export, binds to both poly(A)<sup>+</sup> RNA and nuclear pores.“ *Embo J* 16(11): 3256-71.
- Siomi, H. and G. Dreyfuss (1995). „A nuclear localization domain in the hnRNP A1 protein.“ *J Cell Biol* 129(3): 551-60.
- Siomi, M. C., P. S. Eder, et al. (1997). „Transportin-mediated nuclear import of heterogeneous nuclear RNP proteins.“ *J Cell Biol* 138(6): 1181-92.
- Smith, A. E., B. M. Slepchenko, et al. (2002). „Systems analysis of Ran transport.“ *Science* 295(5554): 488-91.
- Stewart, M. (2007). „Molecular mechanism of the nuclear protein import cycle.“ *Nat Rev Mol Cell Biol* 8(3): 195-208.
- Stewart, M. (2007). “Ratcheting mRNA out of the nucleus.” *Mol Cell* 25(3): 327-30.
- Stochaj, U., P. Banski, et al. (2006). „The N-terminal domain of the mammalian nucleoporin p62 interacts with other nucleoporins of the FXFG family during interphase.“ *Exp Cell Res* 312(13): 2490-9.
- Stoffler, D., B. Fahrenkrog, et al. (1999). „The nuclear pore complex: from molecular architecture to functional dynamics.“ *Curr Opin Cell Biol* 11(3): 391-401.
- Stoffler, D., B. Feja, et al. (2003). „Cryo-electron tomography provides novel insights into nuclear pore architecture: implications for nucleocytoplasmic transport.“ *J Mol Biol* 328(1): 119-30.
- Strahm, Y., B. Fahrenkrog, et al. (1999). „The RNA export factor Gle1p is located on the cytoplasmic fibrils of the NPC and physically interacts with the FG-nucleoporin Rip1p, the DEAD-box protein Rat8p/Dbp5p and a new protein Ymr 255p.“ *Embo J* 18(20): 5761-77.
- Strawn, L. A., T. Shen, et al. (2004). „Minimal nuclear pore complexes define FG repeat domains essential for transport.“ *Nat Cell Biol* 6(3): 197-206.

## CHAPTER 1: INTRODUCTION: NUCLEOPORINS OF THE CENTRAL REGION OF THE NPC

Suzuki, A., Y. Ito, et al. (2002). “t(7;11)(p15;p15) Chronic myeloid leukaemia developed into blastic transformation showing a novel NUP98/HOXA11 fusion.” *Br J Haematol* 116(1): 170-2.

Timney, B. L., J. Tetenbaum-Novatt, et al. (2006). „Simple kinetic relationships and nonspecific competition govern nuclear import rates in vivo.“ *J Cell Biol* 175(4): 579-93.

Tran, E. J. and S. R. Wentz (2006). „Dynamic nuclear pore complexes: life on the edge.“ *Cell* 125(6): 1041-53.

Trotta, C. R., E. Lund, et al. (2003). „Coordinated nuclear export of 60S ribosomal subunits and NMD3 in vertebrates.“ *Embo J* 22(11): 2841-51.

Vasu, S., S. Shah, et al. (2001). „Novel vertebrate nucleoporins Nup133 and Nup160 play a role in mRNA export.“ *J Cell Biol* 155(3): 339-54.

Vetter, I. R., A. Arndt, et al. (1999). “Structural View of the Ran-Importin  $\beta$  Interaction at 2.3 Å Resolution.” *Cell* 97: 635-646.

von Lindern, M., S. van Baal, et al. (1992). “Can, a putative oncogene associated with myeloid leukemogenesis, may be activated by fusion of its 3' half to different genes: characterization of the set gene.” *Mol Cell Biol* 12(8): 3346-55.

Walther, T. C., A. Alves, et al. (2003). „The conserved Nup107-160 complex is critical for nuclear pore complex assembly.“ *Cell* 113(2): 195-206.

Weirich, C. S., J. P. Erzberger, et al. (2004). „The N-terminal domain of Nup159 forms a beta-propeller that functions in mRNA export by tethering the helicase Dbp5 to the nuclear pore.“ *Mol Cell* 16(5): 749-60.

Wen, W., J. L. Meinkoth, et al. (1995). „Identification of a signal for rapid export of proteins from the nucleus.“ *Cell* 82(3): 463-73.

Wesierska-Gadek, J., H. Hohener, et al. (1996). „Autoantibodies against nucleoporin p62 constitute a novel marker of primary biliary cirrhosis.“ *Gastroenterology* 110(3): 840-7.

## CHAPTER 1: INTRODUCTION: NUCLEOPORINS OF THE CENTRAL REGION OF THE NPC

- Worman, H. J. and J. C. Courvalin (2003). "Antinuclear antibodies specific for primary biliary cirrhosis." *Autoimmun Rev* 2(4): 211-7.
- Yang, Q., M. P. Rout, et al. (1998). "Three-dimensional architecture of the isolated yeast nuclear pore complex: functional and evolutionary implications." *Mol Cell* 1(2): 223-34.
- Yang, W., J. Gelles, et al. (2004). "Imaging of single-molecule translocation through nuclear pore complexes." *Proc Natl Acad Sci U S A* 101(35): 12887-92.
- Yang, W. and S. M. Musser (2006). "Nuclear import time and transport efficiency depend on importin beta concentration." *J Cell Biol* 174(7): 951-61.
- Yao, W., M. Lutzmann, et al. (2008). "A versatile interaction platform on the Mex67-Mtr2 receptor creates an overlap between mRNA and ribosome export." *Embo J* 27(1): 6-16.
- Yaseen, N. R. and G. Blobel (1999). "Two distinct classes of Ran-binding sites on the nucleoporin Nup-358." *Proc Natl Acad Sci U S A* 96(10): 5516-21.
- Yasuhara, N., N. Shibasaki, et al. (2007). "Triggering neural differentiation of ES cells by subtype switching of importin-alpha." *Nat Cell Biol* 9(1): 72-9.
- Zeitler, B. and K. Weis (2004). "The FG-repeat asymmetry of the nuclear pore complex is dispensable for bulk nucleocytoplasmic transport in vivo." *J Cell Biol* 167(4): 583-90.
- Zemp, I. and U. Kutay (2007). "Nuclear export and cytoplasmic maturation of ribosomal subunits." *FEBS Lett* 581(15): 2783-93.
- Zuccolo, M., A. Alves, et al. (2007). "The human Nup107-160 nuclear pore subcomplex contributes to proper kinetochore functions." *Embo J* 26(7): 1853-64.



## **Domain topology of the p62 complex within the 3-D architecture of the nuclear pore complex**

**Kyrill Schwarz-Herion, Bohumil Maco, Ursula Sauder, and Birthe Fahrenkrog\***

*M.E. Müller Institute for Structural Biology, Biozentrum, University of Basel, Klingelbergstrasse 70,  
CH-4056 Basel, Switzerland*

\*Corresponding author, Fax: +41-61-267-2109

E-mail address: [birthe.fahrenkrog@unibas.ch](mailto:birthe.fahrenkrog@unibas.ch)

Key words: nuclear pore complex; p62-complex; nucleoporins; FG-repeats;  
immuno-electron microscopy



### Summary

The nuclear pore complex (NPC) is the only known gateway for exchange of macromolecules between the cytoplasm and nucleus of eukaryotic cells. One key compound of the NPC is the p62 sub-complex, which consists of the nucleoporins p62, p54, and p58/p45 and is supposed to be involved in nuclear protein import and export. In this study we show the localization of different domains of the p62 complex by immuno-electron microscopy using isolated nuclei from *Xenopus* oocytes. To determine the exact position of the p62 complex, we examined the localization of the C- and N-terminal domains of p62 by immunolabeling using domain-specific antibodies against p62. In addition, we expressed epitope-tagged versions of p62, p54, and p58 in *Xenopus* oocytes and localized the domains with antibodies against the tags. This first systematic analysis of the domain topology of the p62 complex within the NPC revealed that the p62 complex is anchored to the cytoplasmic face of the NPC most likely by the coiled-coil domains of the three nucleoporins. Furthermore, we found the phenylalanine-glycine (FG)-repeat domain of p62, but not of p58 and p54, to be mobile and flexible nature.

## 2.1. Introduction

The nuclear pore complex (NPC) is one of the largest known complexes in mammalian cells, estimated to have a molecular weight of ~120 MDa (Reichert, Holzenburg et al. 1990). The NPC mediates the import and export of macromolecular cargos in and out of the nucleus, and proteomic studies of yeast and mammalian NPCs showed that the NPC is composed of about 30 different proteins, called nucleoporins (Rout, Aichison et al. 2000; Tran and Wentz 2006 ; Cronshaw, Krutchinsky et al. 2002; Bednenko, Cingolani et al. 2003; Fahrenkrog and Aebi 2003). The NPC consists of three major parts: the cytoplasmic ring moiety with the cytoplasmic fibrils, the nuclear ring moiety with the nuclear basket, and the central framework (Fahrenkrog, Köser et al. 2004; Schwartz, 2005). From the cytoplasmic ring eight kinky fibrils, ~50 nm in length, emanate into the cytoplasm. Eight filaments with a length of ~75 nm are attached to the nuclear ring and join into a massive distal ring, thereby forming the nuclear basket. The dominant building block in the central region of the NPC is the central framework, which is embedded in the nuclear envelope (NE) and composed of eight multidomain spokes. The central framework, which is continuous with a cytoplasmic and a nuclear ring moiety, has a height of ~80 nm and it encloses the central pore, which has a diameter of about 40 nm, being narrowest in the midplane of the NE and widening to ~70 nm at its cytoplasmic and nuclear periphery (Fahrenkrog and Aebi 2003; Stoffler, Feja et al. 2003).

A major structural feature of about one third of the nucleoporins is the phenylalanine-glycine (FG)-repeat domains, which are composed of hydrophobic FG patches, that are spaced by hydrophilic linkers of variable length and sequence. FG-repeat domains, which are reported to interact directly with transport receptors, may play an important role in the context of nucleoplasmic transport (Matsuura, Lange et al. 2003; Bayliss, Littlewood et al. 2000; Hu, Guan et al. 1996). Biophysical measurements and X-ray crystallography indicated that FG-repeat domains are unstructured and highly flexible domains (Bayliss, Littlewood et al. 2000; Denning, Uversky et al. 2002; Denning, Patel et al. 2003). The findings were further supported by ultra-structural immunogold localization studies of different domains of the nucleoporin Nup153 and Nup214 (Fahrenkrog, Maco et al. 2002). Both nucleoporins appear to be anchored to the NPC by their non-FG-repeat domains, whereas the FG-repeat domains were found to be flexible and mobile within the NPC in a transport and energy-dependent manner (Fahrenkrog, Maco et al. 2002; Paulillo, Phillips et al. 2005; Paulillo, Powers et al. 2006). Moreover, atomic force microscopy studies further unveiled that the FG-repeat domain of Nup153 is an extended molecule with a length of about 200 nm and surface tethered FG-repeats behave like a polymer brush acting as entropic barrier and selective trap in the near field of the NPC (Lim, Aebi et al. 2006a; Lim, Huang et al. 2006b ).



The nucleoporin p62 is one of the first characterized vertebrate nucleoporins and was found to form a subcomplex together with the nucleoporins p54, p58 and p45 – a splicevariant of p58 (Davis and Blobel 1986; Hu and Gerace, 1998; Hu, Guan et al. 1996; Cordes and Krohne 1993; Guan, Muller et al. 1995; Finlay, Meier et al. 1991; Davis and Blobel 1987). Based on its amino acid sequence, vertebrate p62 is organized in three different domains: (i) a N-terminal FG-repeat domain of about 170 residues, which contains five FG-repeats; (ii) a threonine-rich linker region, 120 residues long; (iii) a C-terminal 270 residue  $\alpha$ -helical rod coiled-coil domain (Sergej Strelkov [personal communication]) (Finlay, Meier et al. 1991; David and Blobel 1986; Denning, Patel et al. 2003). p54 has an overall similar domain organization as compared to p62 with a shorter FG-repeat domain of  $\sim$  100 residues (Hu, Guan et al. 1996). The nucleoporin p58, in contrast, exhibits two FG-repeat domains, a shorter N-terminal domain ( $\sim$ 85 residues) and a longer C-terminal domain ( $\sim$ 110 residues), which are spaced by  $\alpha$ -helical coiled-coil domain (Hu, Guan et al. 1996). Finlay et al. could show that depletion of p62, p54, or p58 from *Xenopus* nuclear extracts yielded reconstituted nuclei that were defective for nuclear import (Finlay, Meier et al. 1991). Additionally, this study showed that the depletion of one component of the p62 complex led to co-immunoprecipitation of all three components of the complex, indicating strong protein-protein interactions between these three nucleoporins.

Further biochemical characterizations of the p62 complex by Hu et al. showed that all three nucleoporins can bind directly to distinct nuclear import factors, such as importin  $\beta$ , and can deplete nuclear import activity from the cytosol (Hu, Guan et al. 1996). Attempts to determine the localization of the p62 complex on the ultrastructural level have led to controversial results locating this complex to either the cytoplasmic face or both sides of the NPC (Cordes and Krohne 1993; Guan, Muller et al. 1995; Dabauvalle, Benavente et al. 1988). Epitopes recognized by the employed antibodies in the distinct studies have remained unknown.

To overcome the inconsistency of previous immunolocalization data of the p62 complex, we used domain-specific antibodies in combination with expressing epitope-tagged versions of the p62 complex nucleoporins to map six distinct domains of the complex in the 3-D structure of the NPC by immunogold-EM in *Xenopus* oocyte nuclei. We show here that the p62 complex is anchored to the cytoplasmic face of the NPC by the coiled-coil domains of p62, p58, and p54. In addition, we found the FG-repeat domain of p62 to be flexible and mobile within the NPC, whereas the FG-repeat domains of p58 and p54 appear immobile.

## 2.2. Results

### 2.2.1. Production and characterization of an antibody against the C-terminus of p62

In order to gain a better understanding of the topology of the p62 complex within the 3-D architecture of the NPC, we raised an antibody against the C-terminal coiled-coil domain of *Xenopus* p62 (residues 332-547; Fig. 2.1 (a)) in rabbits. This antibody was tested in an immunoblot, using extracts from *Xenopus* eggs as well as HeLa cells. As shown in Fig. 2.1 (b), the antibody recognized p62 among a complex array of proteins in *Xenopus* egg (lane 1) and HeLa cell extract (lane 2). In order to detect the N-terminal region of p62, we used a monoclonal antibody against residues 24-178 of the human p62 (Fig. 2.1 (a)), which recognizes the N-terminal epitope in a wide range of vertebrates (BD Bioscience, Franklin Lakes NJ) (Buss and Stewart 1995; Carmo-Fonseca, Kern et al. 1991).

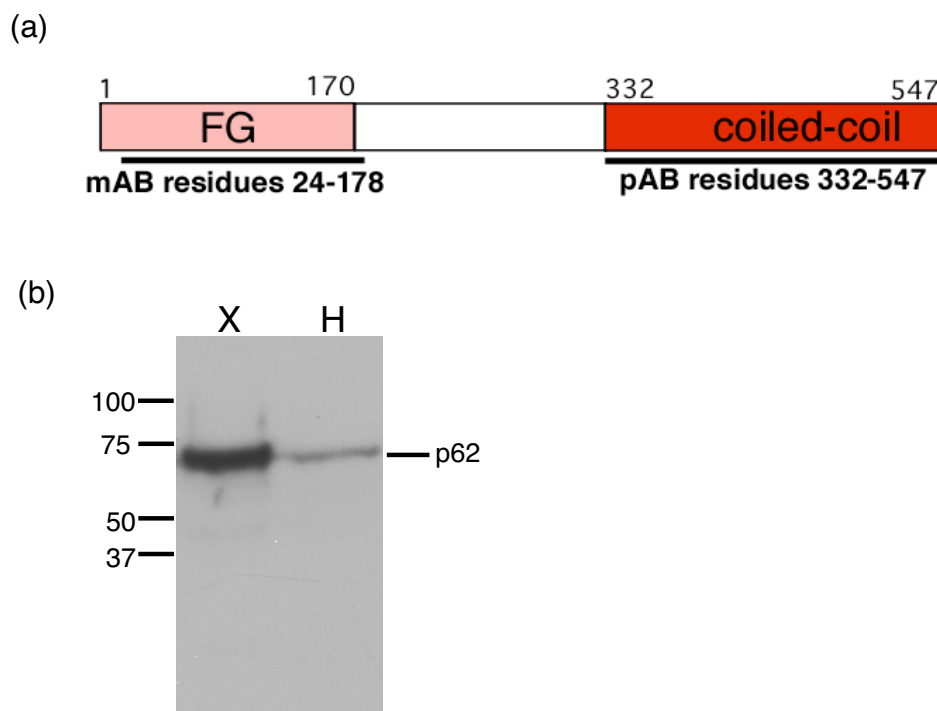


**Figure 2.1.** Domain-specific antibodies against p62 (a) The overall domain organization of *Xenopus* p62 is schematically illustrated. A commercially available monoclonal antibody, which was raised against the FG-repeat domain (residues 24-178), was used and a polyclonal antibody against the C-terminal coiled-coil domain (residues 332-547; p62-C antibody) was raised. (b) Domain-specific anti-p62-C antibody recognizes a protein of about 60 kDa in immunoblots of *Xenopus* egg extracts (lane 1) or HeLa cell extracts (lane 2). The positions of the marker in kilodaltons are indicated.

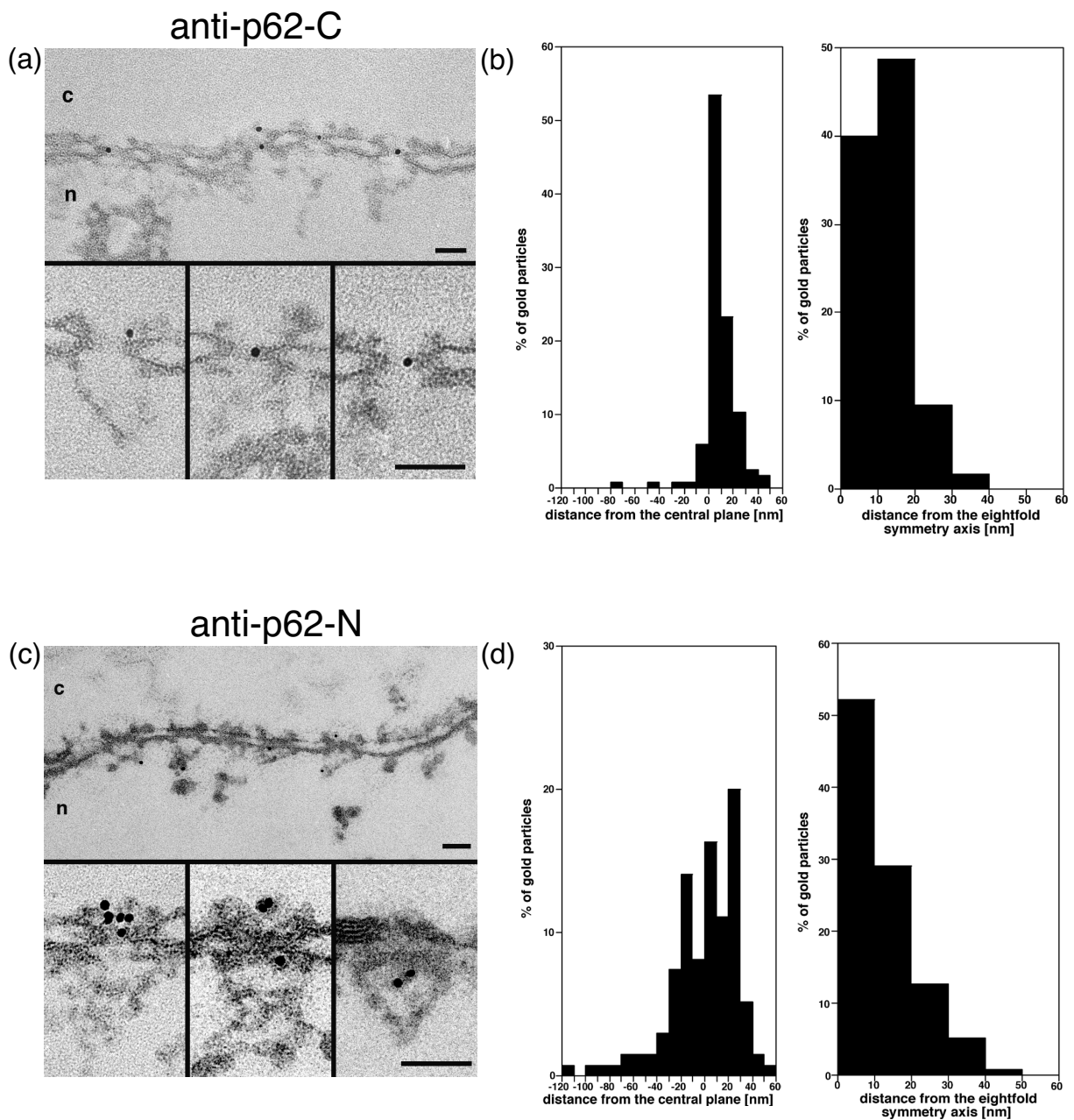


**Figure 2.2.** Domain topology of p62 within the nuclear pore complex. (a) Intact isolated nuclei were preimmunolabeled with the polyclonal anti-p62-C antibody directly coupled to 8-nm colloidal gold and prepared for EM by Epon embedding and thin-sectioning. A view along a cross-sectioned NE stretch with labeled NPCs is shown, together with a gallery of selected examples of gold-labeled NPC in cross-sections. (b) Quantitative analysis of the gold particles associated with the NPC after labeling with the anti-p62-C antibody. 115 gold particles were scored. (c) The localization of the N-terminal domain of p62 in isolated, intact *Xenopus* nuclei was determined with a monoclonal anti-p62-N antibody directly coupled to 8-nm colloidal gold. A stretch along the NE in cross-sections and a gallery of selected examples of gold-labeled NPCs in cross-sections (bottom) are shown. (d) Histograms show quantitative analysis of anti-p62-N labeled NPCs. Total number of analyzed particles was 133. c, cytoplasm; n, nucleus. Scale bars, 100 nm

### 2.2.2. p62 has a distinct domain topology in the NPC

To determine the localization of distinct domains of p62 within the 3-D architecture of the NPC, we used the domain specific antibodies against p62 for immuno-EM. To do so, we isolated intact nuclei from *Xenopus* oocytes and incubated them with the respective antibody that has been directly coupled to 8-nm colloidal gold. After incubation at room temperature, the labeled nuclei were prepared and embedded for thin-section EM or quick-freeze/freeze-drying/rotary metal-shadowing (see Material and Methods). We first mapped the epitope that is recognized by the antibody directed against the C-terminal region of p62 (anti-p62-C). As highlighted in Fig. 2.2 (a), this anti-p62-C antibody recognizes an epitope close to the central pore of the NPC. Quantification of the gold particle distribution (Fig. 2.2 (b)) with respect to the central plan of the NPC indicated that more than 80% of the gold particles were found at distances between 0 and +20 nm from the central plane of the NPC with a peak at  $5.4 \text{ nm} \pm 14.1 \text{ nm}$ . Together with the corresponding average radial distances of  $9.4 \text{ nm} \pm 6.0 \text{ nm}$  this corresponds to a localization at the cytoplasmic entry side of the central pore. This localization of the C-terminal domain of p62 was further confirmed by quick-freeze/freeze-drying/rotary metal-shadowing EM (Jarnik, 1991; Fahrenkrog, 2002). Stereo pictures allowed the visualization of the epitope, which is recognized by the anti-p62-C antibody in 3-D. As shown in Fig. 2.6 (a), gold particles decorate the NPC close to the central plane of the NPC at a distance of about 15 nm in average.

Next, we analyzed the location of the N-terminal FG-repeat domain of p62 within the NPC, using the monoclonal anti-p62-N antibody conjugated to 8-nm colloidal gold in *Xenopus* oocyte nuclei. We found that this anti-p62-N antibody recognized epitopes on the cytoplasmic as well as on the nuclear face of the NPC (Fig. 2.2 (c)). Quantification of the gold particle distribution revealed that ~ 60% of the gold particles were found on the cytoplasmic side at an average distance of  $16.3 \text{ nm} \pm 12.1 \text{ nm}$  from the central plane of the NPC, whereas 40% were detected on the nuclear face of the NPC at an average distance of  $-25.3 \text{ nm} \pm 25.4 \text{ nm}$  (Fig. 2.2 (d)). Together with corresponding average radial distances of  $9.8 \text{ nm} \pm 8.7 \text{ nm}$  this corresponds to epitopes close to the cytoplasmic and nuclear entry/exit sites of the central pore. Stereo pictures of a quick-frozen/freeze-dried/rotary metal-shadowed NE in Fig. 2.6 (b) show the nucleoplasmic face of the NPC further supporting the notion that the N-terminal FG-repeat domain of p62 can reach its nucleoplasmic face.

Taken together, our data suggest that p62 is anchored to the cytoplasmic face of the NPC by its C-terminal coiled-coil domain, whereas its N-terminal FG-repeat domain is flexible and mobile within the central pore region of the NPC.

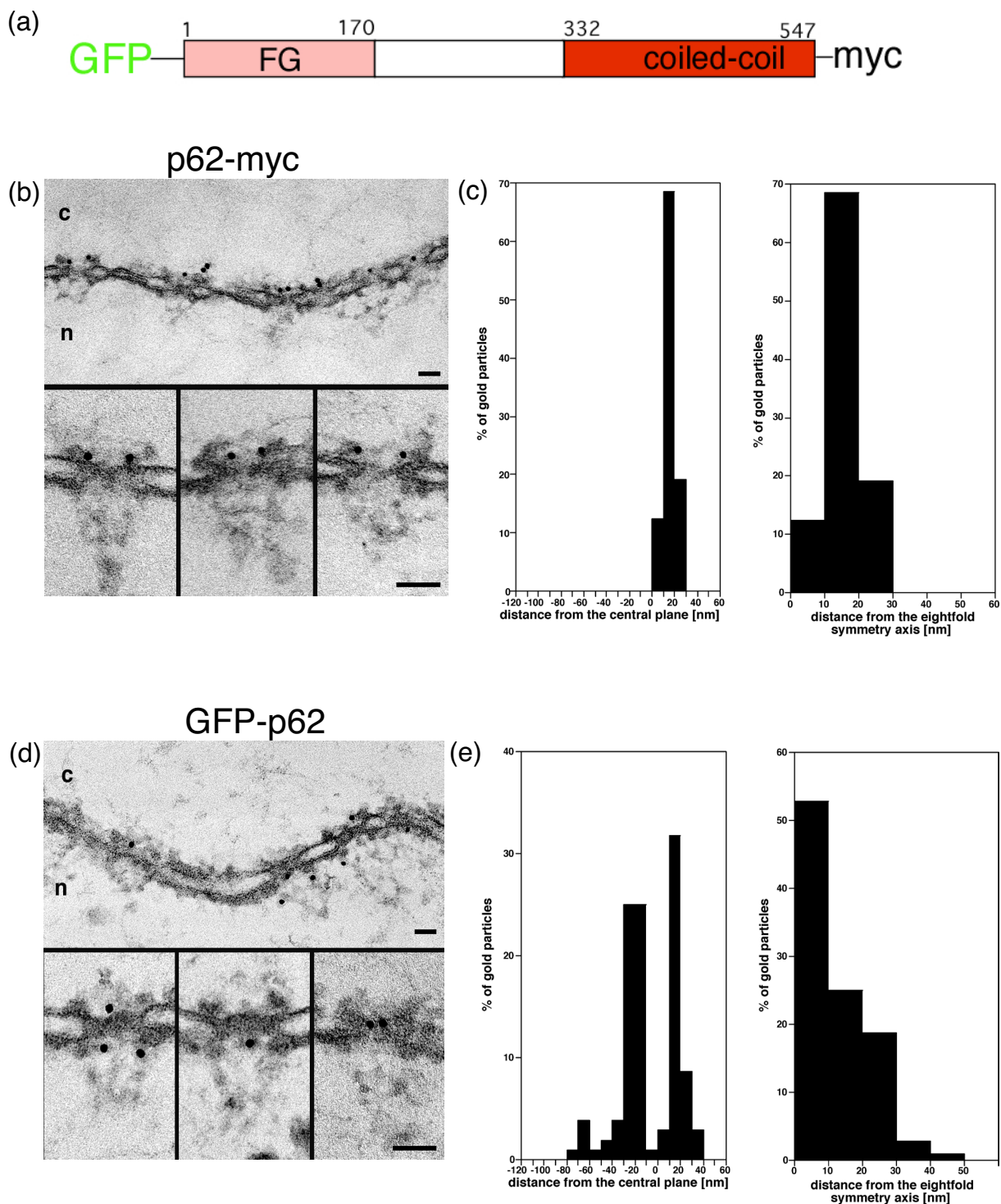


**Figure 2.3.** Domain topology of epitope-tagged nucleoporin *Xenopus* p62 within the nuclear pore complex. (a) The overall organization of tagged p62 is illustrated. (b) Myc-tagged C-terminal domain of p62 was detected in microinjected, isolated *Xenopus* nuclei by anti-myc antibody directly coupled to 8-nm colloidal gold. An overview along the NE in cross-sections and a gallery of selected examples of gold-labeled NPCs in cross-sections (bottom) are shown. (c) Quantitative analysis of the scored gold particles is shown in histograms. 73 gold particles were analyzed. (d) The GFP-tagged N-terminal domain of p62 in intact, isolated *Xenopus* nuclei was detected by an anti-GFP antibody directly coupled to 8-nm colloidal gold. Micrographs show a stretch along the NE in cross-sections and a gallery of selected examples of cross sections (bottom). (e) Gold particles, which were associated with the NPC were analyzed with respect to the central plane and the eight fold symmetry axis of the NPC. 104 gold particles were scored. c, cytoplasm; n, nucleus. Scale bars, 100 nm.

### 2.2.3. Recombinant expression of epitope-tagged p62 in *Xenopus* NPCs

To confirm the results obtained by using the domain-specific antibodies against the C-terminal and N-terminal domain of p62, we next expressed C-terminal myc-tagged and N-terminal GFP-tagged *Xenopus* p62, respectively, in *Xenopus* oocytes (Fig. 2.3 (a)). For this purpose, we microinjected the corresponding plasmid in *Xenopus* oocyte nuclei. The presence of the cytomegalovirus (CMV) promoter allowed expression of GFP-p62 and myc-p62 directly in the oocytes. The location of the incorporated protein was determined by using a monoclonal antibody against the myc-tag and a polyclonal antibody against the GFP-tag (see Materials and Methods) directly conjugated to 8-nm colloidal gold.

Fig. 2.3 (b) and (c) document that the p62 myc-tagged C-terminus is exclusively found at the cytoplasmic face of the NPC with a distance of  $\sim 16.5 \text{ nm} \pm 4.7 \text{ nm}$  from the central plane. Quantification of the gold particle distribution with regard to the eightfold symmetry axis resulted in a distance of  $\sim 14.3 \text{ nm} \pm 7.2 \text{ nm}$  (Fig. 2.3 (c), right panel). By contrast, the antibody-gold particles, which recognize the GFP-tagged N-terminal epitope of p62, could be detected at both the cytoplasmic (38% of the particles) and the nucleoplasmic (62% of the particles) side of the NPC (Fig. 2.3 (d)). Quantitative analysis of the distribution of the particles with respect to the central plane resulted in a peak at  $12.4 \text{ nm} \pm 8.7 \text{ nm}$  (Fig. 2.3 (e)). Taken together, our immuno-EM data using domain-specific antibodies and incorporation of epitope-tagged p62 into *Xenopus* oocyte NPCs suggest that p62 is anchored to the cytoplasmic side of the NPC by its C-terminal coiled-coil domain, whereas the N-terminal FG-repeat domain is mobile and can localize to both sides of the NPC.

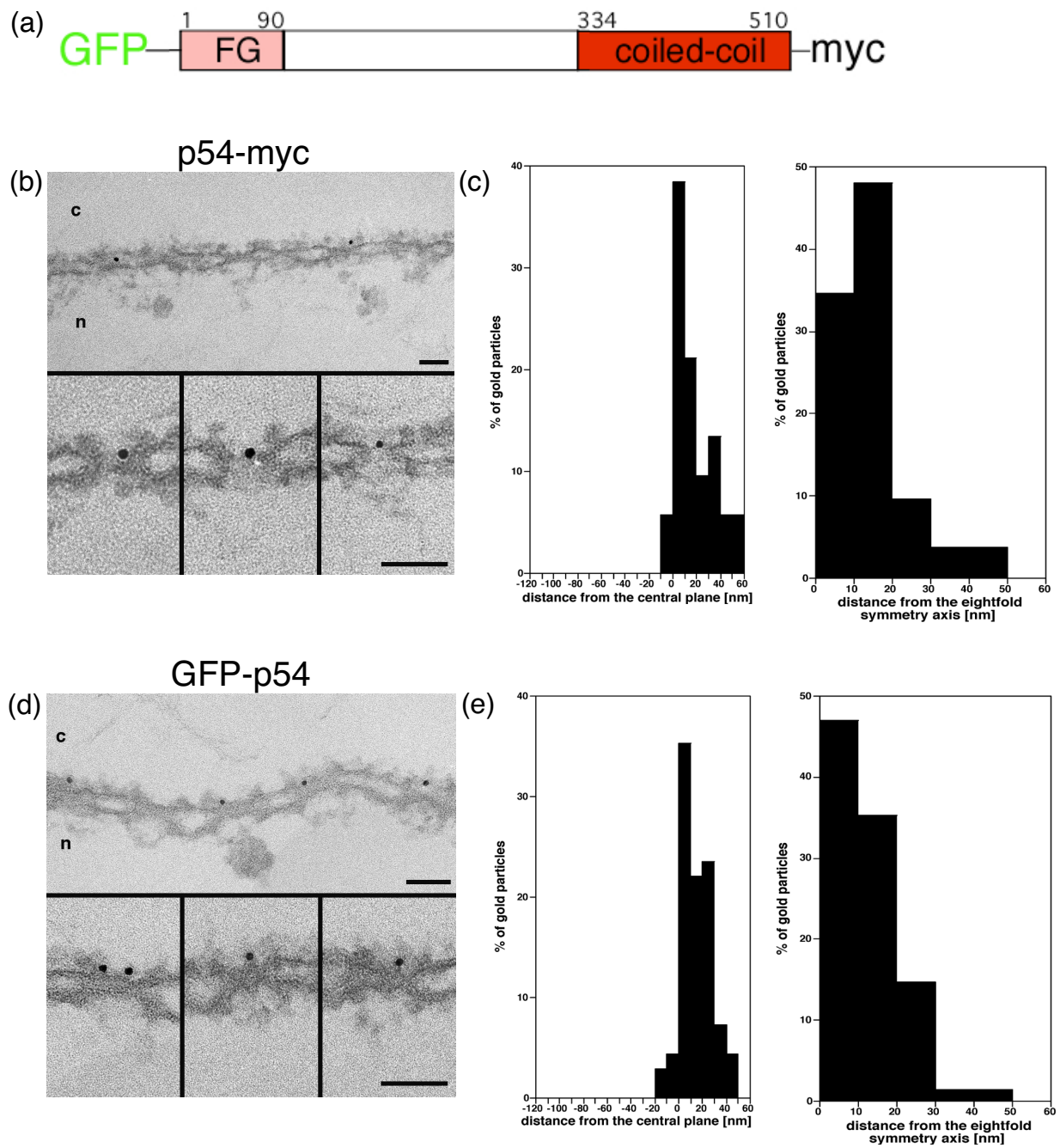


**Figure 2.4.** Domain topology of epitope-tagged rat p54 within the NPC (a) The overall organization of tagged rat p54 is illustrated. (b) Microinjected, isolated and intact *Xenopus* nuclei were immunolabeled with anti-myc antibody directly conjugated to 8-nm colloidal gold to detect the C-terminus of p54. The corresponding histograms are shown in (c). 51 gold particles were scored. (d) The N-terminal GFP-tag of p54 was detected with an anti-GFP antibody conjugated to 8-nm colloidal gold by preimmunolabeling in *Xenopus* oocyte nuclei. A view along a cross-sectioned NE stretch with labeled NPCs is shown together with a gallery of selected examples of gold-labeled NPC in cross-sections (bottom). The corresponding histograms to (d) are shown in (e). 130 gold particles were scored. c, cytoplasm; n, nucleus. Scale bars, 100 nm.

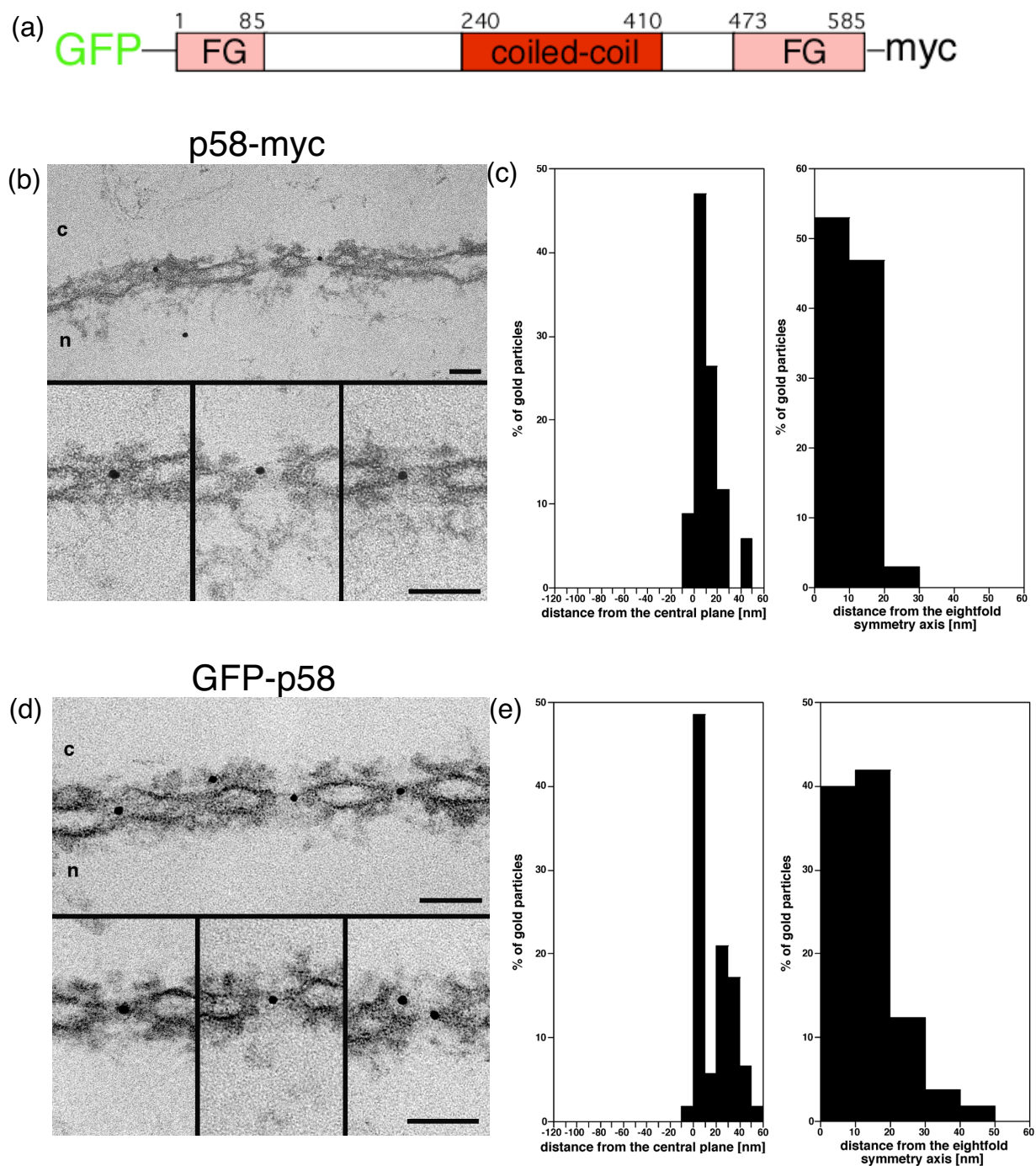


**Figure 2.5.** Domain topology of epitope-tagged nucleoporin rat p58 within the NPC. (a) The domain organization of tagged rat p58 is illustrated. (b) Microinjected, isolated and intact nuclei were immunolabeled with anti-myc antibody directly conjugated to 8-nm colloidal gold to detect the myc-tagged C-terminus of p58. The corresponding histograms to (b) are shown in (c). 35 gold particles were scored. (d) In microinjected, isolated nuclei N-terminal GFP-tagged of p58 was detected by an anti-GFP antibody conjugated to 8-nm colloidal gold in combination with preimmunolabeling of *Xenopus* oocyte nuclei. A view along a cross-sectioned NE stretch with labeled NPCs is shown together with a gallery of selected examples of gold-labeled NPC in cross-sections (bottom). The corresponding histograms to (d) are shown in (e). 110 gold particles were scored. c, cytoplasm; n, nucleus. Scale bars, 100 nm



### 2.2.4 Localization of epitope-tagged p54 and p58 within the NPC

To complete the mapping of the members of the p62-complex in the 3-D-architecture of the NPC, rat p54 and rat p58 were cloned into vectors to express fusion proteins with a myc-tagged C-terminus and a GFP-tagged N-terminus, respectively (Fig. 2.4 (a)). The corresponding plasmids under control of the CMV-promoter were microinjected and expressed in *Xenopus* oocytes, and the isolated nuclei were either labeled with an anti-myc antibody or an anti-GFP-antibody, respectively, both directly coupled to 8-nm colloidal gold. As shown in Fig. 2.4 (b), the anti-myc antibody exclusively labels the cytoplasmic face of the NPC of *Xenopus* oocyte nuclei expressing myc-p54. Quantitative analysis of the gold-labeled C-terminal domain of p54 with respect to the central plane revealed that 83% of the gold particles were detected between 0 and +40 nm at the cytoplasmic side of the NPC (Fig. 2.4 (c), left panel; average distance  $15.3 \text{ nm} \pm 16.8 \text{ nm}$ ). Together with the corresponding radial distances of  $11.8 \text{ nm} \pm 9.8 \text{ nm}$  (Fig. 2.4 (c), right panel) this corresponds to a localization close to the cytoplasmic entry side of the central pore

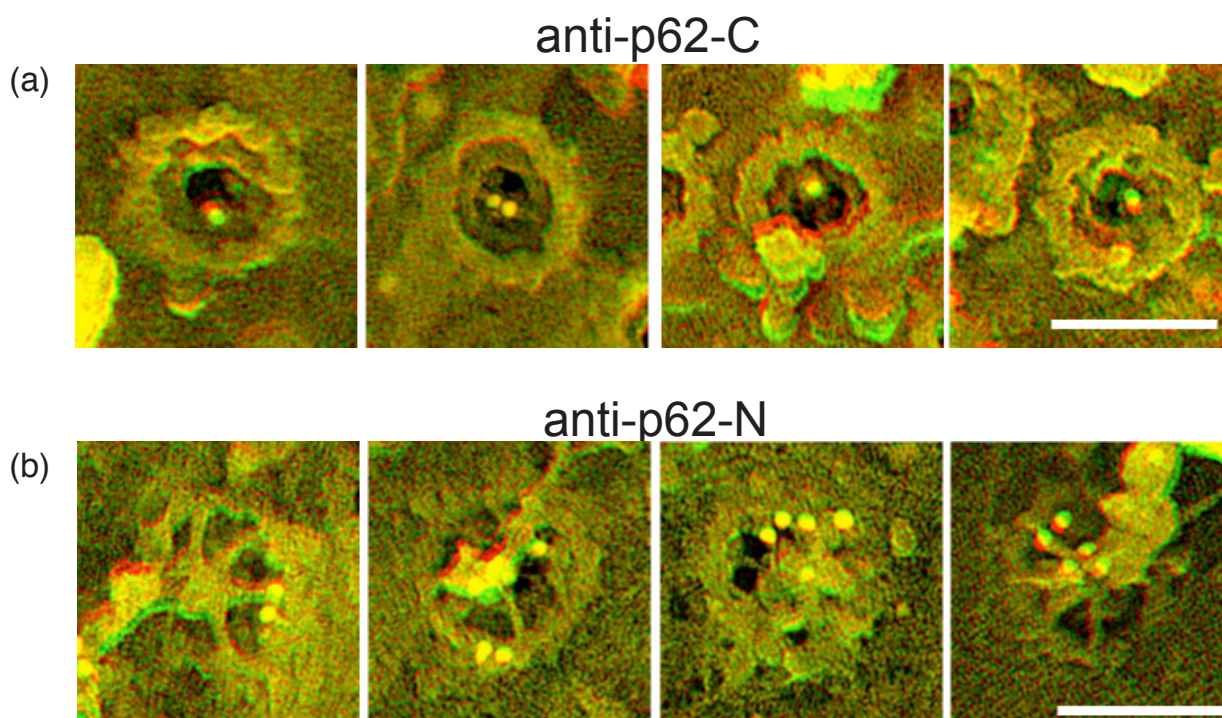


**Figure 2.6.** Localization of the p62 domains at the cytoplasmic and the nuclear face of the NPC. Intact *Xenopus* oocyte nuclei were incubated with antibody directly conjugated to 8-nm colloidal gold, spread on an EM grid and further prepared for quick-freeze/freeze-drying/rotary metal-shadowing. (a) Anaglyph stereo images of selected examples, revealing the cytoplasmic face of NPCs labeled with domain-specific anti-p62-C antibody. (b) Gallery of anaglyph stereo images shows the nuclear face of NPCs labeled with anti-p62-N antibody directly conjugated to 8-nm gold. Scale bars, 100 nm.

of the NPC. The GFP-tagged N-terminus of p54, containing 7 FG- repeats, was localized by anti-GFP-antibodies. 88% of the gold particles could be detected at the cytoplasmic face of the NPC between 0 and +40 nm (Fig. 2.4 (e), right panel; average distance  $17.5 \text{ nm} \pm 9.6 \text{ nm}$  from the central plane of the NPC). Fig. 2.4 (e), left panel, shows the radial distribution of the gold-labeled GFP-tagged N-terminus of p54.

The nucleoporin p58 differs from p62 and p54 by having two FG-repeat domains both at the N-terminus (4 FG-repeats) and at the C-terminus (8 FG-repeats) (Fig. 2.5 (a)). The myc-tagged C-terminus of p58 was visualized by pre-embedding immuno-labeling in thin-sections of *Xenopus* nuclei. Analysis of the spatial distribution of the myc-tagged C-terminus of p58 resulted in 85% of gold particles being associated with the cytoplasmic side of the NPC between 0 and +30 nm (average distance  $9.0 \text{ nm} \pm 14.4 \text{ nm}$  with respect to the central plane of the NPC) and a vertical distribution from the eightfold symmetry axis of  $7.6 \text{ nm} \pm 9.0 \text{ nm}$  (Fig. 2.5 (b) and (c)). Finally, the p58 N-terminal domain was examined by the immuno-gold technique. Fig. 2.5 (d) shows that the GFP-tagged N-terminal domain of p58 is located at the cytoplasmic face of the NPC close to its central plane. Quantitative analysis of the distribution of the gold particles (Fig. 2.5 (e)) showed that 92% of the particles were detected between 0 and +40 nm at an average distance  $14.7 \text{ nm} \pm 15.8 \text{ nm}$  from the NPC's central plane with a vertical distribution of  $11.1 \text{ nm} \pm 9.0 \text{ nm}$  from the eightfold symmetry axis corresponding to a location in the cytoplasmic central pore region of the NPC.

## 2.3. Discussion

Previous immuno-EM studies concerning nucleoporin localization typically dealt with antibodies, which were raised against full-length proteins without specifying the epitope that is recognized by the antibody or with one-site tagged nucleoporins, which were detected by antibodies against the tags. More recent studies, however, showed that for larger nucleoporins, which have a structurally distinct domain organization, such as Tpr, Nup153 and Nup214, domain-specific antibodies and expression of nucleoporins, that are tagged at their N-terminus and C-terminus, were prerequisite to determine more specifically the overall organization of these nucleoporins within the NPC (Frosst, Guan et al. 2002; Fahrenkrog, Maco et al. 2002; Krull, Thyberg et al. 2004; Paulillo, Phillips et al. 2005).

By following the same strategy, we show here that such a systematic analysis of nucleoporin domain distribution within the 3-D structure of the NPC is also favourable for smaller nucleoporins with nevertheless distinct domain organization. Our study demonstrates a cytoplasmic anchorage site of the p62 subcomplex of the NPC by coiled-coil domains with only the rather short FG-repeat of p62 being flexible within the NPC.

### 2.3.1. The coiled-coil domains mediate the anchoring of the p62 complex to the cytoplasmic side of the NPC

The EM localization data of the C-terminal domain of p62 with domain-specific antibodies as well as with C-terminal myc-tagged p62 demonstrate a cytoplasmic location of this epitope within the NPC (Figs. 2.2, 2.3, 2.7 (a) and (b)). Similarly the myc-tagged C-terminal domain of p54 localizes to the cytoplasmic face of the NPC (Figs. 2.4 (b) and (c); 2.7 (c)). These data coincide with earlier findings in biochemical studies, which have shown, that the C-terminal predicted coiled-coil domain of p62 binds to the C-terminal predicted coiled-coil domain of p54, suggesting that both domains co-localize within the 3-D structure of the NPC (Buss and Stewart 1995). Based on biochemical data, we assume that also the coiled-coil domain of p58, which is located in the center of the protein, is anchored to the cytoplasmic face of the NPC, similar to the coiled-coils of p62 and p54 (Buss and Stewart 1995). Interestingly, the crystal structure of the coiled coil domain of p58 has recently been resolved (Melcak, Hoelz et al. 2007). In the crystal, p58 forms tetramers consisting of two antiparallel dimers that can adopt various conformations leading to a lateral displacement between tetramers and an intermolecular sliding mechanism, which may contribute to adjust the diameter of the central pore of the NPC in response to transport acti-

vity. Our study locating the p62 complex and, in particular, the coiled-coil domains of the complex to the cytoplasmic periphery of the central pore may further support the notion that the p62 complex critically contributes to regulate the opening and closing of the central pore.

### 2.3.2. Domain topology of the FG-repeat domain of p62, p54 and p58

In the present immuno-EM study, we detected the FG-repeats of p62 at both the cytoplasmic and the nuclear side of the NPC by using domain-specific antibodies against this domain as well as by expressing N-terminal GFP-tagged p62 in *Xenopus* oocytes (Figs: 2.2, 2.3, 2.6, 2.7). These findings support previous studies, which showed that the FG-repeat domains of Nup214 and Nup155 are mobile and flexible within the NPC (Fahrenkrog, Maco et al. 2002; Paulillo, Phillips et al. 2005; Paulillo, Powers et al. 2006). In contrast to the FG-repeat domain of p62, the FG-repeat domains of p54 and p58 do not appear to be flexible as they were found to reside exclusively on the cytoplasmic side of the NPC. By comparing the length and the distribution of FG-repeats within the domains of p62, p54, and p58, some differences become obvious: whereas the p62 FG-repeat domain bears six FG-repeats nearly equally distributed over a length of 170 residues, the different FG-repeat domains of p54 and p58 contain five to seven FG-repeats, which are spread over a length of 85-110 residues. Given that the FG-repeat domains have an extended conformation (i.e. 3.06 Å per residue) (Fahrenkrog, Maco et al. 2002; Strelkov, Herrmann et al. 2002), the FG-repeat domain of p62 would have a length of about 52 nm if fully extended, compared to 28 nm for the FG-repeat domains of p54 and 26 nm or 34 nm for the two FG-repeat domains of p58, respectively.

These differences in length may account for the fact that the FG-repeat domain of p62 can span the ~50 nm central pore from the cytoplasmic anchoring site to the nuclear face, in contrast to the shorter FG-repeat domains of p58 and p54.

Besides their differences in length, the different spatial distribution of the distinct FG-repeat domains of the p62 complex can also be interpreted by a recent model of Lim et. al. (Lim, Huang et al. 2006). In this model, FG-repeat domains were found to behave like a polymer brush without interactions between individual FG-repeat domains. This would suggest that differently anchored FG-repeat domains extend in different directions from their anchoring point. With respect to our localization data shown here, this might imply that the FG-repeat domains of p62, p54 and those of p58 have slightly different anchoring points within the NPC coinciding with different degrees of freedom in the 3-D structure of the NPC, and in turn a different spatial distribution.

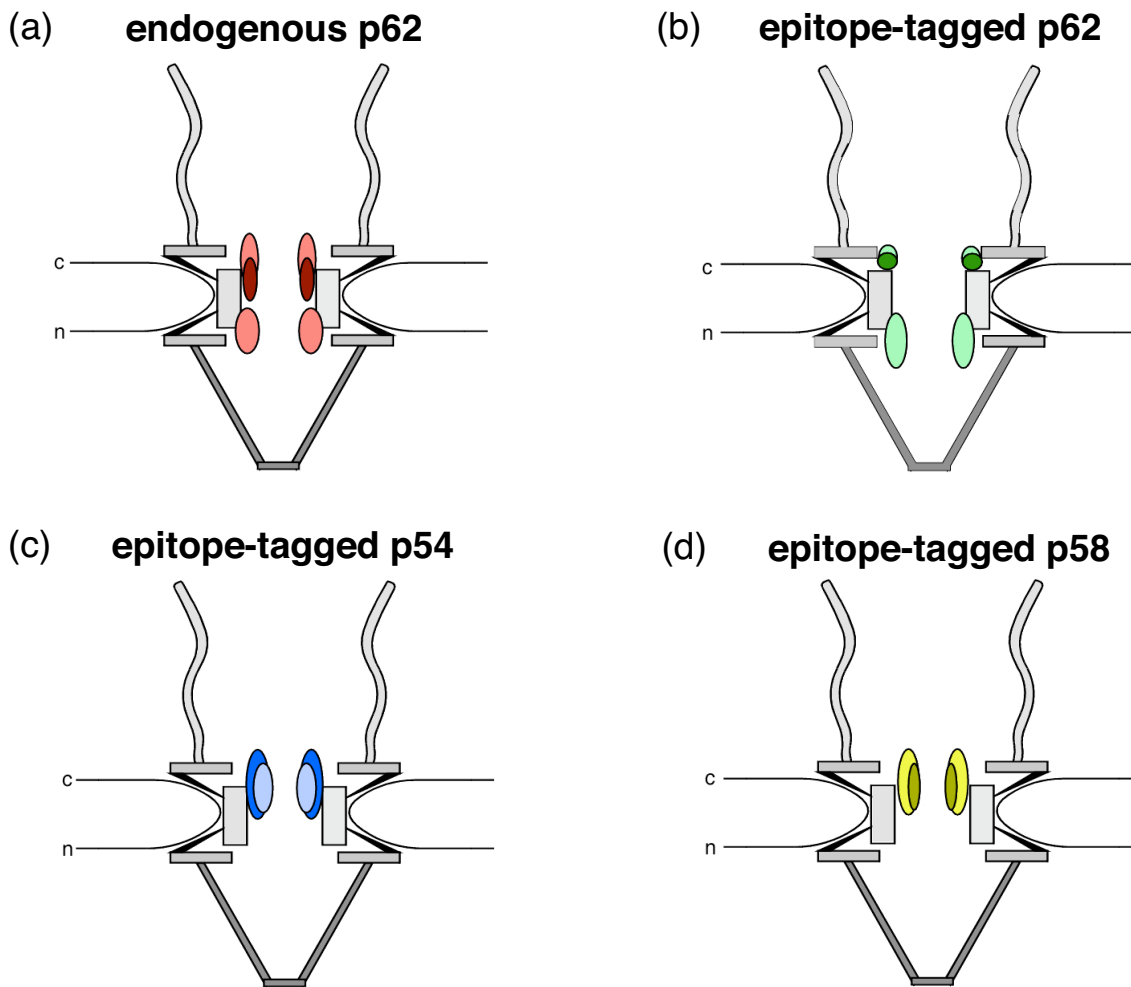


**Figure 2.7.** Schematic representation of the epitope distribution of the different domains of the p62 complex within the 3-D architecture of the NPC revealed by domain-specific antibodies and expression of epitope-tagged nucleoporins p62, p54, and p58. The N-terminal domain of p62 is localized close to the entry and exit of the NPC’s central pore as determined by employing domain specific antibodies (a; light red) or expression of N-terminally GFP-tagged p62 (b; light green). The C-terminus of p62 localizes to the cytoplasmic entry side of the central pore (dark red in (a), dark green in (b)). The center of each elliptic “location cloud” represents the mean distance from the central plane and the central eightfold symmetry axis, respectively, of the NPC. The radii of the elliptic clouds are defined by the standard deviation of the vertical and radial distances. (c) The myc-tagged C-terminus of p54 (dark blue) and the GFP-tagged N-terminus of p54 (light blue) both localize to the cytoplasmic entry side of the central pore. (d) Myc-tagged C-terminus of p58 (dark yellow) and the GFP-tagged N-terminus of p58 (light yellow) show a position for both domains at the cytoplasmic entry side of the central pore..

### 2.3.3. The nucleoporins of the p62 complex are asymmetric nucleoporins

Based on their localization within the NPC, nucleoporins are distinguished between symmetrical nucleoporins, i.e. those nucleoporins, which reside on the cytoplasmic and the nuclear side of the NPC and asymmetrical nucleoporins, i.e. nucleoporins, which locate to either the cytoplasmic or the nuclear side of the NPC. This distribution of distinct nucleoporins is thought to have an impact on nucleocytoplasmic transport through the NPC. The Wentz lab has recently shown that the depletion of different FG-repeat domains affect nucleocytoplasmic transport and viability of yeast cells depending on whether these nucleoporins are located symmetrically or asymmetrically in the NPC architecture (Strawn, Shen et al. 2004). In this context, asymmetric FG-repeat domains were found to be dispensable for the survival of the cells and nuclear import of cargos, whereas additional disruption of symmetric FG-repeat domains rapidly affects distinct nuclear transport pathways and cell survival, such as the deletion of the FG-repeat domains of Nsp1p, the yeast homologue of p62 (Carmo-Fonseca, Kern et al. 1991). Our study identifying the p62 complex as asymmetric, however, suggest that the disruption of asymmetric FG-repeat domains can cause severe defects in nuclear transport, which might lead to cell death. This indicates that the specific requirement of an individual nucleoporin for nucleocytoplasmic transport might depend more on its specific interaction partners rather than on its asymmetric or symmetric distribution within the NPC.

Taken together, we could show that p62, p54, and, most likely, p58 are anchored to the cytoplasmic face of the NPC by their C-terminal coiled-coil domains. The FG-repeat domain of p62 appears to be mobile within the NPC and can reach into and through the central pore from its cytoplasmic anchoring site to the nuclear face of the NPC. By contrast, the FG-repeat domains of p54 and p58 were detected exclusively close to their anchoring site on the cytoplasmic face of the NPC, suggesting that they exhibit no or only limited structural flexibility (Fahrenkrog, Maco et al. 2002; Strelkov, Herrmann et al. 2002).

Further biophysical and structural studies of the isolated p62 complex will be required to show how the different nucleoporins of the p62 complex precisely interact with each other and the neighbouring subcomplexes of the NPC and how they enable import and export.

## 2.4. Materials and methods

### 2.4.1. Antibody production and purification

A C-terminal fragment of *Xenopus laevis* p62 (residues 332-547) was amplified by PCR and inserted into BamHI-NotI digested pGEX-6P-1 expression vector (Amersham, Pittsburgh, USA), which was modified by insertion of a TEV protease cleavage site upstream to the multiple cloning site, using site directed mutagenesis. N-terminal GST-tagged p62 was expressed in *E. coli* BL21 (DE3) cells and purified on a GSTrap column (Amersham, Pittsburgh, USA). Soluble protein fractions were collected and the GST-tag was removed by digestion with TEV protease, which was fused to a 6xHis-tag, and purification on a second GSTrap column. Finally the TEV protease was removed with a Ni-chelating column (GE Healthcare, Pittsburgh, USA). All buffers were containing 0.1% Triton-100 to increase the amount of soluble p62. Purified protein was used to inoculate a rabbit (Eurogentec, Liege, Belgium) and rabbit serum of the final bleeding was affinity purified using the corresponding recombinant p62 fragment bound to CNBr-activated Sepharose 4 Fast Flow (Amersham, Pittsburgh, USA).

For immunoblotting, *Xenopus* egg or HeLa whole cell extracts were separated on a 12% (w/v) polyacrylamide gel by SDS-PAGE and transferred onto a PVDF membrane. The membrane was blocked with 0.1% I-Block (Applied Biosystems, Lincoln, USA) in PBS containing 0.1% Tween-20. Affinity purified anti-p62 antibody was used at a 1:50 dilution for immunoblots. Antibody signals were detected by chemiluminescence using CDP-Star (Applied Biosystems, Lincoln, USA).

### 2.4.2. Isolation of *Xenopus* oocyte nuclei

Mature (stage 6) oocytes were surgically removed from female *Xenopus laevis* and the nuclei were isolated as described (Pante, Bastos et al. 1994).

### 2.4.3. Direct conjugation of antibodies to colloidal gold

The colloidal gold was prepared and conjugated to antibodies as described previously (Fahrenkrog, Maco et al. 2002).

### 2.4.4. Labeling of isolated nuclei from *Xenopus* oocytes

Labeling, fixation, and quick-freeze/freeze-drying/rotary metal-shadowing was performed as described (Fahrenkrog, Maco et al. 2002). Electron micrographs of thin-sectioned samples were recorded with a Hitachi H-7000 transmission electron microscope (Hitachi, Tokyo, Japan), operated at an acceleration voltage of 100 kV. Images of quick-frozen/freeze-dried/rotary metal-shadowed nuclei were recorded on an EM 912 Omega EFTEM (LEO Electron microscopy, Oberkochen, Germany) at an acceleration voltage of 120 kV equipped with a slow-scan CCD camera with a 2-MHz read-out, 16-bit information depth, 1024×1024-pixel CCD chip, pixel size 19  $\mu\text{m}$ , and a P43 phosphorus scintillator (Proscan, Scheuring, Germany).

### 2.4.5. Quantification of gold labeling at the NPCs and calculation of location clouds

The position of the gold particles associated with the NPCs was measured from electron micrographs of cross-sections along the NE of Epon-embedded, thin-sectioned isolated nuclei. For each gold particle its distance perpendicular to the central plane of the NPC and from the eightfold symmetry axis of the NPC was determined. All counted particles were blotted in histograms. The linear dimensions of the *Xenopus* NPC in Epon-embedded, thin-sectioned isolated nuclei were calculated from unlabeled NEs to estimate the dimensions of the NPC under the experimental conditions used. Location clouds were calculated as described (Fahrenkrog, Aris et al. 2000).

### 2.4.6. Microinjection of tagged p62, p54 and p58

Full-length *Xenopus* p62 was amplified by PCR and cloned between the unique EcoRI and XhoI sites of pcDNA3.1/myc-His (Invitrogen, Carlsbad, CA, USA) to produce C-terminally tagged p62-myc. To produce N-terminally tagged GFP-p62, full length *Xenopus laevis* p62 was amplified by PCR and cloned into EcoRI/BamHI cut pEGFP-C1 (Clontech, Palo Alto, CA, USA). Rat p54 and p58 were amplified by PCR and inserted into the BamHI/NotI cut pcDNA3.1/myc-His vector or cloned between the unique EcoRI and BamHI sites of pEGFP-C1, respectively. Microinjection of the plasmids into *Xenopus* oocytes were performed as described (Fahrenkrog and Aebi, 2002)



## 2.5. Acknowledgements

The authors thank Larry Gerace for providing cDNA of rat p54 and p58 and Volker Cordes for the cDNA of *Xenopus* p62. Ueli Aebi is greatly acknowledged for critical reading the manuscript and Daniel Stoffler for helpful discussions. Vesna Olivieri is acknowledged for experimental and technical support. This work was supported by research grants from the Swiss National Science Foundation (to B.F.), by the Kanton Basel Stadt, and the M.E. Müller Foundation.

## 2.6. References

- Bayliss, R., Littlewood, T. & Stewart, M. (2000). Structural basis for the interaction between FxFG nucleoporin repeats and importin-beta in nuclear trafficking. *Cell* 102: 99-108.
- Bednenko, J., Cingolani, G. & Gerace, L. (2003). Nucleocytoplasmic transport: navigating the channel. *Traffic* 4: 127-35.
- Buss, F. & Stewart, M. (1995). Macromolecular interactions in the nucleoporin p62 complex of rat nuclear pores: binding of nucleoporin p54 to the rod domain of p62. *J Cell Biol* 128, 251-61.
- Carmo-Fonseca, M., Kern, H. & Hurt, E. C. (1991). Human nucleoporin p62 and the essential yeast nuclear pore protein NSP1 show sequence homology and a similar domain organization. *Eur J Cell Biol* 55: 17-30.
- Cordes, V. C. & Krohne, G. (1993). Sequential O-glycosylation of nuclear pore complex protein gp62 in vitro. *Eur J Cell Biol* 60: 185-95.
- Cronshaw, J. M., Krutchinsky, A. N., Zhang, W., Chait, B. T. & Matunis, M. J. (2002). Proteomic analysis of the mammalian nuclear pore complex. *J Cell Biol* 158: 915-27.
- Dabauvalle, M. C., Benavente, R. & Chaly, N. (1988). Monoclonal antibodies to a Mr 68,000 pore complex glycoprotein interfere with nuclear protein uptake in *Xenopus* oocytes. *Chromosoma* 97: 193-7.
- Davis, L. I. & Blobel, G. (1986). Identification and characterization of a nuclear pore complex protein. *Cell* 45: 699-709.
- Davis, L. I. & Blobel, G. (1987). Nuclear pore complex contains a family of glycoproteins that includes p62: glycosylation through a previously unidentified cellular pathway. *Proc Natl Acad Sci U S A* 84: 7552-6.
- Denning, D. P., Uversky, V., Patel, S. S., Fink, A. L. & Rexach, M. (2002). The *Saccharomyces cerevisiae* nucleoporin Nup2p is a natively unfolded protein. *J Biol Chem* 277: 33447-55.
- Denning, D. P., Patel, S. S., Uversky, V., Fink, A. L. & Rexach, M. (2003). Disorder in the nuclear pore complex: the FG repeat regions of nucleoporins are natively unfolded. *Proc Natl Acad Sci U S A* 100: 2450-5.
- Fahrenkrog, B., Aris, J. P., Hurt, E. C., Pante, N. & Aebi, U. (2000). Comparative spatial localization of protein-A-tagged and authentic yeast nuclear pore complex proteins by immunogold electron microscopy. *J Struct Biol* 129: 295-305

- Fahrenkrog, B. & Aebi, U. (2002). The vertebrate nuclear pore complex: from structure to function. *Results Probl Cell Differ* 35: 25-48.
- Fahrenkrog, B., Maco, B., Fager, A. M., Koser, J., Sauder, U., Ullman, K. S. & Aebi, U. (2002). Domain-specific antibodies reveal multiple-site topology of Nup153 within the nuclear pore complex. *J Struct Biol* 140: 254-67.
- Fahrenkrog, B. & Aebi, U. (2003). The nuclear pore complex: nucleocytoplasmic transport and beyond. *Nat Rev Mol Cell Biol* 4: 757-66.
- Fahrenkrog, B., Koser, J. & Aebi, U. (2004). The nuclear pore complex: a jack of all trades? *Trends Biochem Sci* 29: 175-82.
- Finlay, D. R., Meier, E., Bradley, P., Horecka, J. & Forbes, D. J. (1991). A complex of nuclear pore proteins required for pore function. *J Cell Biol* 114: 169-83.
- Frosst, P., Guan, T., Subauste, C., Hahn, K. & Gerace, L. (2002). Tpr is localized within the nuclear basket of the pore complex and has a role in nuclear protein export. *J Cell Biol* 156: 617-30.
- Guan, T., Muller, S., Klier, G., Pante, N., Blevitt, J. M., Haner, M., Paschal, B., Aebi, U. & Gerace, L. (1995). Structural analysis of the p62 complex, an assembly of O-linked glycoproteins that localizes near the central gated channel of the nuclear pore complex. *Mol Biol Cell* 6: 1591-603.
- Hu, T., Guan, T. & Gerace, L. (1996). Molecular and functional characterization of the p62 complex, an assembly of nuclear pore complex glycoproteins. *J Cell Biol* 134: 589-601.
- Hu, T. & Gerace, L. (1998). cDNA cloning and analysis of the expression of nucleoporin p45. *Gene* 221: 245-53.
- Jarnik, M. & Aebi, U. (1991). Toward a more complete 3-D structure of the nuclear pore complex. *J Struct Biol* 107: 291-308.
- Krull, S., Thyberg, J., Bjorkroth, B., Rackwitz, H. R. & Cordes, V. C. (2004). Nucleoporins as components of the nuclear pore complex core structure and Tpr as the architectural element of the nuclear basket. *Mol Biol Cell* 15: 4261-77.
- Lim, R. Y., Aebi, U. & Stoffler, D. (2006a). From the trap to the basket: getting to the bottom of the nuclear pore complex. *Chromosoma* 115: 5-26.
- Lim, R. Y., Huang, N. P., Koser, J., Deng, J., Lau, K. H., Schwarz-Herion, K., Fahrenkrog, B. & Aebi, U. (2006b). Flexible phenylalanine-glycine nucleoporins as entropic barriers to nucleocytoplasmic transport. *Proc Natl Acad Sci U S A* 103: 9512-7.

- Matsuura, Y., Lange, A., Harreman, M. T., Corbett, A. H. & Stewart, M. (2003). Structural basis for Nup2p function in cargo release and karyopherin recycling in nuclear import. *Embo J* 22: 5358-69.
- Melcak, I., A. Hoelz, et al. (2007). "Structure of Nup58/45 suggests flexible nuclear pore diameter by intermolecular sliding." *Science* 315: 1729-32.
- Pante, N., Bastos, R., McMorro, I., Burke, B. & Aebi, U. (1994). Interactions and three-dimensional localization of a group of nuclear pore complex proteins. *J Cell Biol* 126: 603-17.
- Paulillo, S. M., Phillips, E. M., Koser, J., Sauder, U., Ullman, K. S., Powers, M. A. & Fahrenkrog, B. (2005). Nucleoporin domain topology is linked to the transport status of the nuclear pore complex. *J Mol Biol* 351: 784-98.
- Paulillo, S. M., Powers, M. A., Ullman, K. S. & Fahrenkrog, B. (2006). Changes in nucleoporin domain topology in response to chemical effectors. *J Mol Biol* 363: 39-50.
- Reichelt, R., Holzenburg, A., Buhle, E. L., Jr., Jarnik, M., Engel, A. & Aebi, U. (1990). Correlation between structure and mass distribution of the nuclear pore complex and of distinct pore complex components. *J Cell Biol* 110: 883-94.
- Rout, M. P., Aitchison, J. D., Suprapto, A., Hjertaas, K., Zhao, Y. & Chait, B. T. (2000). The yeast nuclear pore complex: composition, architecture, and transport mechanism. *J Cell Biol* 148: 635-51.
- Schwartz, T. U. (2005). Modularity within the architecture of the nuclear pore complex. *Curr Opin Struct Biol* 15: 221-6.
- Stoffler, D., Feja, B., Fahrenkrog, B., Walz, J., Typke, D. & Aebi, U. (2003). Cryo-electron tomography provides novel insights into nuclear pore architecture: implications for nucleocytoplasmic transport. *J Mol Biol* 328: 119-30.
- Strawn, L. A., Shen, T., Shulga, N., Goldfarb, D. S. & Wentz, S. R. (2004). Minimal nuclear pore complexes define FG repeat domains essential for transport. *Nat Cell Biol* 6: 197-206.
- Strelkov, S. V., Herrmann, H., Geisler, N., Wedig, T., Zimbelmann, R., Aebi, U. & Burkhard, P. (2002). Conserved segments 1A and 2B of the intermediate filament dimer: their atomic structures and role in filament assembly. *Embo J* 21: 1255-66.
- Tran, E. J. & Wentz, S. R. (2006). Dynamic nuclear pore complexes: life on the edge. *Cell* 125: 1041-53.

## **Influence of antibodies against the p62 complex on nucleocytoplasmic transport**

<sup>1</sup>Kyrill Schwarz-Herion, <sup>2</sup>Tinglu Guan, <sup>1</sup>Ursula Sauder, <sup>2</sup>Larry Gerace, and <sup>1</sup>Birthe Fahrenkrog\*

<sup>1</sup>M.E. Mueller Institute for structural Biology, Biozentrum, University of Basel, Klingelbergstrasse 70,  
4056 Basel Switzerland

<sup>2</sup>The Scripps Research Institute, La Jolla, California 92037, USA



### Summary

Nuclear pore complexes (NPCs) are large protein complexes, which are embedded in the nuclear envelope (NE) and control the traffic of proteins and RNAs between the nucleus and the cytoplasm in a signal-dependent manner. Transport receptors bind cargos and interact particularly with certain nucleoporins. Phenylalanine-glycine (FG) repeat motifs were found in about a third of the nucleoporins, functioning as a major docking site for soluble transport receptors. The p62 complex, which contains several FG repeat domains, was previously described to be involved in protein import and to interact directly with soluble transport receptors. To examine the localization of this docking site and to find out how antibodies against single components of the p62 complex influence nucleocytoplasmic transport, we performed *in vitro* transport assays using nucleoplasmin-GFP as cargo. This cargo was used in transport assays with digitonin-permeabilized HeLa cells, which were treated with antibodies against the p62 complex components, or was directly conjugated to colloidal gold in ultrastructural transport assays, using isolated nuclei from *Xenopus* oocytes. Our data suggest that antibodies against the components of the p62 complex inhibit or reduce transport of cargos through the NPC. The ultrastructural transport studies revealed that the second docking site for cargo/receptor complexes is masked when p62 complex antibodies are used in the transport assay.

### 3.1. Introduction

Nuclear pore complexes (NPCs) are large protein assemblies located in the double-membrane of the nuclear envelope (NE), regulating the transport of proteins and RNAs between the cytoplasm and the nucleus of eukaryotic cells (Fried and Kutay 2003; Pemberton and Paschal 2005). Proteomics studies in mammalian and yeast cells showed that the NPC is composed from multiple copies of about 30 nucleoporins, which are assembled in different subcomplexes (Rout, Aitchison et al. 2000; Cronshaw, Krutchinsky et al. 2002; Schwartz 2005). The 3D-architecture of the NPC was determined by cryo-electron microscopy (cryo-EM) studies in yeast and higher eukaryotes. The NPC architecture exhibits a tripartite architecture with an 8-fold rotational symmetry, an overall dimension of about 180 nm perpendicular to the plane of the NE, and a total mass of about 125 MDa (Reichelt, Holzenburg et al. 1990; Hinshaw, Carragher et al. 1992; Akey and Radermacher 1993; Stoffler, Fahrenkrog et al. 1999; Fahrenkrog and Aebi 2003; Stoffler, Feja et al. 2003; Beck, Forster et al. 2004). The NPC is composed of a central framework, which is embedded in the double membrane of the NE and is sandwiched between a cytoplasmic ring moiety and nuclear ring moiety (Stoffler, Feja et al. 2003). Eight short, kinky fibrils emanate from the cytoplasmic ring moiety, whereas the nuclear ring is capped with a cage-like structure, termed nuclear basket. The central framework encloses the central pore of the NPC, which is the transport channel for all trafficking between the nucleus and cytoplasm. The central pore has a length of about 90 nm and has a diameter of about 45-50 nm at its narrowest point (Fahrenkrog and Aebi 2003; Stoffler, Schwarz-Herion et al. 2006).

Nuclear import of proteins and RNPs is mediated by a large, evolutionarily conserved family of transport receptors, the importin- $\beta$  family (Conti, Muller et al. 2006). Importins bind to their cargos in the cytoplasm via recognition of its nuclear localization sequence (NLS) (Lanford and Butel 1984; Adam, Lobl et al. 1989). The importin/cargo complex translocates into the nucleus via interaction with NPC proteins (Bednenko, Cingolani et al. 2003; Lim, Koser et al. 2007). In the nucleus, the importin/cargo-complex is dissociated by RanGTP, replacing the cargo from the importin/cargo complex (Stewart 2006). While the biochemical regulation of the transport of cargos into the nucleus is well understood, the exact mechanism of translocation and interaction of transport receptors with the NPC is still elusive. Recent studies, however, proposed a new mechanism for the selective gating of transport receptors (Lim, Aebi et al. 2006; Lim and Fahrenkrog 2006; Lim, Fahrenkrog et al. 2007). The transport receptors bind during the translocation process mainly to phenylalanine-glycine (FG) repeat motifs, which are found in about



a third of the nucleoporins (Patel, Belmont et al. 2007). These repeat domains are composed of hydrophobic FG patches, that are spaced by hydrophilic linkers (Denning and Rexach 2007). The nucleoporins possessing FG-repeat domains are mainly distributed at the cytoplasmic and the nucleoplasmic face of the NPC, respectively (Fahrenkrog and Aebi 2003).

One prominent subcomplex, containing several FG-repeat domains involved in nucleocytoplasmic transport, is the p62 complex (Finlay, Meier et al. 1991). Biochemical dissection of the p62 complex revealed that it is composed of 3-4 nucleoporins, which directly interact with each other (Finlay, Meier et al. 1991; Guan, Muller et al. 1995; Hu, Guan et al. 1996). The nucleoporins of the p62 complex – p62, p54, p58, and p45 – contain FG-repeat domains, which bind to transport receptors and coiled-coil domains, which probably mediate the interaction with each other and with neighbored NPC subcomplexes (Dabauvalle, Benavente et al. 1988; Finlay, Meier et al. 1991; Hu, Guan et al. 1996). Additionally, the nucleoporins p62 and p58 are glycosylated by O-acetylglucosamin. The influence of the p62 complex on nucleocytoplasmic transport was shown in p62-complex-depleted, reconstituted nuclei as well as in cells, which were treated with antibodies against p62 (Dabauvalle, Benavente et al. 1988; Finlay, Meier et al. 1991). A RNAi study of the p62 complex homologues in *C. elegans* revealed leaking NPCs, i.e. an increase of diffusion of large cargos without NLS when the components of the p62 complex were depleted by RNAi (Galy, Mattaj et al. 2003; Schetter, Askjaer et al. 2006). Based on the X-ray structure of the p58/p45 dimer, a sliding mechanism was proposed for the p62 complex, changing the diameter of the central channel to facilitate the transport of cargos (Melcak, Hoelz et al. 2007).

The transport of cargos through the NPC was examined on the level of fluorescence microscopy as well as on electron microscopy level (Adam, Sterne-Marr et al. 1992; Pante and Aebi 1996; Yang, Gelles et al. 2004; Yang and Musser 2006). Ultrastructural studies of nuclear export with microinjected gold-conjugated proteins showed that nuclear import of macromolecules occurs through the nuclear pores. Studies with gold-conjugated nucleoplasmin, microinjected into oocytes of *Xenopus laevis*, revealed distinct binding steps of the import complex during the transport through the NPC (Pante and Aebi 1996; Rollenhagen, Muhlhauser et al. 2003). In the first translocation step, the import complex binds at about 50 nm from the central plane of the NPC at the cytoplasmic filaments, which mainly consist of the nucleoporin Nup358 (Melchior, Guan et al. 1995; Yokoyama, Hayashi et al. 1995). The second docking site of the import complex is located at the cytoplasmic periphery of the NPC about 13 nm from the central channel of the NPC. At the nuclear side of the NPC, the import complex was predominantly found at 10-

20 nm from the central channel. A fourth docking site was observed in cells at the nuclear basket when import is followed in the presence of a mutant form of importin  $\beta$ , that does not bind Ran (Gorlich, Pante et al. 1996). Blocking of the central channel by microinjection of WGA-coated gold particles leads to an accumulation of import complexes at the cytoplasmic filaments, inhibiting the delivery from the first binding region to the second binding region at the entry to the gated channel. WGA is a lectine, which recognizes about 10 glycosylated nucleoporins, including the components of the p62 complex (Pante and Aebi 1996). A phenomenon, which was also observed during the translocation process, was the inward bending of cytoplasmic filaments to the entry of the central channel, handing the cargo over to the second binding site (Pante and Aebi 1996). In the papers of Beck et al. about a 3D-reconstruction of native NPCs, based on cryo-Tomography, changes in the conformation of cytoplasmic filaments binding to cargos were observed (Beck, Forster et al. 2004; Beck, Lucic et al. 2007). Different conformational states of the NPC were analyzed, and one of these conformational changes was interpreted as slow incorporation or release of cargo complexes into or from the FXFG-framework residing in the central channel, which involves interaction with the cytoplasmic filaments.

*In vitro* transport assays were developed to observe nucleocytoplasmic transport of fluorescence-labeled cargos in digitonin permeabilized cells (Adam, Sterne-Marr et al. 1992). Quantification of this assay can be achieved by using fluorescence-activated cell sorting (FACS)(Paschal and Gerace 1995). Some studies deal with microinjection of labeled cargos in the cytoplasm or nucleoplasm to get insight into the kinetics of nucleocytoplasmic transport (Riddick and Macara 2005).

In recent years, the transport was also examined by single molecule microscopy. Yang et al. showed how a single fluorescence-labeled cargo travels through the NPC and revealed the binding kinetics of cargos to the NPC. The import complex spends the majority of its 10-ms interaction time with the NPC, moving within a comparatively small region corresponding to the NPC central region (Yang, Gelles et al. 2004). The movement of the cargo through the NPC bears the characteristics of a bi-directional, rapid random walk and is rate-limited by only one or at most a few reaction steps (Yang, Gelles et al. 2004). Kubitschek et al. examined the dwell times at the NPC of the fluorescence-labeled transport receptors NTF2 and transportin in a single-molecule fluorescence experiment (Kubitschek, Grunwald et al. 2005). The dwell-times for NTF2 and transportin ranged between 5.8 and 7.2 ms, respectively, indicating a different transport time for different receptors. Import kinetics of karyopherins was also quantified *in vivo* in single yeast cells and reconstituted nuclei (Timney, Tetenbaum-Novatt et al. 2006; Kopito and Elbaum

2007). This study showed that import rates are simply governed by the concentration of the karyopherins, the concentration of their cargo, and the affinity between them (Timney, Tetenbaum-Novatt et al. 2006).

To determine the influence of antibodies against full length p62, p54, and p58 on the importin  $\beta$  import pathways, we used nucleoplasmin-GFP as a cargo in an *in vitro* transport assay. The assay was performed with permeabilized, unfixed HeLa cells on fluorescence microscopy level; isolated nuclei from *Xenopus* oocytes were used for an assay to observe the import assay of gold-conjugated nucleoplasmin on ultrastructural level. Our data indicate the influence of the p62 complex and its compounds on nucleoplasmic transport and confirm the localization of the p62 complex at the entry of the central channel

### 3.2. Results

#### 3.2.1. Ultrastructural nuclear import assay

To study the role of the p62 complex in nuclear protein import at the ultrastructural level, we used isolated nuclei from *Xenopus laevis* oocytes to employ an *in vitro* transport assay. To do so, the nuclei were first incubated for 30 minutes in low salt buffer (LSB) or LSB containing antibodies against p62 complex nucleoporins, respectively. Next, the nuclei were transferred into transport buffer containing cytosolic extracts from HeLa cells, ATP, an energy regenerating system, and GFP-nucleoplasmin, that has been directly conjugated to 8-nm colloidal gold as cargo. The import of the cargo was stopped after different points in time (5, 10 or 30 min) by fixation with 2% glutaraldehyde. Fixed samples of nuclei were processed for embedding and thin sectioning EM as described in Materials and Methods.

As shown in Fig. 3.1. (a), 3.1. (c) and 3.1. (d), GFP-nucleoplasmin first binds to the cytoplasmic filaments (i.e. at a distance of 30-60 nm from the NPC's central plane) and next to the cytoplasmic entrance of the central pore (i.e. at a distance of 10-25 nm from the central plane). After translocation through the central pore, the GFP-nucleoplasmin was found at the nuclear entrance/exit of the central pore (i.e. at a distance of -30 nm from the central plane) and, finally, at the nuclear basket (i.e. at a distance of -100 to -120 nm from the central plane). Together, the results of the ultrastructural assay correspond well with the results of similar ultrastructural import assays, using equally nucleoplasmin as an import cargo (Pante and Aebi 1996; Rutherford, Goldberg et al. 1997).

The results from the ultrastructural transport should be confirmed by assays in HeLa cells, that allowed to visualize whole nuclei and the accumulation of GFP-nucleoporin in the nucleus over time. The *in vitro* transport experiments in digitonin-permeabilized HeLa cells show transport of GFP-nucleoplasmin into the nucleus at different points in time at fluorescence microscope level. 5 minutes after the start of the transport assay, a rim stain of the GFP-labeled cargo was observed. After 15 minutes, the rim stain was significantly reduced and the cargo was dispersed in the nucleus. After 30 minutes, the green fluorescence signal completely accumulated in the nucleus (Fig. 3.1. (b)). Together, these *in vitro* experiments show the accumulation of import cargos over time and confirm the functionality of the ultrastructural *in vitro* assay.

To analyze the import pathways of the imported GFP-nucleoplasmin gold particles at the different import points in time were scored and analyzed in histograms regarding their distances from the central plane of the NPC or their distance to the 8-fold symmetry axis. The histograms in Fig. 3.1. (c) demonstrate the distribution of 8-nm gold particles, which were directly conjugated to GFP-nucleoplasmin, in the 3D structure of the NPC. The histograms on the left side show the distribution of the cargos relatively to the central plane of the NPC, whereas the histograms at the right side show the distribution of the gold-conjugated nucleoplasmin with regard to the 8-fold symmetry axis of the NPC. The ultrastructural import assay was done for the points in time 5, 15, and 30 minutes. In Fig. 3.1. (d), the localization of the gold particles during the import process is shown as localization clouds in a 3D-model of the NPC. To get a better overview of the different binding regions and different populations of the import cargo, the NPC was divided in different regions according to the different docking sites for the import complex. The division is described in 3.4. (Materials and Methods).

As schematically represented in Fig. 3.1. (d), the gold-conjugated cargo binds at the cytoplasmic filaments with an average distance of  $52.1 \pm 14.3$  nm from the central plane. Next, the binding region at the cytoplasmic entry of the central channel is located at about  $20.5 \pm 13.5$  nm from the central pore. At this time, only 8% of the gold particles are attached to the nuclear side of the NPC.

15 minutes after the start of the import assay, 29.3% of the counted gold particles were attached to the nuclear side. The number of particles attached to the cytoplasmic filaments was reduced from 77.8% after 5 minutes to 52.7% after 15 minutes. While the number of gold particles at the periphery of the central channel increased to 16.4%, 14.5% of the gold particles were found at the nuclear periphery of

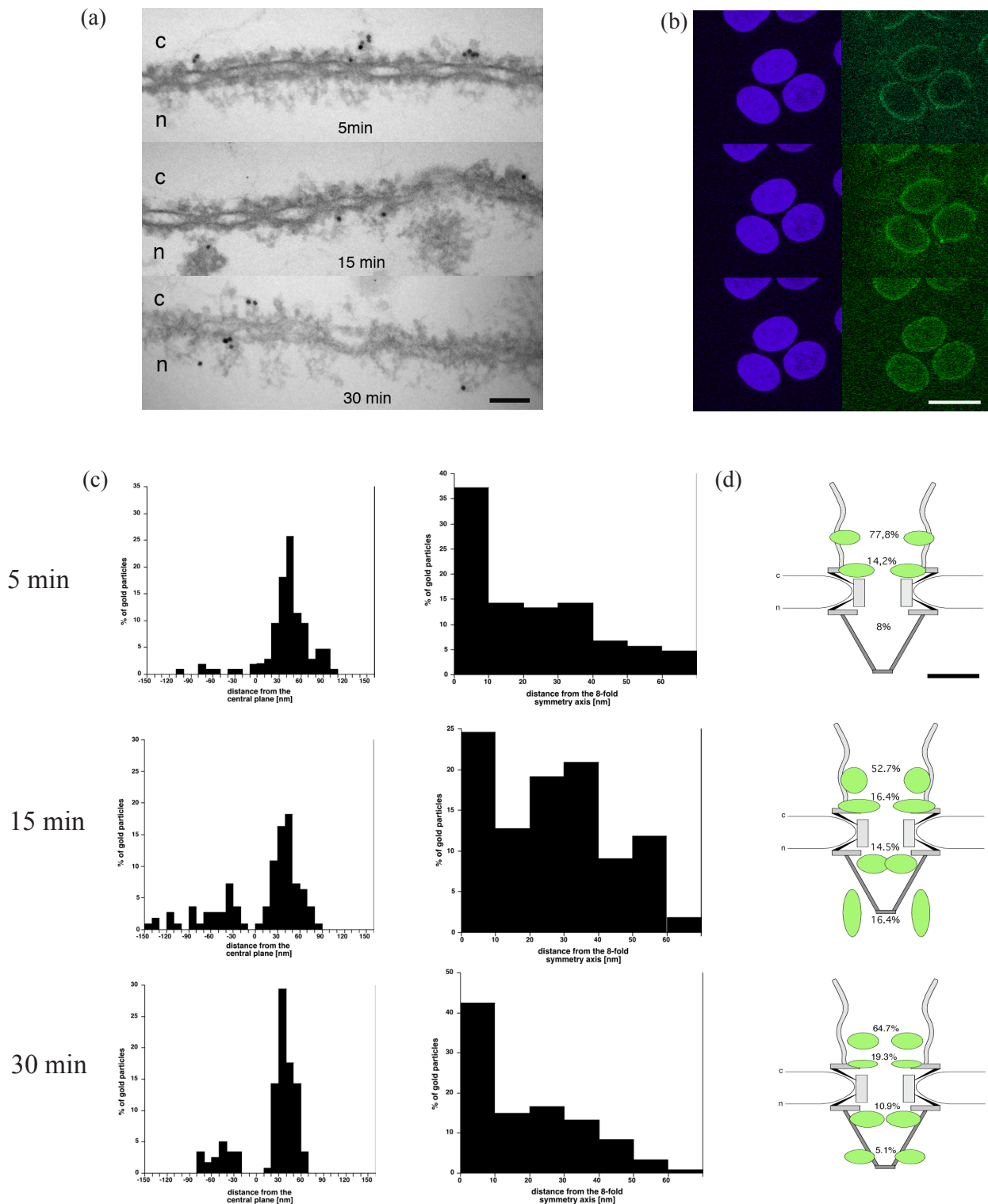


**Figure 3.1.** The nuclear import of gold-labeled nucleoplasmin-GFP. (a) Nuclear envelope cross sections from *Xenopus* nuclei are shown. The overview of the transport process shows the binding of the import complex to different parts of the NPC at the points in time 5, 15 and 30 minutes. Scale bar represents 100 nm. (b) The survey shows the corresponding import experiment with time-lapse fluorescence microscopy. The nucleus was stained with the blue DNA-binding dye DAPI. The fluorescence pictures at the different points in time show the stepwise accumulation of the green fluorescent cargo in the nucleus. Scale bar represents 20  $\mu$ m. (c) The histograms show the distribution of cargo gold particles in the 3D-architecture of the NPC during the import process. statistics at point in time 119 particles were counted. (d) Schematic representation of the distribution of cargo/importin-complexes within the 3-D architecture of the NPC at different points in time were attached to the nuclear basket.

the central channel at an average distance of  $-33.6 \pm 9.4$  nm from the central plane of the NPC and at an average distance of  $14.3 \pm 15.9$  nm from the 8-fold symmetry axis. As shown in the model at time 15 minutes, the distances of the localization clouds at the cytoplasmic and the nuclear entry of the central channel differed significantly regarding the distance from the 8-fold symmetry axis. The cargos transported to the nuclear basket of the NPC seem to diffuse away from the nuclear basket as demonstrated by the bigger distance from the 8-fold symmetry axis of  $33.3 \pm 9.0$  nm (average distance from the central plane:  $-80.9 \pm 23.3$ ).

Altogether, at the point in time 30 minutes, the number of gold particles attached to the nuclear side of the NPC was reduced to 16.0%. Compared to the distances at the points in time 5 and 15 minutes, the distance between gold particles attached to the cytoplasmic filaments and the 8-fold symmetry axis was reduced to  $20.4 \pm 15.2$  nm.

### 3.2.2. Transport of nucleoplasmin is delayed by antibodies against the C-terminal domain of p62

To test whether or not antibodies against single compounds of the p62 complex influence the nuclear import of GFP-nucleoplasmin, its import was studied after preincubation of *Xenopus* oocytes nuclei with a polyclonal antibody against the full length rat nucleoporin p62, a polyclonal antibody against the C-terminal region of the *Xenopus* p62, and a monoclonal antibody against the N-terminal region of the mammalian p62, respectively (Carmo-Fonseca, Kern et al. 1991; Hu, Guan et al. 1996).

We found that in HeLa cells an excess of the N-terminal p62 antibody leads to a slight delay of the nuclear import of GFP-cargo, as compared to control experiments, but does not lead to a complete inhibition of nuclear import (Fig. 3.1 and 3.2. (a)). In contrast, the antibodies against full length rat p62 and the C-terminal domain of p62 (Fig. 3.2 (b) and (c)) lead to a partial inhibition of nuclear import of GFP-nucleoplasmin, indicated by an accumulation of the cargo at the nuclear rim.

In the ultrastructural import experiment with the antibody against the N-terminus of p62, the amount of attached cargos at the nucleoplasmic side of the NPC after 30 minutes transport was higher than at the same time in the control experiment (25.4% vs. 16.0%). A detail, which could be observed at 15 minutes after start of the experiment, is that the amount of gold-conjugated cargos at the region 0-30 nm from the central plane of the NPC was significantly reduced to 4.5% of all events compared to 17.9% in the control experiment.

In the transport experiments with the antibody against the full length p62 (3.2. (e)), at the time 30 minutes the number of gold particles attached to the nuclear side was significantly reduced compared to the control experiment (the percentage of counted gold particles at the nuclear side dropped from 16.0% to 4.5%), whereas at point in time 5 minutes there was a slightly increased number of gold particles at the nuclear side (11.4% vs. 8%).

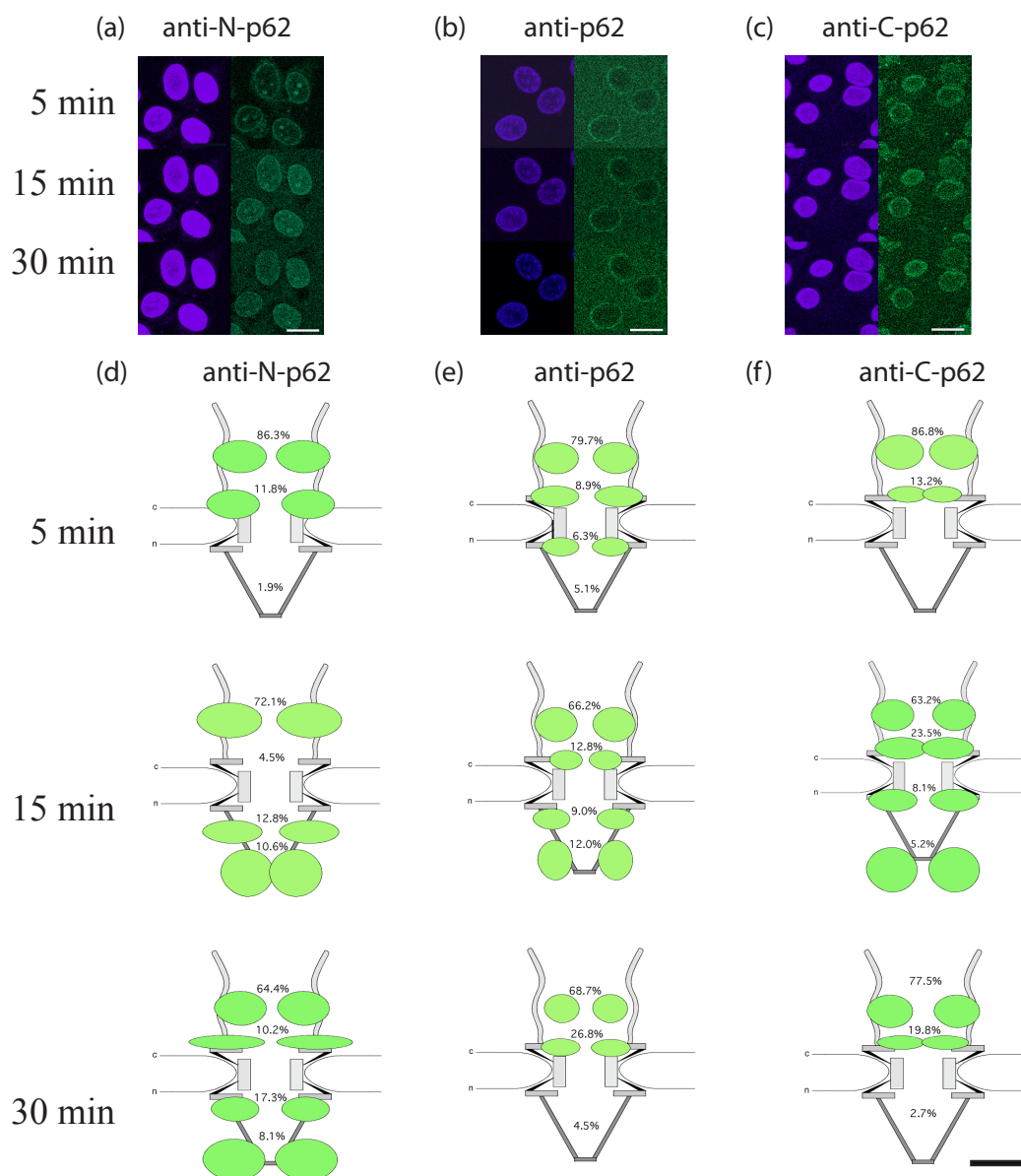
In the import assay using the C-terminal p62 antibody, a significant reduction of import cargo at the nuclear side was observed as well (Fig. 3.2. (f)). At the time 5 minutes, import of cargos was completely blocked. The amount of gold particles attached to the nuclear side of the NPC at time 15 minutes was reduced from 29.3% in the control experiment to 13.3% with the C-terminal p62 antibody. There were nearly no gold particles found at the nuclear side at the point in time 30 minutes.

### **3.2.3. Antibodies against the nucleoporins p54 and p58 have different impact on the nuclear import of GFP-nucleoplasmin**

Next, the influence on the nucleocytoplasmic transport of antibodies raised against the full length mammalian nucleoporins p54 and p58 was examined (Fig. 3.3.).

In the ultrastructural transport experiment using the p54 antibody (Fig. 3.3.(c)), the import of the cargo was first promoted at the time 5 minutes (an increase to 26.2% of counted gold particles compared to 8% gold particles at the nuclear side in the control experiment). The percentage of transport cargos attached to the nuclear side dropped down to 4.5% and 5.4% at the points in time 15 minutes and 30 minutes, respectively.

Nucleocytoplasmic transport was affected by the polyclonal antibody raised against the full length rat p58 in a different way. At the time 5 minutes, the import of any cargo is completely inhibited. At the time 15 minutes, 13.9% gold particles were found at the nuclear side. At the time 30 minutes, the percentage of gold particles bound to the nuclear part of the NPC increased to 21.1% , which means a higher percentage of attached gold particles than in the control experiment. Summarizing the key feature of Fig. 3.3. (d), this means that the import of cargos is delayed when the p58 antibody is added to the ultrastructural import assay.



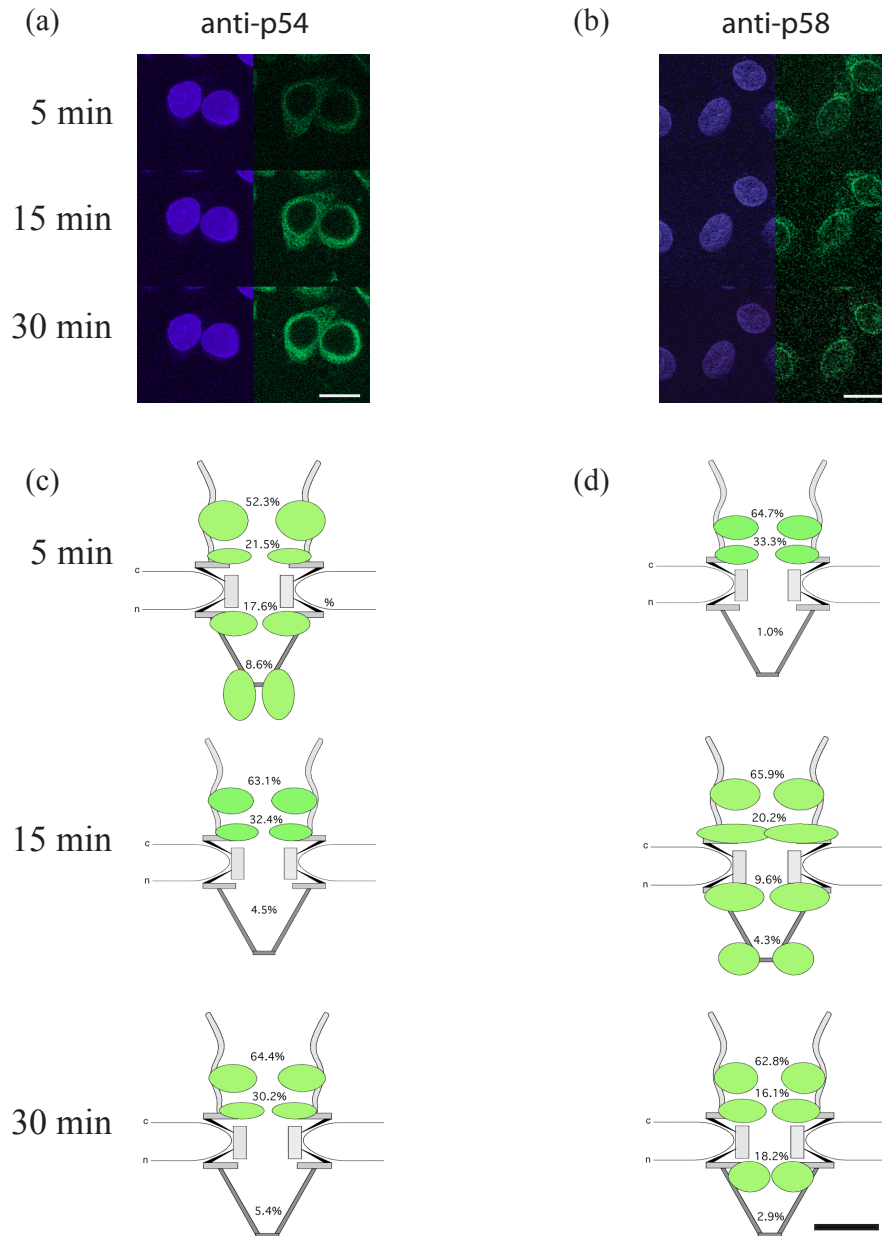
**Figure 3.2.** Influence of antibodies against different domains of the mammalian nucleoporin p62 on nuclear transport. (a) Fluorescence import assay with digitonin-permeabilized HeLa cells is illustrated. Before the import assay was started, cells were treated with 0.016 mg/ml monoclonal antibodies against the N-terminal domain of p62 (anti-N-p62). The survey shows the accumulation of nucleoplasmin-GFP (green) over time in the nucleus (blue). (b) Fluorescence import assay with digitonin-permeabilized HeLa cells is shown. Before the import assay was started, cells were treated with 0.016 mg/ml polyclonal antibodies against full length p62 (anti-p62). The survey shows the accumulation of nucleoplasmin-GFP (green) over time in the nucleus (blue). (c) Fluorescence import assay with digitonin-permeabilized HeLa cells is illustrated. Before the import assay was started, cells were treated with 0.016 mg/ml polyclonal antibodies against the C-terminal domain of *Xenopus* p62 (anti-C-p62). Scale bars: 20  $\mu$ m (d) Schematic representation of the distribution of cargo/importin-complexes within the 3-D architecture of the NPC at different points in time is shown. Transport assay was performed with 0.016 mg/ml antibody against anti-N-p62. For the different points in time following numbers of particles were counted: 50 for time 5 minutes, 89 for time 15 minutes and 197 for the point in time 30 minutes. (e) Schematic representation of the distribution of cargo/importin-complexes within the 3-D architecture of the NPC at different points in time is shown. Transport assay was performed with 0.016 mg/ml anti-p62. For the different points in time following numbers of particles were counted: 79 for time 5 minutes, 134 for time 15 minutes and 179 for time 30 minutes. (f) Schematic representation of the distribution of cargo/importin-complexes within the 3-D architecture of the NPC at different points in time is illustrated. Transport assay was performed with 0.016 mg/ml anti-C-p62. For the different points in time following numbers of particles were counted: 71 for time 5 minutes, 70 for time 15 minutes and 142 for time 30 minutes. Scale bar: 100 nm.



Fig. 3.3.(a) shows how the p54 antibody affects nucleocytoplasmic transport on fluorescence microscopy level. At the different points in time 5 min, 15 min, and 30 min, the rim stain of the GFP-labeled cargo showed that transport is completely inhibited during this time range. There is no indication that there is a higher import rate at point in time 5 minutes. The time-lapse fluorescence microscopy experiment with the p58 antibody in Fig 3.3.(b) shows that there is a visible rim stain at all points in time with some, few import of cargos but does not reflect the transport rates, which could be assumed from the ultrastructural experiment.

### **3.2.4. A combination of antibodies against the p62 complex inhibits nucleocytoplasmic import**

Next, we intended to analyze how antibodies against the p62 complex nucleoporins in combination affect the nuclear import of GFP-nucleoplasmin. The survey of micrographs in Fig. 3.4. (a) shows the accumulation of gold-conjugated cargos at the time 30 minutes when the import assay was performed with a mixture of antibodies against full length rat p62, p54, and p58. The ultrastructural nuclear import was also performed with a mixture of antibodies against different components of the p62 complex (Fig. 3.4. (d)). In all “snapshots” of the nuclear import event at point in time 30 minutes, only a very little amount of particles was observed at the nuclear side. Only slight differences regarding the percentages of gold particles attached to the first or second docking sites were observed. Again, when an antibody combination was used, which contains the antibody against full length p58, the localization cloud was focused at the cytoplasmic second docking site with an average distance from the central plane of about 25 nm. The fluorescence import assay in Fig. 3.4. (b) in the time range between 5 and 30 minutes, using antibodies against full length rat p62, p54, and p58, shows that the import is completely inhibited. The rim stain in this experiment is consistent with the control experiment in Fig. 3.4. (c). In the control experiment, the monoclonal antibody mAb414 is used, which recognizes mainly p62 but also a number of different FG-repeat domains and which is known to inhibit nuclear transport.



**Figure 3.3.** Influence of antibodies against the full length mammalian nucleoporins on nuclear transport. (a) Fluorescence import assay with digitonin-permeabilized HeLa cells is shown. Before the import assay was started, cells were treated with 0.016 mg/ml polyclonal antibodies against the nucleoporin p54 (anti-p54). The survey shows the transport of nucleoplasm-GFP (green) over time in the nucleus (blue). The green signal in the nucleus was weak at all points in time whereas the green rim staining increased over time. (b) Fluorescence import assay with digitonin-permeabilized HeLa cells is illustrated. Before the import assay was started, cells were treated with 0.016 mg/ml polyclonal antibodies against the nucleoporin p58 (anti-p58). The survey shows the transport of nucleoplasm-GFP (green) over time in the nucleus (blue). At all points in time a clear rim stain could be observed but there was also a slight increase of the green signal in the nucleus. Scale bars: 20  $\mu$ m (c) Schematic representation of the distribution of cargo/importin-complexes within the 3-D architecture of the NPC at different points in time is shown. Transport assay was performed with 0.016 mg/ml anti-p54. For the different points in time following numbers of particles were counted: 132 for the point in time 5 minutes, 111 for the point in time 15 minutes and 205 for the point in time 30 minutes. (d) Schematic representation of the distribution of cargo/importin-complexes within the 3-D architecture of the NPC at different points in time is illustrated. Transport assay was performed with 0.016 mg/ml anti-p58. For the different points in time, the following numbers of particles were counted: 96 for time 5 minutes, 96 for time 15 minutes and 137 for time 30 minutes. Scale bar: 100 nm.

### 3.3. Discussion

The mechanisms of selective import and export of cargos through the NPC are still elusive. Valuable information can be gleaned from ultrastructural import assays. Several studies, which dealt with nucleoplasmic transport on ultrastructural level, used microinjection of cargos and antibodies into *Xenopus* oocytes to dissect transport pathways (Pante and Aebi 1996; Rollenhagen, Muhlhauser et al. 2003; Zhong, Shio et al. 2006). It was demonstrated before that antibodies, which recognize a bunch of different FG-repeats, inhibit nuclear import and that, in such cases, cargos accumulate at the cytoplasmic filaments (Dabauvalle, Benavente et al. 1988; Pante and Aebi 1996). Significant progress was done in recent years in the field of single molecule fluorescence microscopy revealing the import steps and the kinetics of the nuclear import process (Yang, Gelles et al. 2004; Kubitscheck, Grunwald et al. 2005; Lill, Lill et al. 2006; Timney, Tetenbaum-Novatt et al. 2006; Kopito and Elbaum 2007). Equally, RNAi studies of nucleoporins combined with fluorescence microscopy showed further details, to which extent certain nucleoporins are involved in nucleocytoplasmic import (Galy, Mattaj et al. 2003; Hutten and Kehlenbach 2006; Schetter, Askjaer et al. 2006).

To give new insights into the mechanism of import, nucleoplasmin was used as an example of an import cargo. We examined the import of this cargo *in vitro* by fluorescence and electron microscopy. The nucleoporins of the p62 complex are known as putative docking sites for the importin/cargo complex. Until nowadays, it was not clear where the second docking site for an import complex is exactly located and how antibodies against single FG-repeat domains affect transport. To get information about the import pathway of nucleoplasmin and the role of the p62 complex in this context, we used antibodies against different domains of the p62 complex. We applied the antibodies in a concentration-dependent manner to be sure that they are used in excess relative to the antigen. We found that the nucleocytoplasmic system is robust and tolerates the masking of single FG-repeat domains. When certain domains, such as the N-terminal FG-repeat domain of p62, are masked, the import of nucleoplasmin into the nucleus is rather accelerated than delayed. When blocking transport by applying antibodies against the compounds of the p62 complex, the gold particles accumulated at a place above the putative position of the p62 complex in the 3D structure of the NPC. This observation supports localization data of the p62 complex domains recently published (Schwarz-Herion, Maco et al. 2007).

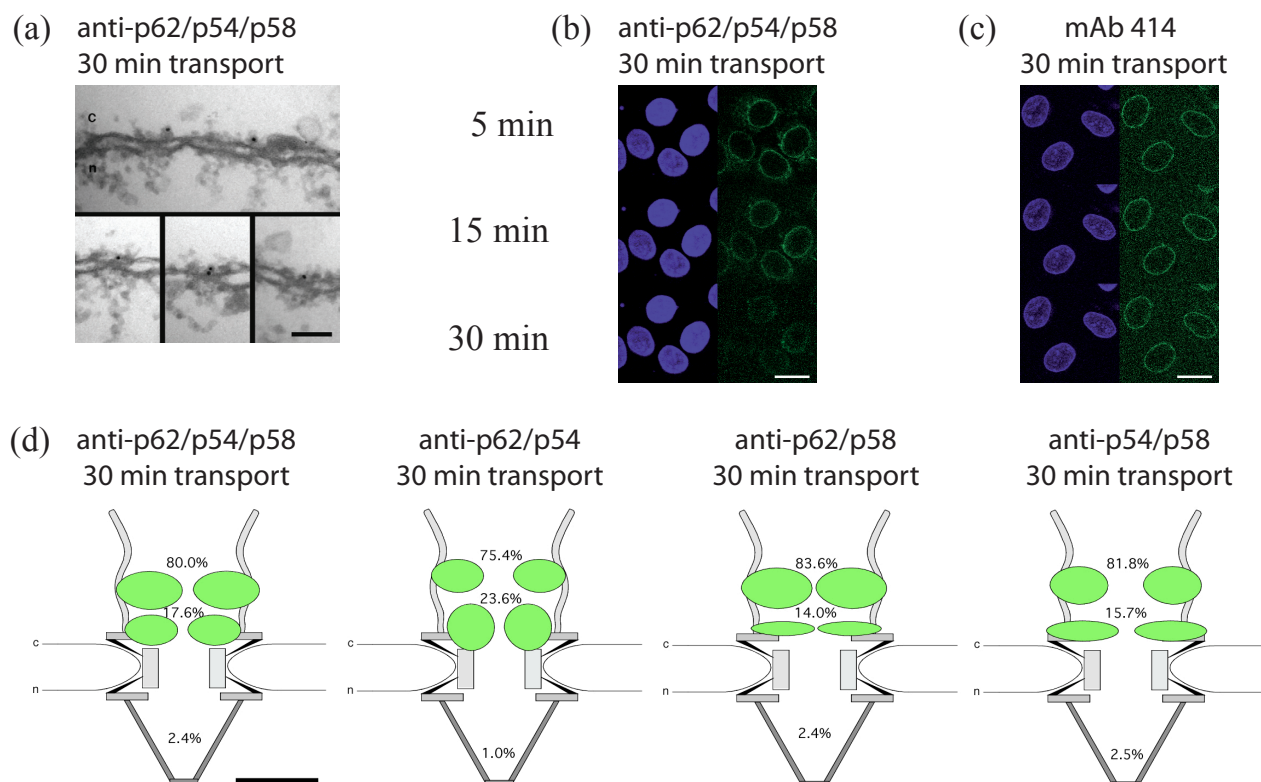


**Figure 3.4.** The nuclear import of gold-labeled nucleoplasmin-GFP. (a) Nuclear envelope cross sections from *Xenopus* nuclei are illustrated. Selected examples of gold-labeled NPCs in cross-section are shown. The selected micrographs show the binding of the import complex to the cytoplasmic face of the NPC at the point in time 30 minutes. (b) Fluorescence import assay with digitonin-permeabilized HeLa cells is shown. Before the import assay was started, cells were treated with 0.016 mg/ml of mixed polyclonal antibodies against the nucleoporins p62, p54 and p58 (anti-p62/p54/p58). The transport process at the points in time 5, 15 and 30 minutes is illustrated. (c) Control fluorescence import assay with digitonin-permeabilized HeLa cells is illustrated. Before the import assay was started, cells were treated with the monoclonal antibody mAb414 (excess; 1:1000 dilution of the commercial batch), which recognize different FG-repeat domains of several FG-repeat nucleoporins. The fluorescence microscopy pictures show the accumulation of the GFP-labeled cargo at the points in time 5, 15 and 30 minutes. Scale bars: 20  $\mu$ m (d) Schematic representation of the distribution of cargo/importin-complexes within the 3-D architecture of the NPC at points in time 30 minutes is shown. The experiment was performed with differently combined antibodies against the nucleoporins p62, p54, and p58. In all experiments only a minor population of 2.4% and 2.5%, respectively, of gold particles could be detected at the nuclear side after 30 minutes of transport. For the different experiments with different antibody mixtures following numbers of particles were counted: 170 particles in the experiment with anti-p62/p54/p58; 203 particles in the experiment with anti-p62/p54; 165 particles in the experiment with anti-p62/p58; 313 particles in the experiment with anti-p54/p58. Scale bar: 100 nm.

### 3.3.1. Interpretation of the results from the fluorescence and ultrastructural assay

First of all, the experiments on a fluorescence and ultrastructural level are not directly comparable for several reasons. The experiments on fluorescence level function as proof of concept, e.g. to test the functionality of the *in vitro* transport assay on a macroscopic level. The state of nuclear import was determined by the intensity of the fluorescence signal in the nucleus and the cytoplasm at different points in time.

In contrast, at the ultrastructural level, the accumulation of the cargos in the nucleus was not detected but the binding of cargos in transition to the different elements of the NPC at different points in time could be examined. The different points in time in the ultrastructural assay cannot be directly compared with the points in time in the fluorescence microscopy assay. Rather the binding of the cargos to the different parts of the NPCs can be interpreted as “snapshots” at different points in time of cargos in transit like in the paper of Beck et al. (Beck, Lucic et al. 2007). The transport rate and speed in both *in vitro* assays is lower than in *in vitro* and *in vivo* transport assays described before (Adam, Sterne-Marr et al. 1992; Riddick and Macara 2005; Timney, Tetenbaum-Novatt et al. 2006). In the paper of Kopito et al., it is discussed that the transport rate is limited and proportional to the concentration of transport receptors in transport assay and the binding affinity to the cargo (Kopito and Elbaum 2007). We also assume that in our experiment the transport rate is limited by the supply of transport receptors and the competition between the cargos in the HeLa extract and the supplied GFP-nucleoplasmin for binding sites of the transport receptors. It was also described before that the transport efficacy of cargos with multiple NLSs is reduced (Beck, Lucic et al. 2007). Taking also in consideration that the gold conjugated GFP-nucleoplasmin is sterically unfavourable as cargo, the low transport rates, especially in the ultrastructural assay, can be explained. A further possible interpretation for the reduced number of gold particles observed at the nuclear side at time point 30 minutes is the decreasing efficiency of the supplemented energy regenerating system after a certain period. Last, a high diffusion rate of gold particles from the nuclear side of the NPC inside the nucleus could mean that the gold particles attached to the nuclear side do not reflect the total number of gold particles transported into the nucleus. In this way, the ultrastructural import assay is only suitable to reveal the cargo docking sites at the NPC with and without antibodies against components of the p62 complex but not to quantify time-dependent nuclear import on the ultrastructural level.

### 3.3.2. Docking sites of the import complex during transport

During the import process, four docking sites are described: at the cytoplasmic filaments (30-60 nm from the central p lane), at the entry of the central channel (15-25 nm from the central plane), at the exit of the central channel (-30 nm from the central plane), and at the nuclear basket (-100 to -120 nm from the central plane). Not only the localization of the docking site changed when conditions for the nuclear import were modified but also the size of the gold particles population when antibodies were applied. When applying antibodies to the import assay, docking sites for the importin/cargo complex were modified.

First of all, none of the different p62 antibodies completely inhibit nuclear import of the cargo. The monoclonal N-terminal p62 AB rather supports nucleoplasmic transport than inhibiting it (3.2. (d)). When an excess of antibodies against the N-terminal FG-repeat domain of p62 was used in the ultrastructural import assay, the population at the second docking site at the entry of the central channel dropped down from 17.9% to 4.5%. It means that the docking of the nuclear import complex is influenced by the antibody against the N-terminal domain of p62. One possible explanation for this effect is that the FG-repeat domain of p62 collapses because of its binding to the monoclonal antibody comparable ,e.g., to the binding of transport receptors to the FG-repeats (Lim, Fahrenkrog et al. 2007). This way, we can also explain the increased import traffic at time 30 minutes: the entropic barrier breaks down and more cargos can enter the nucleus. This interpretation is also supported by the fluorescence data in Fig. 3.2 (a), which show an increase of the fluorescence signal over time. Compared to the control experiment, the parameters of the third and fourth docking sites changed, too. At the second docking site, the distance from the 8-fold symmetry axis increased from  $14.3 \pm 15.9$  nm to  $30.3 \pm 24.0$  nm at the time 15 minutes, whereas at the fourth docking site the average distance of the gold particles population from the 8-fold symmetry axis decreased from  $33.3 \pm 9.0$  nm to  $16.9 \pm 12.2$  nm. Equally, at time 30 minutes, the localization data of the localization clouds in the antibody-treated samples were different compared to the control experiment. At the third docking site, the distance from the central axis was also increased from  $17.2 \pm 16.8$  nm to  $28.0 \pm 19.1$  nm. The second docking site showed a wider spread of the standard deviation along the horizontal axis than in the control experiment ( $\pm 30.3$  to  $\pm 14.5$ ). One possible explanation for the observed import pathways with different (wider) distances to the 8-fold symmetry in the experiments with the N-terminal p62 antibody, compared to the control experiment, is the overtake of the transported cargo by other FG-repeat domains like Nup358, Nup214, or Nup98, which results in different distances from the central axis for the third and fourth docking site (Paulillo, Phillips et al. 2005). Both phenomena described above, show once again the flexibility and the robustness of the transport machinery when single FG-repeat domains are masked or depleted as it was demonstrated already before (Strawn, Shen et al. 2004).

### **3.3.3. The effects of antibodies against full length p62 and its C-terminal domain**

Using the antibody against the full length rat nucleoporin p62 in the import assay (3.2.(e)) leads to a breakdown of the import process after a while. After 5 minutes of transport, the percentage of transported cargo gold particles is higher than in the control experiment. At the time 15 minutes, the percen-

tage of transported particles stands back the percentage in the control experiments. After 30 minutes of transport, the nuclear import of gold particles is nearly completely inhibited. At the time 15 minutes, the distance from the 8-fold symmetry axis at the third docking site has significantly increased compared to the control experiment. In contrast, the fluorescence microscopy experiment (Fig. 3.2.(b)) shows an overall reduction of the nuclear import, pointed out by a visible nuclear rim stain at all points in time.

The transport experiment with the antibody against the C-terminus (3.2.(c)) of p62 bears indications to interpret the position of the p62 complex in the 3D structures of the NPC. At all three points in time of observation (5, 15, and 30 minutes), the average distance of the second docking site from the central plane was between 20-25 nm. That means that the gold particles accumulate above the proposed position of the p62 complex at  $16.5 \pm 4.7$  nm from the central plane (Schwarz-Herion, Maco et al. 2007). A further point is the overlap of localization clouds at the second docking site at all points in time. The gold particles seem to concentrate above the central entry of the central channel, hindered to enter the nucleus by a barrier, possibly consisting of antibodies which extend into the central region of the NPC and thus cover the entry to the central channel. Altogether, the transport rate through the central channel or the number of gold particles attached to the nuclear side of the NPC, respectively, is strongly reduced, and at the time 5 minutes transport was even completely blocked. Similarly, the fluorescence transport experiment revealed also a reduced transport rate, indicated by a nuclear rim stain at all points in time.

Considering the results from the experiments with the N-terminal- and the C-terminal p62 antibodies, the observation of the experiments can be interpreted as a combination of the opposed effects of both domain-specific antibodies. Anyway, this interpretation is speculative because the epitopes, which are recognized by the full length p62 antibody, are unknown.

### **3.3.4. Antibodies against full length rat p54 and p58 affect transport in different ways**

When the import assay was performed against full length rat p54 (Fig. 3.3.(c)), the import of cargo seemed to be accelerated at the beginning (at the time 5 minutes) and to be inhibited afterwards (at the points in time 15 and 30 minutes). This corresponds to the results described above with the antibody against full length p62. In contrast, the transport experiment with the same antibody on fluorescence level revealed an overall block of the cargo import. In contrary to the results with antibodies against the full length p54, the transport of the import cargo was not influenced in the same way by the antibody

against the full length nucleoporin p58 (Fig. 3.3.(b)). The results of a partly delayed import (at the time 5 and 15 minutes, less particles were imported compared to the control experiment) and a partly increased import (more particles were found at the nuclear part of the NPC compared to the control experiment) lets suggest that the antibody influences the transport by the partial collapse of the entropic barrier formed by the FG-repeats. One interesting feature of the ultrastructural assay at point in time 15 minutes is that the localization clouds between 0 and 30 nm from the central plane overlap at an average distance of 23.1 nm from the central plane, indicating an accumulation of import cargos above the supposed position of the p62 complex within the 3D structure of the NPC. The results of the transport assay with the p58 antibody let suggest that the epitopes recognized by the antibody are mainly the FG-repeat domains of p58 but like with the other full length antibodies, the epitopes, which are recognized by the antibodies, remain elusive. The corresponding experiment on fluorescence level (Fig. 3.3.(c) and (d)) showed an inhibition of transport, indicated by a nuclear rim stain at all points in time and did not seem to correlate with the ultrastructural import experiments.

### **3.3.5. A combination of the antibodies against the p62 complex inhibits transport**

When antibodies against full length p62, p54, and p58 are used together in an import assay, a clear inhibition of the transport at fluorescence as well as at ultrastructural level after 30 minutes could be observed. The gallery of nuclear pore complexes in Fig. 3.4. (a) shows that the import complexes – represented by the gold particles – stick mainly to the cytoplasmic filaments and the periphery of the central channel, the supposed docking sites of the importin/cargo-complexes at the NPC. The representation of the stuck import cargos as localization clouds in Fig. 3.4.(d) reveals slight differences regarding the combination of the applied antibodies: When the combination of p62/p54 antibodies and p54/p58 antibodies were used, the localization clouds had a different conformation compared to the experiment where a combination of p62/p54 antibodies was used. The reason for this difference could be that the entropic barrier, which is built up by the FG-repeat domains, might be disturbed by the antibodies against the full length p62 complex in different ways, resulting in different docking sites for the import cargos. On fluorescence level, the application of antibodies against full length p62, p54, and p58 in the import assay (Fig. 3.4. (b)) resulted in the same way in a rim stain at all points in time as in the control experiment using the mAb 414 (Fig. 3.4 (c)).

Taken together, the new study regarding the function of the p62 complex gave new insights into the



location of the p62 complex in the NPC and its role as a putative docking site for importin/cargo-complexes. The observations described above, also support the results of a recent study about the domain topology of the p62 complex in the 3D structure of the NPC (Schwarz-Herion, Maco et al. 2007). The observation that only a combination of different antibodies against the p62 complex can inhibit nuclear import also supports the assumption that the regulation of the nucleoplasmic transport is robust and tolerates the deletion of certain FG-repeat domains. It was already shown before that the removal of several FG-repeat domains by genetic engineering in yeast have only minor influence in nucleocytoplasmic transport (Strawn, Shen et al. 2004). But masking of single components by antibodies can have different effects compared to a depletion like, e.g., inter- and intramolecular crosslinking or the break down of polymer brushes. Equally, the special role of the FG-repeats of the nucleoporin p62 in nucleoplasmic transport is demonstrated in the ultrastructural experiment, using antibodies against the FG-repeat domain. When using antibodies against the p62 FG-repeats, the second docking site of the import complex was significantly affected, indicating that the FG-repeat domains of the p62 complex is an important element of the second docking site.

The study equally describes on ultrastructural level the pathways of importin/cargo-complexes in detail. Anyway, to specify the import (or export) pathways, it is necessary to do the same experiments with antibodies against each domain of the p62 complex or, at least, the FG-repeat nucleoporins, which are mainly involved in nucleocytoplasmic transport. Additionally, it is necessary to repeat the experiments also with shorter time frames to get a broader experimental foundation for the interpretation of the transport event. Thus, the ultrastructural import assays together with extensive studies with single molecule fluorescence techniques (Kubitscheck, Grunwald et al. 2005; Yang and Musser 2006) might give new insight into the kinetics and mechanism of the nuclear protein import. The import studies with GFP-labeled cargo shown in this paper, make not the claim for giving new insight into the kinetics of the transport event but rather for showing similarities or differences of nuclear import on fluorescence and ultrastructural level when nucleoporin-specific antibodies were applied in the transport assay.

## 3.4. Material and Methods

### 3.4.1. Recombinant protein expression

His-tagged recombinant GFP-nucleoplasmin was expressed in *E. coli* BL21 cells. The protein was purified via a His-trap column loaded with NiSO<sub>4</sub> (GE Healthcare, Pittsburgh, USA) and eluted with a buffer containing 200 mM imidazole. The collected fractions were analyzed by SDS-PAGE, and fractions containing purified GFP-nucleoplasmin were pooled. The purified GFP-nucleoplasmin was concentrated to 1 mg/ml and finally dialyzed against PBS pH 7.4.

### 3.4.2. Isolation of *Xenopus* oocyte nuclei

Mature (stage 6) oocytes were surgically removed from female *Xenopus laevis* and the nuclei were isolated as described (Pante, Bastos et al. 1994).

### 3.4.3. Direct conjugation of nucleoplasmin-GFP to colloidal gold

Colloidal gold particles with an diameter of about 8 nm were prepared and conjugated to nucleoplasmin-GFP as described (Baschong and Wrigley 1990; Fahrenkrog, Maco et al. 2002).

### 3.4.4. Antibodies

The antibody against the C-terminal domain of the mammalian p62 was generated and purified as described (Schwarz-Herion, Maco et al. 2007). As antibody recognizing the N-terminal domain of p62, we used a monoclonal antibody against residues 24–178 of human p62, which recognizes the N-terminal epitope in a wide range of vertebrates (BD Bio-science, Franklin Lakes NJ)(Carmo-Fonseca, Kern et al. 1991). The antibodies against the full length rat nucleoporins p62, p54, and p58 were generated and purified as described (Hu, Guan et al. 1996).

### 3.4.5. Ultrastructural Nuclear Import Assay in isolated *Xenopus* oocytes nuclei

Isolated nuclei of *Xenopus* oocytes were incubated for 30 minutes in low salt buffer (LSB) supple-

mented with antibodies against the nucleoporins p62, p54, and p58, respectively. After incubation with the antibodies, nuclei were transferred to 180  $\mu$ l transport mixture (20 mM HEPES pH 7.3, 110 mM potassium acetate, 5 mM sodium acetate, 2 mM magnesium acetate, 1 mM EGTA, 2 mM DTT, 1  $\mu$ g/ml Aprotinin, 1  $\mu$ g/ml Leupeptin, 1  $\mu$ g/ml Pepstatin A, 50 % v/v cytosolic HeLa extract, 20 units/ml creatine phosphokinase, 20 mM creatine phosphatase; 1 mM ATP), supplemented with 20  $\mu$ l gold-conjugated nucleoplasmin-GFP as cargo. The nuclei were incubated in the transport mixture at room temperature (RT) for 5, 15 or 30 minutes, respectively, washed with LSB, supplemented with 0.1% BSA, and fixed in LSB containing 2% glutaraldehyde and 0.3% tannic acid. Fixed nuclei were washed twice with LSB, embedded in 2% agarose, and postfixed with 4% OsO<sub>4</sub>. Fixed samples were dehydrated, embedded in Epon 812 resin (Fluka, Buchs, Switzerland), and processed for thin-sectioning EM as described previously (Pante, Bastos et al. 1994). Thin sections were cut on a Reichert Ultracut microtome (Reichert-Jung Optische Werke, Vienna, Austria) using a diamond knife (Diatome, Biel, Switzerland). The sections were collected on parlodion-coated copper grids and stained with 6% uranyl acetate for 1 h, followed by 2% lead citrate for 2 min. Electron micrographs were recorded with a FEI Morgani 268D (Philips) transmission electron microscope, operated at an acceleration voltage of 80 kV.

### 3.4.6. Quantification of gold labeling at the NPCs and calculation of location clouds

The positions of the gold particles associated with the NPC during nuclear import were measured from electron micrographs of cross-sections along the NE of Epon-embedded, thin-sectioned isolated nuclei. For each gold particle, its distance perpendicular to the central plane of the NPC and from the 8-fold symmetry axis of the NPC was determined. All analyzed gold particles were blotted into histograms. The linear dimensions of the *Xenopus* NPC in Epon-embedded, thin-sectioned isolated nuclei were calculated from unlabeled NEs to estimate the dimensions of the NPC under the experimental conditions used. Gold particles which have a distance of 90 to -120 nm from the central plane of the NPC were taken in calculation. Location clouds were calculated as described (Fahrenkrog, Aris et al. 2000).

### 3.4.7. Fluorescence Microscopy Nuclear Import Assay in HeLa cells

HeLa cells were grown as monolayers on Lab-Tec chambered coverslips to 80% confluence in Dulbecco's Modified Eagle Medium (DMEM; Sigma, St. Louis, USA), complemented with 10% fetal calf serum and penicillin/streptomycin at 37°C. Cells were permeabilized on ice with 40  $\mu$ g/ml digitonin

in transport buffer (20 mM HEPES pH 7.3, 110 mM potassium acetate, 5 mM sodium acetate, 2 mM magnesium acetate, 1 mM EGTA, 2 mM DTT, 1  $\mu\text{g/ml}$  aprotinin, 1  $\mu\text{g/ml}$  leupeptin, 1  $\mu\text{g/ml}$  pepstatin A), supplemented with 200 ng/ml DAPI. Next, cells were washed two times with transport buffer. The coverglasses were mounted on an inverse confocal microscope LSM 510 (Carl Zeiss, Jena, Germany), and 180  $\mu\text{l}$  transport mixture including an energy regenerating system without ATP, supplemented with 20  $\mu\text{l}$  nucleoplasmin-GFP (1 mg/ml), was added into the chamber. The transport assay was started by addition of 5  $\mu\text{l}$  1 mM ATP. Import into the nucleus was observed starting at time 0 for 30 minutes. Every minute, a picture of the transport experiment was taken with a 63x oil objective. At each point in time, the picture was taken only from one confocal plane but was 8-fold averaged to improve the signal/noise ratio. The excitation wavelength was  $\lambda = 405$  nm for DAPI staining and  $\lambda = 488$  nm for GFP.

### **3.5. Acknowledgements**

We are grateful to Per Rigler for providing access to the LSM 510 and helping with the *in vitro* assay.

### 3.6. References

Adam, S. A., T. J. Lobl, et al. (1989). „Identification of specific binding proteins for a nuclear location sequence.“ *Nature* 337(6204): 276-9.

Adam, S. A., R. Sterne-Marr, et al. (1992). „Nuclear protein import using digitonin-permeabilized cells.“ *Methods Enzymol* 219: 97-110.

Akey, C. W. and M. Radermacher (1993). „Architecture of the *Xenopus* nuclear pore complex revealed by three-dimensional cryo-electron microscopy.“ *J Cell Biol* 122(1): 1-19.

Baschong, W. and N. G. Wrigley (1990). „Small colloidal gold conjugated to Fab fragments or to immunoglobulin G as high-resolution labels for electron microscopy: a technical overview.“ *J Electron Microsc Tech* 14(4): 313-23.

Beck, M., F. Forster, et al. (2004). „Nuclear pore complex structure and dynamics revealed by cryoelectron tomography.“ *Science* 306(5700): 1387-90.

Beck, M., V. Lucic, et al. (2007). „Snapshots of nuclear pore complexes in action captured by cryo-electron tomography.“ *Nature* 449 (7162): 1387-90

Bednenko, J., G. Cingolani, et al. (2003). „Nucleocytoplasmic transport: navigating the channel.“ *Traffic* 4(3): 127-35.

Carmo-Fonseca, M., H. Kern, et al. (1991). „Human nucleoporin p62 and the essential yeast nuclear pore protein NSP1 show sequence homology and a similar domain organization.“ *Eur J Cell Biol* 55(1): 17-30.

Conti, E., C. W. Muller, et al. (2006). „Karyopherin flexibility in nucleocytoplasmic transport.“ *Curr Opin Struct Biol* 16(2): 237-44.

- Cronshaw, J. M., A. N. Krutchinsky, et al. (2002). „Proteomic analysis of the mammalian nuclear pore complex.“ *J Cell Biol* 158(5): 915-27.
- Dabauvalle, M. C., R. Benavente, et al. (1988). „Monoclonal antibodies to a Mr 68,000 pore complex glycoprotein interfere with nuclear protein uptake in *Xenopus* oocytes.“ *Chromosoma* 97(3): 193-7.
- Denning, D. P. and M. F. Rexach (2007). „Rapid evolution exposes the boundaries of domain structure and function in natively unfolded FG nucleoporins.“ *Mol Cell Proteomics* 6(2): 272-82.
- Fahrenkrog, B. and U. Aebi (2003). „The nuclear pore complex: nucleocytoplasmic transport and beyond.“ *Nat Rev Mol Cell Biol* 4(10): 757-66.
- Fahrenkrog, B., J. P. Aris, et al. (2000). „Comparative spatial localization of protein-A-tagged and authentic yeast nuclear pore complex proteins by immunogold electron microscopy.“ *J Struct Biol* 129(2-3): 295-305.
- Fahrenkrog, B., B. Maco, et al. (2002). „Domain-specific antibodies reveal multiple-site topology of Nup153 within the nuclear pore complex.“ *J Struct Biol* 140(1-3): 254-67.
- Finlay, D. R., E. Meier, et al. (1991). „A complex of nuclear pore proteins required for pore function.“ *J Cell Biol* 114(1): 169-83.
- Fried, H. and U. Kutay (2003). „Nucleocytoplasmic transport: taking an inventory.“ *Cell Mol Life Sci* 60(8): 1659-88.
- Galy, V., I. W. Mattaj, et al. (2003). „*Caenorhabditis elegans* nucleoporins Nup93 and Nup205 determine the limit of nuclear pore complex size exclusion in vivo.“ *Mol Biol Cell* 14(12): 5104-15.
- Gorlich, D., N. Pante, et al. (1996). „Identification of different roles for RanGDP and RanGTP in nuclear protein import.“ *Embo J* 15(20): 5584-94.

- Guan, T., S. Muller, et al. (1995). „Structural analysis of the p62 complex, an assembly of O-linked glycoproteins that localizes near the central gated channel of the nuclear pore complex.“ *Mol Biol Cell* 6(11): 1591-603.
- Hinshaw, J. E., B. O. Carragher, et al. (1992). „Architecture and design of the nuclear pore complex.“ *Cell* 69(7): 1133-41.
- Hu, T., T. Guan, et al. (1996). „Molecular and functional characterization of the p62 complex, an assembly of nuclear pore complex glycoproteins.“ *J Cell Biol* 134(3): 589-601.
- Hutten, S. and R. H. Kehlenbach (2006). „Nup214 is required for CRM1-dependent nuclear protein export in vivo.“ *Mol Cell Biol* 26(18): 6772-85.
- Kopito, R. B. and M. Elbaum (2007). „Reversibility in nucleocytoplasmic transport.“ *Proc Natl Acad Sci U S A* 104(31): 12743-8.
- Kubitscheck, U., D. Grunwald, et al. (2005). „Nuclear transport of single molecules: dwell times at the nuclear pore complex.“ *J Cell Biol* 168(2): 233-43.
- Lanford, R. E. and J. S. Butel (1984). „Construction and characterization of an SV40 mutant defective in nuclear transport of T antigen.“ *Cell* 37(3): 801-13.
- Lill, Y., M. A. Lill, et al. (2006). „Single Hepatitis-B Virus Core Capsid Binding to Individual Nuclear Pore Complexes in HeLa Cells.“ *Biophys J* 91(8): 3123-30.
- Lim, R. Y., U. Aebi, et al. (2006). „From the trap to the basket: getting to the bottom of the nuclear pore complex.“ *Chromosoma* 115(1): 15-26.
- Lim, R. Y. and B. Fahrenkrog (2006). „The nuclear pore complex up close.“ *Curr Opin Cell Biol* 18(3): 342-7.



- Lim, R. Y., B. Fahrenkrog, et al. (2007). „Nanomechanical Basis of Selective Gating by the Nuclear Pore Complex.“ *Science* 318(5850): 640-643.
- Lim, R. Y., N. P. Huang, et al. (2006). „Flexible phenylalanine-glycine nucleoporins as entropic barriers to nucleocytoplasmic transport.“ *Proc Natl Acad Sci U S A* 103(25): 9512-7.
- Lim, R. Y., J. Koser, et al. (2007). „Nanomechanical interactions of phenylalanine-glycine nucleoporins studied by single molecule force-volume spectroscopy.“ *J Struct Biol* 159(2): 277-289
- Melcak, I., A. Hoelz, et al. (2007). „Structure of Nup58/45 suggests flexible nuclear pore diameter by intermolecular sliding.“ *Science* 315(5819): 1729-32.
- Melchior, F., T. Guan, et al. (1995). „GTP hydrolysis by Ran occurs at the nuclear pore complex in an early step of protein import.“ *J Cell Biol* 131(3): 571-81.
- Pante, N. and U. Aebi (1996). „Sequential binding of import ligands to distinct nucleopore regions during their nuclear import.“ *Science* 273(5282): 1729-32.
- Pante, N., R. Bastos, et al. (1994). „Interactions and three-dimensional localization of a group of nuclear pore complex proteins.“ *J Cell Biol* 126(3): 603-17.
- Paschal, B. M. and L. Gerace (1995). „Identification of NTF2, a cytosolic factor for nuclear import that interacts with nuclear pore complex protein p62.“ *J Cell Biol* 129(4): 925-37.
- Patel, S. S., B. J. Belmont, et al. (2007). „Natively unfolded nucleoporins gate protein diffusion across the nuclear pore complex.“ *Cell* 129(1): 83-96.
- Paulillo, S. M., E. M. Phillips, et al. (2005). „Nucleoporin domain topology is linked to the transport status of the nuclear pore complex.“ *J Mol Biol* 351(4): 784-98.
- Pemberton, L. F. and B. M. Paschal (2005). „Mechanisms of receptor-mediated nuclear import and nuclear export.“ *Traffic* 6(3): 187-98.

- Reichelt, R., A. Holzenburg, et al. (1990). „Correlation between structure and mass distribution of the nuclear pore complex and of distinct pore complex components.“ *J Cell Biol* 110(4): 883-94.
- Riddick, G. and I. G. Macara (2005). „A systems analysis of importin- $\alpha$ - $\beta$  mediated nuclear protein import.“ *J Cell Biol* 168(7): 1027-38.
- Rollenhagen, C., P. Muhlhauser, et al. (2003). „Importin beta-depending nuclear import pathways: role of the adapter proteins in the docking and releasing steps.“ *Mol Biol Cell* 14(5): 2104-15.
- Rout, M. P., J. D. Aitchison, et al. (2000). „The yeast nuclear pore complex: composition, architecture, and transport mechanism.“ *J Cell Biol* 148(4): 635-51.
- Schetter, A., P. Askjaer, et al. (2006). „Nucleoporins NPP-1, NPP-3, NPP-4, NPP-11 and NPP-13 are required for proper spindle orientation in *C. elegans*.“ *Dev Biol* 289(2): 360-71.
- Schwartz, T. U. (2005). „Modularity within the architecture of the nuclear pore complex.“ *Curr Opin Struct Biol* 15(2): 221-6.
- Schwarz-Herion, K., B. Maco, et al. (2007). „Domain Topology of the p62 Complex Within the 3-D Architecture of the Nuclear Pore Complex.“ *J Mol Biol* 370(4) : 796-806.
- Stewart, M. (2006). „Structural basis for the nuclear protein import cycle.“ *Biochem Soc Trans* 34(Pt 5): 701-4.
- Stoffler, D., B. Fahrenkrog, et al. (1999). „The nuclear pore complex: from molecular architecture to functional dynamics.“ *Curr Opin Cell Biol* 11(3): 391-401.
- Stoffler, D., B. Feja, et al. (2003). „Cryo-electron tomography provides novel insights into nuclear pore architecture: implications for nucleocytoplasmic transport.“ *J Mol Biol* 328(1): 119-30.

- Stoffler, D., K. Schwarz-Herion, et al. (2006). „Getting across the nuclear pore complex: new insights into nucleocytoplasmic transport.“ *Can J Physiol Pharmacol* 84(3-4): 499-507.
- Strawn, L. A., T. Shen, et al. (2004). „Minimal nuclear pore complexes define FG repeat domains essential for transport.“ *Nat Cell Biol* 6(3): 197-206.
- Timney, B. L., J. Tetenbaum-Novatt, et al. (2006). „Simple kinetic relationships and nonspecific competition govern nuclear import rates in vivo.“ *J Cell Biol* 175(4): 579-93.
- Yang, W., J. Gelles, et al. (2004). „Imaging of single-molecule translocation through nuclear pore complexes.“ *Proc Natl Acad Sci U S A* 101(35): 12887-92.
- Yang, W. and S. M. Musser (2006). „Visualizing single molecules interacting with nuclear pore complexes by narrow-field epifluorescence microscopy.“ *Methods* 39(4): 316-28.
- Yokoyama, N., N. Hayashi, et al. (1995). „A giant nucleopore protein that binds Ran/TC4.“ *Nature* 376(6536): 184-8.
- Zhong, H., H. Shio, et al. (2006). „Ultrastructural nuclear import assay.“ *Methods* 39(4): 309-15.



**Depletion of components of the p62 complex by RNAi  
leads to mitotic arrest and increased apoptosis**

**Kyrill Schwarz-Herion and Birthe Fahrenkrog**

*M.E. Müller Institute for Structural Biology, Biozentrum, University of Basel, Klingelbergstrasse 70,  
CH-4056 Basel, Switzerland*



## Summary

During the past few years, evidence accumulated that distinct nuclear pore complex proteins do not only function in the nucleocytoplasmic transport, but also in the regulation of other cellular processes, such as mitosis. To study the function of the p62-complex (i.e. p62, p54, and p58) in a cellular context, we depleted its components from HeLa cells by RNA interference, which led to an arrest in cell growth and an increase of apoptotic cells as analyzed by fluorescence activated cell sorting. *In vitro* transport studies of p62- and p54-depleted HeLa cells further showed that the depletion of these p62 complex components had a significant inhibitory effect on nuclear protein import. Taken together, these results indicate that the p62 complex is not only critical for mediating nuclear protein import, but also for cell growth and cell division.

## 4.1. Introduction

In eukaryotic cells, the cytoplasm is separated from the nucleus by two nuclear membranes, called nuclear envelope (NE). Embedded in the NE are nuclear pore complexes (NPCs), which enable the exchange of macromolecules between cytoplasm and nucleus (Fahrenkrog and Aebi 2003; Stoffler, Schwarz-Herion et al. 2006). Vertebrate NPCs are huge protein complexes with an estimated mass of 125 MDa and exhibit a tripartite structural organization with 8-fold rotational symmetry (Reichelt, Holzenburg et al. 1990; Stoffler, Feja et al. 2003; Beck, Forster et al. 2004). The NPCs consist of about 30 different proteins, the so-called nucleoporins (or Nups), which assemble into several subcomplexes to form the NPC (Rout, Aitchison et al. 2000; Cronshaw, Krutchinsky et al. 2002; Schwartz 2005).

One of these subcomplexes is the p62 complex, which is involved in the nuclear import of proteins and in RNA export (Finlay, Meier et al. 1991; Hu, Guan et al. 1996; Schetter, Askjaer et al. 2006). The p62 complex is composed of four different proteins, p62, p54, p58, and p45, with p45 being a splice variant of p58 (Davis and Blobel 1987; Carmo-Fonseca, Kern et al. 1991; Finlay, Meier et al. 1991; Buss and Stewart 1995; Guan, Muller et al. 1995; Hu and Gerace 1998). The p62 complex nucleoporins are exhibiting phenylalanine-glycine (FG)-repeat motifs and coiled-coil domains (Dabauvalle, Benavente et al. 1988; Cordes and Krohne 1993; Schwarz-Herion, Maco et al. 2007). While the coiled-coil domains mediate the anchoring of the p62 complex to the NPC, the FG-repeat domains act as docking sites for nuclear import or export complexes to facilitate the passage of cargos through the NPC (Hu, Guan et al. 1996). Consequently, the p62 complex is known to play a role in nuclear protein import as well as in RNA export (Dabauvalle, Benavente et al. 1988; Finlay, Meier et al. 1991; Paschal and Gerace 1995; Hu, Guan et al. 1996).

Former biochemical studies revealed that nuclei containing NPCs devoid of the p62 complex are defective in nuclear transport (Finlay, Meier et al. 1991). Biochemical studies further demonstrated a direct binding of p62 to transport receptors, cargos, and RNA (Paschal and Gerace 1995). An RNAi study by Sabri et al. revealed an nuclear import defect in 54-depleted cells from *Drosophila melanogaster* (Sabri, Roth et al. 2007) In addition, studies with deletion mutants in yeast showed that all the FG domains in the cytoplasmic fibrils and nuclear basket Nups can be removed without significant impact on Kap95 (yeast importin  $\beta$ ) import and and that the components of the Nsp1 complex – the putative yeast homologue of the p62 complex – belong to the so-called minimal pore (Strawn, Shen et al. 2004; Tran and Wentz 2006). Microinjection of monoclonal antibodies, specifically against p62, caused mitotic arrest of cells in late



telophase (Fukuhara, Sakaguchi et al. 2006). Depletion of the homologue genes of p62 complex in *C. elegans* showed a dramatic effect in mitosis and the viability of the cells (Schetter, Askjaer et al. 2006).

Recently, we have shown by immuno-electron microscopy that the p62 complex is located near the cytoplasmic entry side of the NPC's central pore (Schwarz-Herion, Maco et al. 2007). To study the function of the p62 complex in human cells, we depleted the human nucleoporins p62, p54, and p58 by RNA interference from HeLa cells. We found that p62 and p54 have some influence on the viability of cells and that the regulation of cell growth. p62- and p54-depleted cells additionally showed a nuclear protein import defect. Additionally, overexpression of either p62, p54, or p58 leads to changes in the distribution of different states of the cell cycle stages. Taken together, this study gave new insights into the role of p62, p54, and p58 in the regulation of cell growth, cell division, and the nuclear import of proteins.

## 4.2. Results

### 4.2.1. Depletion of p62, p54, and p58 by RNA interference

To study the functional role of the p62 complex in a cellular context, we depleted the three components of the p62 complex, i.e. p62, p54, and p58, respectively, in HeLa cells by using gene-specific small interfering RNAs (siRNAs). To do so, HeLa cells were either mock-transfected or transfected with siRNAs against p62, p54, and p58, respectively. To analyze the knock-down efficiency of the siRNAs, protein levels were determined by immunoblotting. As shown in Fig. 4.1., treatment of HeLa cells with siRNA against human p62 leads to a significantly reduced level of p62 to an estimated level of ~30% after 4 days as compared to mock-transfected cells, whereas the levels of importin  $\beta$  remained unaffected by siRNA against p62. Similarly, the expression level of p54 was nearly completely reduced in cells treated with siRNAs against p54. In cells treated with siRNAs against p58, however, the expression levels of p58 were only reduced to about 80% as compared to mock-transfected cells, indicating an inefficient knock-down. Therefore, we continued our experiments only with p62- and p54-depleted HeLa cells, respectively.

### 4.2.2. Immunofluorescence analysis of p62- and p54-depleted cells

Cells with reduced levels of p62 and p54 were also examined by indirect immunofluorescence to study the effect of p62 and p54 on the association of other nucleoporins with the NPC. The cells were stained with mAb414, an antibody, which recognizes a set of FG-repeat nucleoporins and with Alexa488-labeled anti-mouse antibody as secondary antibody. The nucleus of the cells was visualized by the DNA-stain DRAQ5. As shown in Fig.4.2. (a), cells treated with p62 siRNA show significantly reduced nuclear rim stain (arrow) of mAb414 as compared to mock-transfected cells or cells, which were not transfected. In cells transfected with a p54 siRNA, the reduction of the rim stain was not as obvious as in the p62-depleted cells (Fig. 4.2.(b)). No reduction in the staining of mAb414 was observed in mock-transfected cells (Fig. 4.2. (c)).

### 4.2.3. Analysis of cell growth with fluorescence activated cell sorting (FACS) assay

To study the cell growth of the RNAi-treated cells, the proliferation of the cells was measured by a CFSE (carboxyfluorescein succinimidyl ester)/FACS-assay as described in Material and Methods. CFSE binds to amines of cellular proteins, and after each cell division, the intensity of the CFSE signal decreases. To quantify the state of proliferation, the mean va-

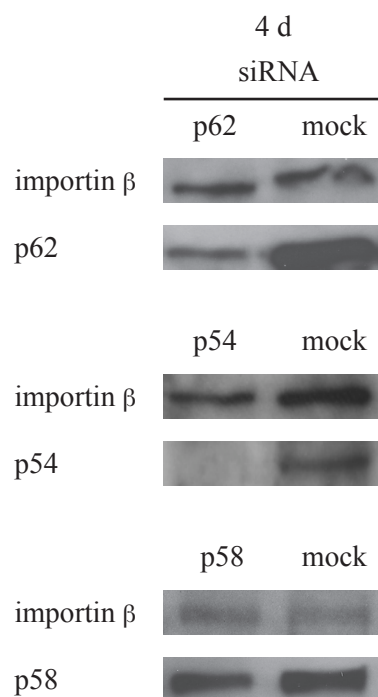


**Figure 4.1.** Depletion of the nucleoporins p62, p54, and p58 by siRNA. Lysates of HeLa cells, 48 h after transfection with mock (right) or nucleoporin-specific siRNAs (left: p62, p54, p58), were immunoblotted with antibodies against mammalian p62, p54, or p58 (lower) and importin  $\beta$  (upper) as a loading control. Cells, transfected with p62, p54, or p58 siRNAs, showed a significant reduction of p62, p54, or p58 level, whereas importin  $\beta$  was not affected.

lues of the fluorescence signal were determined for each cell population (Fig. 4.3. (a)). A high mean corresponds to a low proliferation rate, whereas a low mean reflects a high proliferation rate.

4 days after transfection, p62- and p54-depleted cells, respectively, showed a strongly reduced proliferation rate as compared to mock-transfected cells, demonstrated by higher fluorescence mean values of the p62- and p54-depleted cells (Fig. 4.3.(a)). The mean fluorescence signal of the p54-depleted cells exceeded the mean fluorescence value of the mock-transfected cells by 40%, whereas the p62-depleted cells exceeded it by 24% (Fig.4.3. (a)). A typical steplike pattern of the fluorescence signal decay over time is shown in the histogram of the control experiment in Fig. 4.3. (b). The corresponding histograms in Fig 4.3. (b) of the p62- and p54-depleted cells show an arrest of the fluorescence signal at higher values, pointing to a cell growth arrest in these cells because the fluorescence signal of the CFSE was not transmitted to the daughter cells during mitosis.

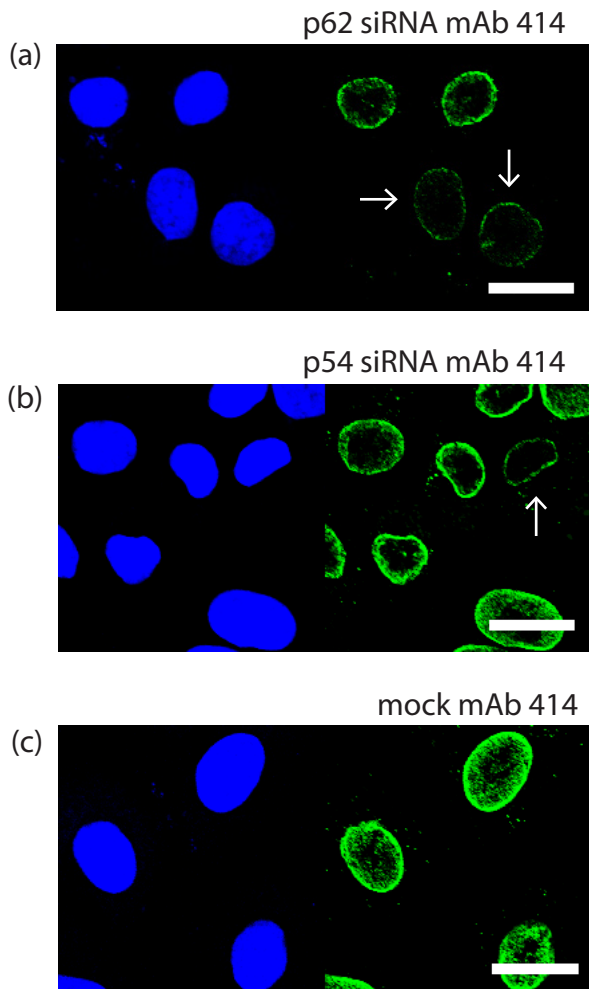


**Figure 4.2.** Immunofluorescence analysis of p62 and p54 depletion. HeLa cells labeled with mAb414 were analyzed by immunofluorescence microscopy. (a) p62 siRNA treated cells showed reduced nuclear rim staining (arrow) (b) Some cells transfected with siRNA against p54 showed reduced rim stain (arrow). (c) Mock-transfected HeLa cells displayed regular nuclear rim staining. Scale bars: 20  $\mu$ m.

#### 4.2.4. Analysis of viability

To reveal the cause of the cell growth arrest, we performed distinct FACS assays. First, the viability of the RNAi-treated cells was analyzed, using an annexinV/propidium iodide (PI) assay. Cells in the early apoptotic phase are recognized by FITC-labeled annexinV, whereas dead cells are visualized by the DNA stain PI. Three days after transfection of the cells with siRNA against p62 or p54, the number of cells, which show an apoptotic and/or PI-positive fluorescence signal, were significantly increased (Fig. 4.4. (a)). An even stronger increase in cell death could be observed in the apoptosis assay after 4 days (Fig. 4.4. (b)). In the annexinV/PI assay, an overlap of annexin-FITC and PI signals was not considered.

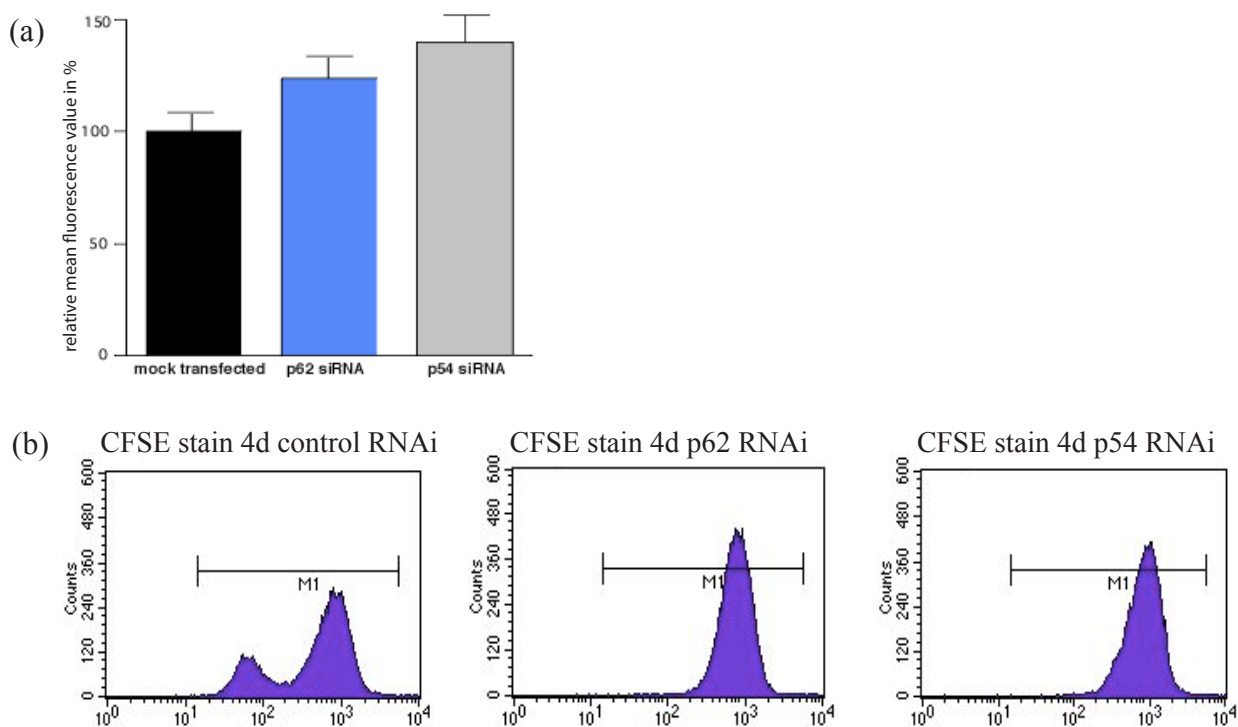


**Figure 4.3.** Proliferation assay using CFSE-staining. (a) CFSE-labeled cells were transfected with siRNAs against p62 or p54. CFSE values 4 days after transfection were measured with FACS and the relative shift to higher values of the FL1 (fluorescence channel 1; green fluorescence) mean values of the nucleoporin-depleted cells as compared to the mean value of mock-transfected cells were determined. (b) The histograms of the CFSE-assay visualize the inhibited proliferation of mock-transfected cells compared to the nucleoporin-depleted cells.

To determine the amount of apoptotic cells in late apoptotic phase after transfection with siRNAs, we performed an assay with hypertonic PI. In this assay, cells, which show degraded DNA, were considered as apoptotic cells. The black columns in Fig. 4.4. (c) demonstrate the amount of cells, which are in apoptosis three days after transfection, whereas the patterned columns show the number of apoptotic cells four days after transfection. The total amount of cells in apoptosis was lower than in the corresponding annexin/PI experiment. After 3 days, the number of apoptotic cells increased by 42% in p62 siRNAi transfected cells, whereas the number of apoptotic cells in a p54-depleted cell population did not increase as compared to the control experiment. 4 days after transfection with siRNA, an increase of apoptotic cells by 94% in the p62-depleted cell population was detected and by 39 % in the p54-depleted cell population as compared to mock-transfected cell population. Together, these data show that after knock-down of p62 and p54, respectively, the viability of cells was significantly decreased as compared to the control experiment.

4.2.5. Cell cycle analysis

Next, we performed cell cycle analysis using PI staining, followed by flow cytometry to distinguish between cells in G0/G1 stage and cells in S/G2 stage. Fig 4.4. (d) shows the distribution of

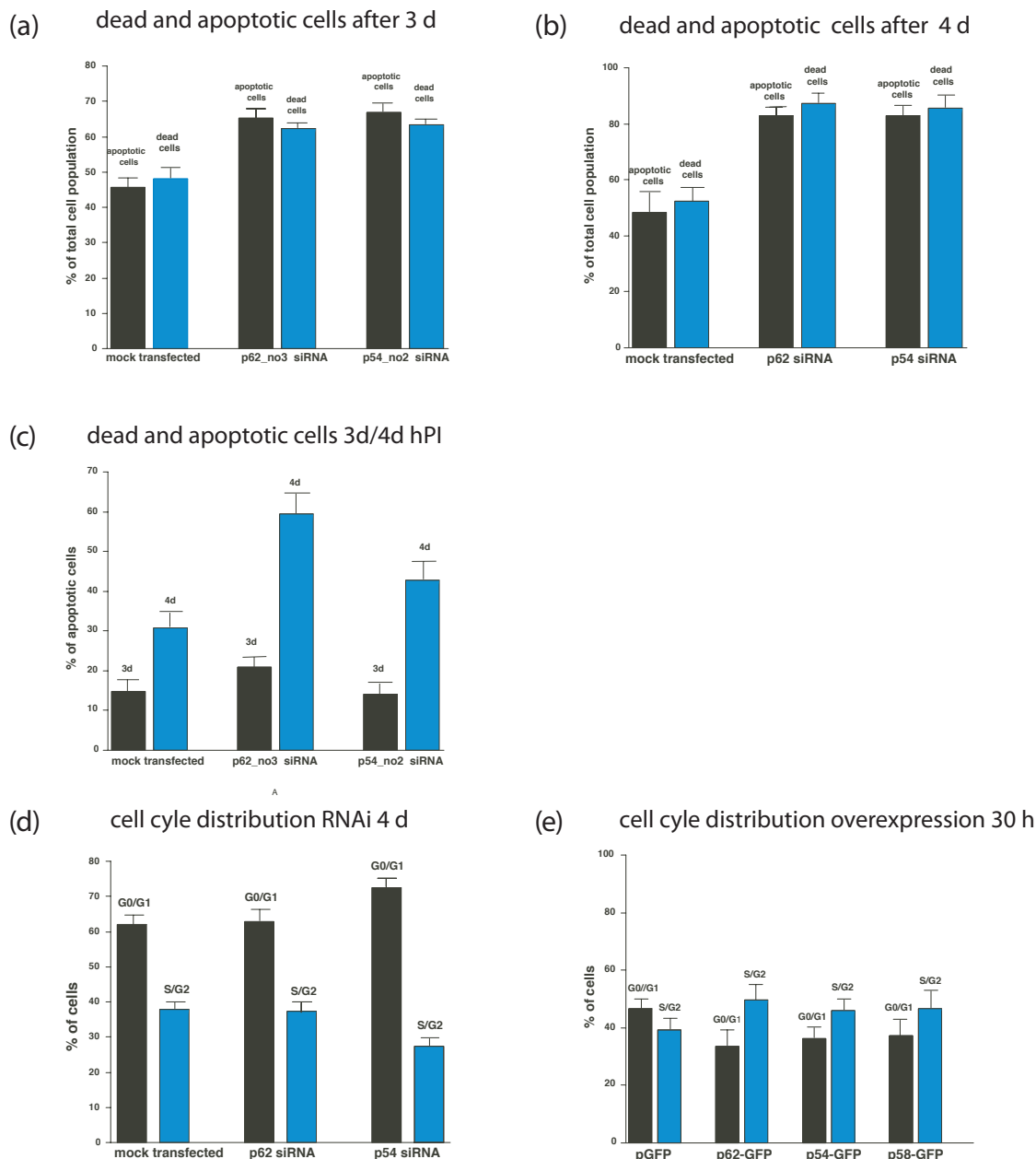


**Figure 4.4.** Apoptosis assay and cell cycle distribution. (a) An apoptosis assay using PI and Annexin-FITC revealed the increase of the number of dead and apoptotic cells 3 days after transfection with nucleoporin-specific siRNAs in comparison to mock-transfected cells. (b) Viability of mock- or siRNA-transfected cells 4 days after transfection. is shown. (c) Quantitative analysis of apoptotic cells 3 or 4 days after transfection using FACS assay with hypertonic PI is illustrated. (d) Mock- or siRNA-treated cells were treated with hypertonic PI stain for cell cycle distribution and analyzed by flow cytometry. Percentages of cells in different stages of the cell cycle are indicated. (e) Cells overexpressing p62-GFP, p54-GFP, or p58-GFP were treated with hypertonic PI stain and analyzed by FACS. Percentages of cells in different stages of the cell cycle are indicated.

cell cycle states of p62- and p54-depleted HeLa cells 3 days after transfection. The G0/G1: S/G2 ratio of 1.68 for p62-depleted cells does not differ significantly from that of the mock-transfected cells (ratio: 1.68), whereas the G0/G1:S/G2 ratio of the p54-depleted cells differs significantly (ratio: 2.4).

Cell cycle analysis was also performed with cells, which were electroporated and transfected with plasmids coding for p62-GFP, p54-GFP, or p58-GFP, respectively. The cells were analyzed 30 h after transfection. Fig. 4.4. (e) shows the different cell cycle states of the PI-stained samples. The GFP-transfected control sample shows a G0/G1:S/G2 ratio of 1.2, whereas cells transfected with p62-GFP, p54-GFP, and p58-GFP, respectively, all show ratios smaller than 1.0 (i.e. p62-GFP: 0.67; p54-GFP: 0.78; p58-GFP: 0.79), indicating that overexpression of all three nucleoporins of the p62 complex leads to an increase of cells in mitosis. Taken together, depletion of p54 and the overexpression of components of the p62 complex seem to have a significant influence on the cell cycle, e.g. the arrest in the G0/G1 phase or the arrest in S/G2 phase, respectively.

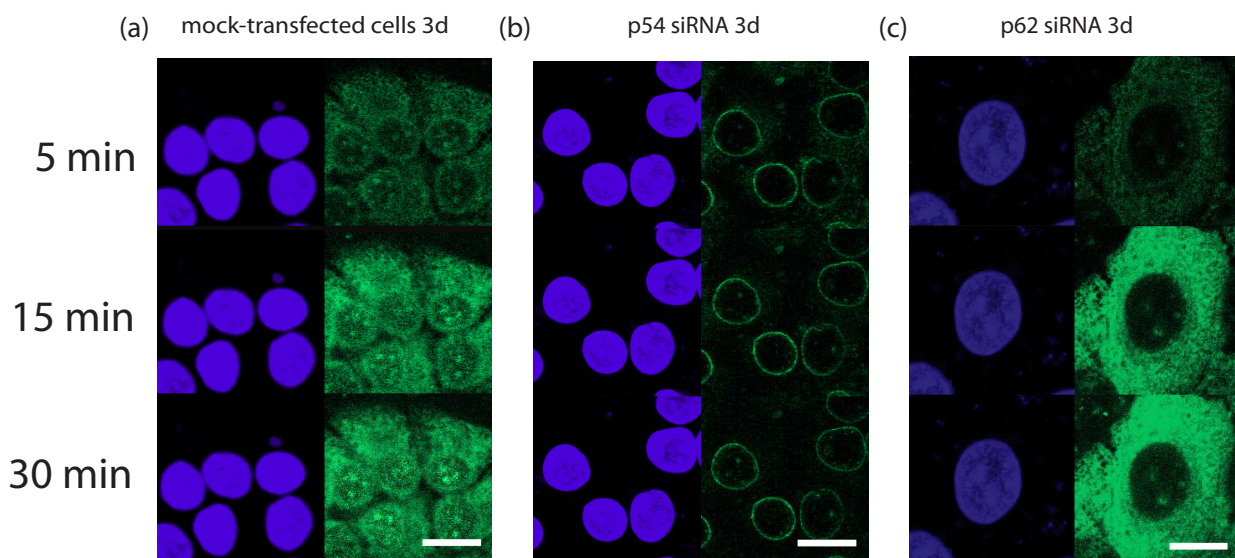


**Figure 4.5.** p62 and p54 are required for nuclear protein import. Nuclear import (a) into digitonin-permeabilized, mock-transfected HeLa cells (b) into digitonin-permeabilized HeLa cells transfected with siRNAs against p54 and (c) into digitonin-permeabilized HeLa cells transfected with siRNAs against p62 with GFP-nucleoplamin as reporter cargo. During the nuclear import assays, cells were imaged after 5 min, 15 min, and 30 minutes. Scale bar: 20  $\mu$ m

#### 4.2.6. In vitro transport studies with nucleoporin-depleted cells

Finally, nucleocytoplasmic transport was tested in p62 complex-depleted cells. The effect of p62-depletion on nucleocytoplasmic transport had been tested previously in reconstituted nuclei and by RNAi in *C.elegans* embryos (Schetter, Askjaer et al. 2006). To study the effect of p62 complex depletion on nuclear protein import in human cells, we used GFP-nucleoplasmin, a substrate for the importin  $\alpha/\beta$  pathway, as model cargo. GFP-nucleoplasmin was added to an import mixture supplemented with a fresh ATP regenerating system and applied to digitonin-permeabilized HeLa cells, that have been treated with siRNA against p62 and p54, respectively, and import of GFP-nucleoplasmin was followed by time lapse confocal microscopy. As shown in Fig. 4.5. (a), in mock-transfected HeLa cells an increase of GFP-nucleoplasmin import over time (5 min, 15 min, 30 min) into the nucleus was observed. In contrast, in p54-depleted cells nuclear import of GFP-nucleoplasmin is abolished as indicated by the accumulation of the cargo at the nuclear rim (Fig. 4.5. (b)). Similarly, depletion of p62 causes inhibition of GFP-nucleoplasmin import (Fig. 4.5. (c)), indicating that both p62 and p54 are required for nuclear protein import in human cells.



### 4.3. Discussion

Based on the biochemical characterization of the NPC, the nucleoporin p62 and its complex partners p58 and p54 are considered as core components for the transport function of the NPC (Davis and Blobel 1986; Davis and Blobel 1987; Dabauvalle, Benavente et al. 1988; Carmo-Fonseca, Kern et al. 1991; Finlay, Meier et al. 1991). Biochemical depletion of the p62 complex in reconstituted nuclei resulted in a lack of nuclear import activity (Finlay, Meier et al. 1991). In addition, recent RNAi-based nucleoporin-knock-down studies revealed that the *C. elegans* homologues of mammalian p62, p54, and p58 have direct roles in orienting the mitotic spindle and the maintenance of cell polarity (Schetter, Askjaer et al. 2006). Moreover, Sabri et al. showed that p54-depleted *Drosophila* cells have nuclear import defects (Sabri, Roth et al. 2007), and microinjection of antibodies against the C-terminal domain of p62 have been shown to cause a failure in cell division (Fukuhara, Sakaguchi et al. 2006).

Our results on the deletion of the nucleoporins p62 and p54 and the overexpression of p62, p54, and p58 further support the recent findings that the p62 complex in fact is involved in regulation of mitosis and cell growth. In addition, we could show that depletion of the p62 and p54 from the NPC inhibits nuclear import of proteins in human cells.

#### 4.3.1. Cell growth of p62/p54-depleted cells

Our results employing a CFSE assay showed that p62- and p54-depleted cells grew slower than mock-transfected cells. The slower cell growth of p62- and p54-depleted cells, respectively, by this assay was further confirmed by an assay using annexinV/PI as well as a hypertonic PI assay. Both assays unveiled induction of apoptosis in p62- and p54-depleted cells as the percentage of apoptotic/dead cells increased by about 50% 3 days after transfection with siRNAs against p62 or p54 (Fig. 4.4.(a)). After 4 days of transfection, the percentages of apoptotic/dead cells in the nucleoporin-depleted cell population even doubled as compared to the mock-transfected cell population (Fig. 4.4.(b)). When the number of apoptotic cells was examined with a different method based on hypertonic PI, the number of cells in late apoptosis increased only significantly after 4 days (Fig. 4.4. (c)) This indicates that the detection of apoptotic cells in early apoptosis by annexinV contributes significantly to the population of apoptotic cells, but cells in late apoptotic phase only increased after 4 days. Taken together, the results show a clear induction of apoptosis and an increase of dead cells in p62- or p54-depleted cells. This increase in apoptosis is most likely due to the observed cell division defects (see 4.3.2.).

### 4.3.2. The p62 complex and cell cycle progression

To study the role of p62 and p54 cell division, we depleted p62 and p54, respectively, from HeLa cells by RNAi and studied all cell cycle progression, using hypotonic PI in combination with FACS analysis. As shown in Fig. 4.4. (d) No changes in the G0/G1:S/G2 ratio could be observed when comparing mock-transfected cells (value of ratio: 1.64) with cells transfected with siRNAs against p62 (value of ratio: 1.68), whereas the ratio observed for p54-siRNA transfected cells (value of ratio: 2.4) differed significantly from that of mock-transfected cells. These data suggest that only p54, but not p62 is involved in cell division. To verify this, we tested the influence of enhanced levels of the p62 complex components on cell division. These analyses revealed a significant increase in the number of cells in S/G2 phase in cells, overexpressing either p62-GFP, p54-GFP, or p58-GFP as compared to control cells, indicating a mitotic arrest.

Taken together, the results of the RNAi and the overexpression experiments show that in p54-depleted cells an increase of cells in apoptosis correlates well with an G0/G1 arrest. Interestingly, the increase of the number of apoptotic cells in a p62-depleted cell population does not correlate with a G0/G1 arrest, suggesting that the cause for the increased number of early apoptotic cells in p62-depleted cells is not due to a cell cycle defect. Overexpression of p62 complex components, on the other hand, caused an increase of cells in the S/G2 phase, suggesting that either an arrest in the S/G2 occurs or that mitosis is delayed. Further experiments, such as live cell imaging, are required to more specifically analyse the role of the p62 complex components in the distinct steps of cell cycle progression.

### 4.3.3. The p62 complex and nucleocytoplasmic transport

Earlier studies focusing on the biochemical depletion of the p62 complex (and probably also other nucleoporins) from extracts of *Xenopus* oocytes and reconstituted nuclei, described the important function of the p62 complex in nuclear protein import (Finlay, Meier et al. 1991). While Forbes and co-workers described an inhibition of nuclear import after the depletion of the p62 complex, Schetter et al. described an increase of transported cargos and lack of size exclusion in cells, in which single components of the p62 complex were depleted by RNAi (Schetter, Askjaer et al. 2006).

Our results clearly show an inhibition of nuclear protein import in p54- and p62 depleted cells. Since we could not detect the levels of depletion of p54 and p62 in our experimental setup, no exact assumption for the direct influence of the depletion of these nucleoporins on nuclear protein import could be made. An ex-

perimental setup, by which nucleoporin-depleted cells and non depleted cells can be clearly distinguished, would be a better choice to carry out the assay. But the comparison between the transport assays using either mock-transfected or nucleoporin-depleted cells (Fig. 4.5.) clearly shows the inhibitory effect in the nucleoporin-depleted cells. Experiments in living cells, in which the import of cargo can be induced in combination with siRNAs against p62 and p54, will allow to study the role of the p62 complex in nuclear protein import.

Taken together, our results showed that the depletion of single components of the p62 complex affect proliferation and cell cycle progression. Moreover, nuclear protein import was blocked in p62-and p54-depleted cells as shown in an *in vitro* import assay using digitonin-permeabilized HeLa cells. Consistently, overexpression of both p62 and p54 affects cell cycle progression in HeLa cells, but, however, at a different stage of the cell cycle as compared to p62- or p54-depleted cells.

To achieve a better understanding of the role of the p62 complex in cell cycle progression, it would be interesting to analyze the localization of the components of the p62 complex throughout mitosis in living cells. RNAi-experiments in *C. elegans* previously indicated a role of p62, p54, and p58 in spindle orientation (Schetter, Askjaer et al. 2006), but a role of these nucleoporins in spindle organization in mammalian cells remains to be elucidated.

## 4.4. Materials and Methods

### 4.4.1. Plasmids

Human p62 was amplified by PCR and was inserted into the XmaI and KpnI sites of pEGFP-C1. The PCR-amplified DNA of human p54 was inserted into the SalI and BamHI restriction sites of pEGFP-C1. The sequence encoding for human p58 was PCR amplified and was inserted into the EcoRI and BamHI sites of pEGFP-C1. The plasmid encoding for nucleoplasmin-GFP was a kind gift of K. S. Ullmann (Salt Lake City, Utah, USA).

### 4.4.2. Recombinant protein expression

His-tagged recombinant nucleoplasmin-GFP was expressed in *E. coli BL21* cells. The protein was purified via a His-trap column loaded with NiSO<sub>4</sub> (GE Healthcare, Pittsburgh, USA) and eluted with a buffer containing 200 mM imidazole. The collected fractions were analyzed by SDS-PAGE, and fractions containing pure nucleoplasmin-GFP were pooled. Next, the purified nucleoplasmin was concentrated to 1 mg/ml and finally dialyzed against PBS pH 7.4.

### 4.4.3. Cell culture and transfection of cells

HeLa cells were grown in Dulbecco's modified Eagle medium (DMEM) containing 10% fetal calf serum (FCS), 2 mM glutamine, and 100 µg/ml streptomycin/penicillin. HeLa cells were transfected by electroporation with plasmids of GFP-hp62, GFP-hp54, or GFP-hp58, using Nucleofector Kit R and Amaxa Nucleofector (Amaxa Biosciences, Cologne, Germany). For each transfection, 2 µg plasmid-DNA was used. The transfection was performed according to the instructions of the manufacturer, using the Nucleofector program for high cell survival. The transfected HeLa cells were plated and further analyzed by fluorescence microscopy, or FACS.

### 4.4.4. RNA interference

HeLa cells were transfected with small interfering RNA (siRNA) (Eurogentec; Brussels, Belgium) against human p62 (CCUACAAGCUGGCUGAGA, corresponding to the nucleotides 1296 to 1314), hu-

man p54 ( CUACAUCUGUAGCCAAAUA, corresponding to the nucleotides 1090 to 1108), or siRNA (Invitrogen, Carlsbad, CA, USA) against p58 (GCAGCAUCCACAGGAUUUA, corresponding to the nucleotides 433 to 451) at a final concentration of 100 nM, using Lifoectamine 2000 (Invitrogen, Carlsbad, CA, USA) according to the instructions of the manufacturer. HeLa cells were plated 24 h before transfection and transfected when they reached a confluency of 30-50%.

### 4.4.5. Cell cycle analysis

Mock-treated or nucleoporin-depleted HeLa cells were trypsinized, washed twice with cold PBS pH 7.2, and incubated over night in ice-cold hypotonic propidium iodide solution (0.1% sodium citrate, 0.1% Triton X, 100 µg/ml RNase, 50 µg/ml PI). Cells were analyzed the next day by flow cytometry (Facs-calibur; BD Bioscience, Franklin Lakes, USA), using CellQuest Pro (BD Bioscience, Franklin Lakes, USA).

### 4.4.6. Immunofluorescence microscopy

For immunofluorescence, cells were grown on coverslips for 3 to 4 days, fixed in PBS containing 3.7% formaldehyde, and permeabilized with PBS containing 0.2% Triton X-100. After washing, cells were incubated with primary antibodies (Monoclonal antibody (mAb) 414 diluted 1:1000 in blocking buffer (1% BSA in PBS) for 1h. Anti-mouse Alexa 488 (1:800) was used as secondary antibody (Molecular Probes, Eugene, USA). After washing, cells were stained with DRAQ-5 DNA cell permeable DNA fluorescence dye (1:250, ALEXIS, San Diego, USA) and mounted with Mowiol. Cells were analyzed by fluorescence microscopy using a confocal microscope from Leica (Leica TCS NT/SP1, Leica, Vienna, Austria). Pictures were processed using Adobe Photoshop (Adobe Systems, Mountain View, CA, USA).

### 4.4.7. Apoptosis FACS assay

Mock-treated or nucleoporin-depleted cells were trypsinized, washed with ice-cold PBS, and cells were resuspended in 100 µl cold annexin-binding buffer (10 mM HEPES pH 7.4, 140 mM NaCl, 2.5 mM CaCl<sub>2</sub>; BD Bioscience, Franklin Lakes, USA). Annexin V-FITC and PI (both BD Bioscience, Franklin Lakes, USA) were added to the resuspended cells, and the mixture was incubated for 15 minutes at room temperature. After addition of 400 µl annexin-binding buffer, the cells were analyzed by flow cytometry (Facs-calibur; BD Bioscience, Franklin Lakes, USA), using CellQuest Pro (BD Bioscience, Franklin Lakes, USA).

### 4.4.8. Carboxyfluorescein succinimidyl ester (CFSE) staining

Freshly plated HeLa cells were pelleted and washed with 37°C warm PBS. The cells were resuspended in 1 ml warm PBS, and 1 ml 2  $\mu$ M CFSE solution in PBS was added. The cell suspension was incubated for 10 minutes at 37 °C, and 2 ml DMEM were added to the suspension to block unbound CFSE. The CFSE-stained cells were washed three times with PBS and finally plated in DMEM supplemented with FCS and antibiotics. After one day of incubation at 37°C, the cells were transfected with siRNAs as described above. The CFSE-staining was measured by FACS after 2 or 3 days.

### 4.4.9. SDS-PAGE and immunoblotting

To analyze the efficacy of the knock-down by siRNA, equal amounts of protein were analyzed at days 3 and 4 by sodium dodecyl sulfate-polyacrylamide gel electrophoresis, followed by immunoblotting. Blots were blocked with 0.1% I-Block (Applied Biosystems, Lincoln, USA) in PBS containing 0.1% Tween-20. The anti-p62 antibody was used in a dilution of 1:500 and the anti-importin  $\beta$  antibody was diluted 1:1000 in blocking buffer. Alkaline phosphate-coupled goat anti-mouse IgG (Sigma, St. Louis, MO) or goat anti-rabbit IgG (Sigma, St. Louis, MO, USA) was used in a dilution of 1:10000 as secondary antibody. Antibody signals were detected by chemiluminescence, using CDP-Star (Applied Biosystems, Lincoln, USA). The anti-p62 antibody was used in a dilution of 1:500, and the anti-importin  $\beta$  antibody was diluted 1:1000.

### 4.4.10. Antibodies

An antibody against the N-terminal domain of p62 was used, which recognizes residues 24–178 of the human p62 in a wide range of vertebrates (BD Bioscience, Franklin Lakes, NJ, USA) (Carmo-Fonseca, Kern et al. 1991). The antibodies against the full length rat nucleoporins p62, p54, and p58 were generated and purified as described before (Hu, Guan et al. 1996). The monoclonal antibody mAb414 was obtained from Jackson Immunoresearch laboratories (West Grove, PA, USA). The monoclonal anti-importin  $\beta$  antibody was obtained from BD Biosciences (Franklin Lakes NJ, USA).

### 4.4.11. Fluorescence Microscopy Import Assay in HeLa cells

Mock-transfected and nucleoporin-depleted HeLa cells were grown as monolayers on Lab-Tec cham-

bered coverglasses to 80% confluence in DMEM (Sigma, St. Louis, USA) with 10% fetal calf serum and penicillin/streptomycin at 37°C. Cells were permeabilized on ice with 40 µg/ml digitonin in transport buffer (20 mM HEPES pH 7.3, 110 mM potassium acetate, 5 mM sodium acetate, 2 mM magnesium acetate, 1 mM EGTA, 2 mM DTT, 1 µg/ml aprotinin, 1 µg/ml leupeptin, 1 µg/ml pepstatin A), supplemented with 200 ng/ml DAPI (4',6-Diamidino-2-phenylindol). Next, the cells were washed two times with transport buffer. The coverglasses were mounted on the inverse confocal microscope LSM 510 (Carl Zeiss, Jena, Germany), and 180 µl transport mixture without ATP, supplemented by 20 µl nucleoplasmin-GFP (1 mg/ml), creatine phosphatase, and creatine phosphokinase, were added into the chamber. The transport assay was started by addition of 5 µl 1 mM ATP. Import into the nucleus was observed, starting from time 0 for 30 minutes at 1 min interval, using a 63x oil objective. At each point in time, a picture was taken only from one confocal plane but was 8-fold averaged to improve the signal to noise ratio. The excitation wavelength was  $\lambda = 405$  nm for DAPI staining and  $\lambda = 488$  nm for GFP.

## 4.5. Acknowledgements

The authors thank Larry Gerace for providing the antibodies against rat p54 and p58. Chantal Feder is greatly acknowledged for technical support and helpful discussions concerning the FACS assays. Many thanks also to Gulio Spagnoli for granting access to the Facscalibur of his group. Per Rigler is acknowledged for support concerning the confocal microscope LSM 510. This work was supported by research grants from the Swiss National Science Foundation (to B.F.), by the Kanton Basel Stadt, and the M.E. Müller Foundation.



## 4.6. References

- Beck, M., F. Forster, et al. (2004). „Nuclear pore complex structure and dynamics revealed by cryoelectron tomography.“ *Science* 306(5700): 1387-90.
- Buss, F. and M. Stewart (1995). „Macromolecular interactions in the nucleoporin p62 complex of rat nuclear pores: binding of nucleoporin p54 to the rod domain of p62.“ *J Cell Biol* 128(3): 251-61.
- Carmo-Fonseca, M., H. Kern, et al. (1991). „Human nucleoporin p62 and the essential yeast nuclear pore protein NSP1 show sequence homology and a similar domain organization.“ *Eur J Cell Biol* 55(1): 17-30.
- Cordes, V. C. and G. Krohne (1993). „Sequential O-glycosylation of nuclear pore complex protein gp62 in vitro.“ *Eur J Cell Biol* 60(1): 185-95.
- Cronshaw, J. M., A. N. Krutchinsky, et al. (2002). „Proteomic analysis of the mammalian nuclear pore complex.“ *J Cell Biol* 158(5): 915-27.
- Dabauvalle, M. C., R. Benavente, et al. (1988). „Monoclonal antibodies to a Mr 68,000 pore complex glycoprotein interfere with nuclear protein uptake in *Xenopus* oocytes.“ *Chromosoma* 97(3): 193-7.
- Davis, L. I. and G. Blobel (1986). „Identification and characterization of a nuclear pore complex protein.“ *Cell* 45(5): 699-709.
- Davis, L. I. and G. Blobel (1987). „Nuclear pore complex contains a family of glycoproteins that includes p62: glycosylation through a previously unidentified cellular pathway.“ *Proc Natl Acad Sci U S A* 84(21): 7552-6.
- Fahrenkrog, B. and U. Aebi (2003). „The nuclear pore complex: nucleocytoplasmic transport and beyond.“ *Nat Rev Mol Cell Biol* 4(10): 757-66.
- Finlay, D. R., E. Meier, et al. (1991). „A complex of nuclear pore proteins required for pore function.“ *J Cell Biol* 114(1): 169-83.

- Fukuhara, T., N. Sakaguchi, et al. (2006). „Functional analysis of nuclear pore complex protein Nup62/p62 using monoclonal antibodies.“ *Hybridoma (Larchmt)* 25(2): 51-9.
- Guan, T., S. Muller, et al. (1995). „Structural analysis of the p62 complex, an assembly of O-linked glycoproteins that localizes near the central gated channel of the nuclear pore complex.“ *Mol Biol Cell* 6(11): 1591-603.
- Hu, T. and L. Gerace (1998). „cDNA cloning and analysis of the expression of nucleoporin p45.“ *Gene* 221(2): 245-53.
- Hu, T., T. Guan, et al. (1996). „Molecular and functional characterization of the p62 complex, an assembly of nuclear pore complex glycoproteins.“ *J Cell Biol* 134(3): 589-601.
- Lim, R. Y., B. Fahrenkrog, et al. (2007). „Nanomechanical Basis of Selective Gating by the Nuclear Pore Complex.“ *Science* 318(5850): 640-643
- Paschal, B. M. and L. Gerace (1995). „Identification of NTF2, a cytosolic factor for nuclear import that interacts with nuclear pore complex protein p62.“ *J Cell Biol* 129(4): 925-37.
- Reichelt, R., A. Holzenburg, et al. (1990). „Correlation between structure and mass distribution of the nuclear pore complex and of distinct pore complex components.“ *J Cell Biol* 110(4): 883-94.
- Rout, M. P., J. D. Aitchison, et al. (2000). „The yeast nuclear pore complex: composition, architecture, and transport mechanism.“ *J Cell Biol* 148(4): 635-51.
- Sabri, N., P. Roth, et al. (2007). „Distinct functions of the Drosophila Nup153 and Nup214 FG domains in nuclear protein transport.“ *J Cell Biol* 178(4): 557-65.
- Schetter, A., P. Askjaer, et al. (2006). „Nucleoporins NPP-1, NPP-3, NPP-4, NPP-11 and NPP-13 are required for proper spindle orientation in *C. elegans*.“ *Dev Biol* 289(2): 360-71.
- Schwartz, T. U. (2005). „Modularity within the architecture of the nuclear pore complex.“ *Curr Opin Struct Biol* 15(2): 221-6.

Schwarz-Herion, K., B. Maco, et al. (2007). „Domain Topology of the p62 Complex Within the 3-D Architecture of the Nuclear Pore Complex.“ *J Mol Biol* 370(4): 769-806

Stoffler, D., B. Feja, et al. (2003). „Cryo-electron tomography provides novel insights into nuclear pore architecture: implications for nucleocytoplasmic transport.“ *J Mol Biol* 328(1): 119-30.

Stoffler, D., K. Schwarz-Herion, et al. (2006). „Getting across the nuclear pore complex: new insights into nucleocytoplasmic transport.“ *Can J Physiol Pharmacol* 84(3-4): 499-507.

Strawn, L. A., T. Shen, et al. (2004). „Minimal nuclear pore complexes define FG repeat domains essential for transport.“ *Nat Cell Biol* 6(3): 197-206.

Tran, E. J. and S. R. Wentz (2006). “Dynamic nuclear pore complexes: life on the edge.” *Cell* 125(6): 1041-53.



## **Conclusion and Outlook**



## 5.1. Summary and outlook

### 5.1.1. Domain topology of the p62 complex within the 3D architecture of the NPC

To determine the location of different domains of the p62 complex within the 3D structure of the NPC, we localized the different FG-repeat and coiled-coil domains of this subcomplex with immuno-EM. Previous immuno-EM showed controversial results concerning the anchoring sites and the localization of the p62 complex within the 3D structure of the NPC. Our new data revealed that the p62 complex is anchored with its coiled-coil domains to the cytoplasmic side of the NPC and that its FG-repeat domains show differences in their flexibility and their distribution within the 3D architecture of the NPC. Thus, the FG-repeat domain of the nucleoporin p62 could be found at the cytoplasmic as well as at the nuclear side of the NPC, whereas the FG-repeat domains of p54 and p58 were restricted to the cytoplasmic side. This might be due to different anchoring sites of the distinct FG-repeat domains, the varied length of the FG-repeat domains of the complex, and differences in the biophysical behavior of the FG-repeat domains.

Recently, a complementary technique to immuno-EM was established to observe FG-repeat domains *in vitro* by AFM. Lim et al. examined the biophysical behavior of the FG-repeat domain of Nup153, immobilized to a gold dot, by AFM simulating nuclear import by adding importin  $\beta$  and RanGTP (Lim, Fahrenkrog et al. 2007). The immobilized FG-repeat domains formed a polymer brush with a certain height, which collapsed after addition of importin  $\beta$ . This collapse could be reversed after addition of RanGTP, demonstrating a new biophysical principle for nucleocytoplasmic transport. The AFM-studies were attended by immuno-EM-studies with isolated nuclei of *Xenopus* oocytes, which showed that, after addition of importin  $\beta$ , the FG-repeat domains of Nup153 collapse to their anchoring sites at the nuclear basket.

It would be interesting to use the same experimental approach equally for the different FG-repeat domains of the p62 complex in order to examine if the FG-repeat domains can form polymer brushes similar to the ones formed by the FG-repeat domains of Nup153. Beyond that, it would be worth to uncover the anchoring sites of the FG-repeat domains of the p62 complex by immuno-EM after addition of importin  $\beta$  (Lim, Fahrenkrog et al. 2007). In the near future, progress in EM tomography will facilitate the localization of antibodies against certain nucleoporins without the use of gold particles, which would reveal the exact binding sites of the antibodies to structural elements of the NPC.

### 5.1.2. The role of the p62 complex in nuclear protein import

Several studies on the p62 complex have previously shown that the p62 complex is involved in the nuclear import of proteins and the export of mRNA (Dargemont, Schmidt-Zachmann et al. 1995; Paschal and Gerace 1995). These studies used experimental techniques, such as immuno-EM, reconstituted nuclei from *Xenopus* egg extracts, or biochemical binding assays (Dabauvalle, Benavente et al. 1988; Finlay, Meier et al. 1991; Hu, Guan et al. 1996; Pante and Aebi 1996).

To study the role of the p62 complex in the nuclear import of nucleoplasmin in human cells, we have used a combination of thin-sectioning EM and fluorescence microscopy. Before starting the import assays, the components of the p62 complex were masked by different specific antibodies against the nucleoporins p62, p54, and p58. The results of the ultrastructural import assay showed that the p62 complex is functioning indeed as second docking site during the import of receptor/cargo complexes into the nucleus. The localization clouds, resulting from the quantitative analysis of the nuclear import complexes when the import was blocked by antibodies against full length p62, p54, and p58, correspond to the localization data of the immuno-EM experiments with antibodies against the tagged nucleoporins p62, p54, and p58. The immunofluorescence experiments showed that nuclear import of GFP-nucleoplasmin is slowed down or blocked when antibodies against the full length nucleoporins p62, p54, or p58 are used in the import assay, whereas the usage of a domain-specific antibody against the FG-repeat domain of p62 seems to accelerate the nuclear import of the cargo.

In the future, it might be useful to repeat the same experiment with antibodies against each single domain of the p62 complex to get a broader experimental foundation. Single fluorescence molecule tracking experiments, combined with specific antibodies against certain nucleoporins will give further insight into the mechanism of nucleocytoplasmic transport through the NPC.

### 5.1.3. Depletion of p62 and p54 causes defects in cell growth and nuclear protein import

Finally, the depletion of p62 and p54 from HeLa cells was examined. Depletion of p62 and p54 by RNAi resulted in an increase of cells undergoing apoptosis and a delay of cell growth demonstrated by FACS-assays. Cell cycle analysis by PI-staining of p54-depleted cells showed an arrest of the cells in the G0/G1 state, whereas p62-depleted cells showed no defect in the cell cycle. Overexpression of mammalian p62, p54, or p58 revealed a significant increase of the S/G2 phase in all transfected cells. Taken



together, modification of the expression levels of the p62, p54 or p58 resulted in changes of the cell cycle phases and depletion of p62 and p54 in decreased viability of the cells. These results partly correspond with results from RNAi-experiments with p62-complex genes in *C. elegans* embryos (Schetter, Askjaer et al. 2006).

We also performed nuclear import assays with p62- and p54-depleted cells, using GFP-nucleoplasmin as cargo. These experiments revealed that nuclear import is blocked in p54- and p62-depleted cells. The inhibition of nuclear protein import in p54-depleted cells corresponds well with a recent RNAi study in *Drosophila melanogaster* cells (Sabri, Roth et al. 2007). Additionally, overexpression and depletion of mammalian p62 and p54 resulted in irregular morphological changes of the nucleus and overexpression of p62 in focal points in the cytoplasm of HeLa cells (our unpublished data).

Taken together, our RNAi study with components of the p62 complex showed that changes in the protein level of p62 and p54 in mammalian cells affect the cell cycle, the viability, and the nuclear protein import significantly.

To get a better understanding of the cell cycle effects, especially live cells imaging of the p62-complex-depleted cells, would be very useful. The nuclear import studies with the nucleoporin-depleted cells should be repeated with cells containing fluorescence reporter cargos, which can be induced *in vivo*.

### **5.1.4. Further biochemical experiments regarding the p62 complex and complexes, which interact with the p62 complex**

To examine the p62 complex regarding its biochemical composition and biophysical properties in detail, the rat p62 complex should be expressed and purified recombinantly. The genes of the mammalian p62 complex (p62, p54, p58, and p45) were cloned into two different Duet vectors (pET Duet1; pRSF; Invitrogen, Carlsbad, USA) and coexpressed together in *E.coli BL21* cells. The expressed p62-complex was purified by a His6-tag fused to the N-terminal domain of p58. Analysis of the purified protein fraction by SDS-Page showed that the complex was partially digested (our unpublished results). A reason for the fast digestion of the complex could be the protease sensitivity of the FG-repeats (Jochen Köser and Roderick Lim personal communications). Cloning of p62, p54, and p58 in one tricistronic vector failed. There are, up to now, no structural data regarding the recombinantly expressed p62 complex in its entirety; the x-ray structure of the coiled-coil p58/p45 dimer, however, was solved recently (Melcak, Hoelz et al. 2007).

Another focus of my work was the examination of interaction between the p62 complex and other subcomplexes of the central nuclear pore complex. Immunoprecipitation of p62 by a p62-specific antibody confirmed the well known strong interaction between p62 and Nup88/Nup214 (our unpublished data; Stochaj, Banski et al. 2006). A further interaction recently confirmed is the interaction of the p62 complex with Nup205 and Nup93 (Schetter, Askjaer et al. 2006). It was previously reported that Nup205 and Nup93 form a stable subcomplex together with Nup188, which could be isolated by immunoprecipitation (Miller, Powers et al. 2000). Biochemical and RNAi studies revealed that also Nup155 and Nup35 interact with the Nup205-Nup93 subcomplex (Grandi, Dang et al. 1997; Franz, Askjaer et al. 2005; Hawryluk-Gara, Shibuya et al. 2005; Mansfeld, Guttinger et al. 2006). To express all these interacting proteins, Nup205, Nup93, Nup35, Nup155, and Nup188 in one single bacteria cell, the corresponding human genes were cloned into three different bicistronic Duet vectors (pET Duet1; pRSF; pCDF; Invitrogen, Carlsbad, United States). The cloning was performed in collaboration with GATC Biotech AG (Konstanz, Germany). The five nucleoporins were transformed into *E.coli BL21* cells and purified by a His6-tag fused to the N-terminus of Nup205. The purified complex should be analyzed by single particle electron microscopy and mass spectroscopy. A similar experimental approach was already successfully performed with the yeast Nup84 subcomplex (Siniosoglou, Lutzmann et al. 2000; Lutzmann, Kunze et al. 2005). The project was stopped in an early phase. The X-ray structure of the yeast Nup93 homologue Nic96p was solved recently and a model how Nic96 could interact with the coiled-coil core structure of the Nsp1p-complex (the putative yeast homologue of the p62 complex) was proposed (Fig. 5.2.; Schrader, Stelter et

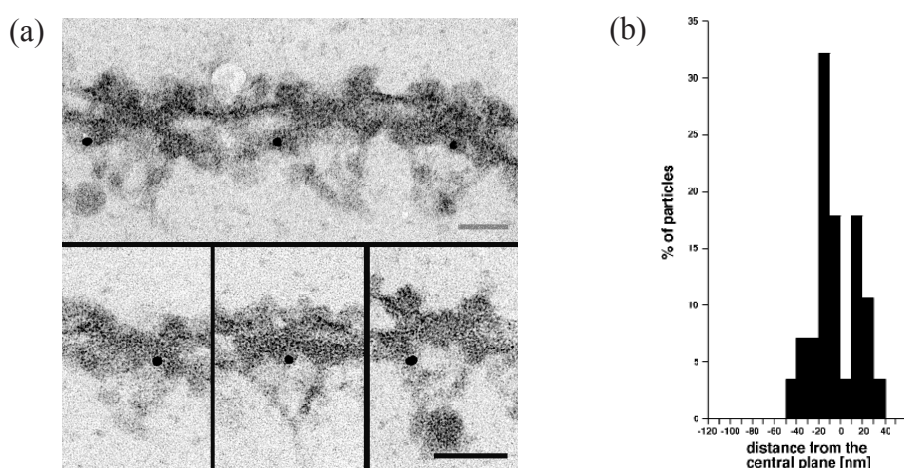


**Figure 5.1.** Domain topology of the epitope-tagged nucleoporin human Nup35 within the nuclear pore complex. (a) GFP-tagged N-terminal domain of Nup35 was detected in microinjected, isolated *Xenopus* nuclei by anti-GFP antibody directly coupled to 8-nm gold. An overview along the NE in cross-sections and a gallery of selected examples of gold-labeled NPCs in cross-sections are shown. Scale bar: 100 nm (b) Quantitative analysis of the scored gold particles is shown in the histogram. 38 gold particles were analyzed.

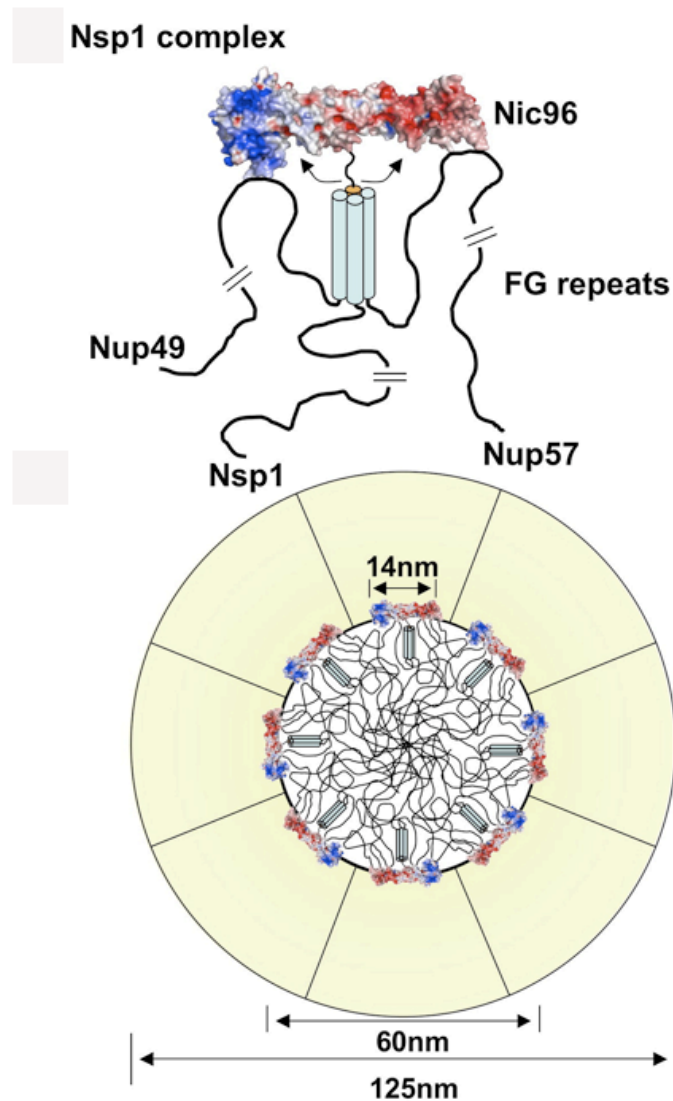


**Figure 5.2.** Model of the interaction between the Nsp1p complex and Nic96p. It is assumed that the N-terminal domain of Nic96p interacts with the coiled-coil domains of the Nsp1p complex. The arrows demonstrate the flexibility of the linker region between the N-terminal domain and the rod domain (X-ray structure) of Nic96p. The model is also transferred to the dimensions of the yeast nuclear pore (Schrader Stelter et al. 2008).

al. 2008).

In the course of this project, the localization of the nucleoporin Nup35 within the 3-D structure of the NPC was solved for the first time. We expressed N-terminal GFP-tagged human Nup35 in *Xenopus* oocytes. The location of the incorporated protein was determined by using a polyclonal antibody against the GFP-tag directly conjugated to 8-nm gold. The gallery in figure 5.1. (a) demonstrates the localization

of the epitope-tagged nucleoporin Nup35 in the 3D structure of the NPC. The corresponding histogram in figure 5.2. (b) shows that Nup35 is localized to both faces of the NPC with an average distance from the central plane of  $-22.6 \text{ nm} \pm 10.6 \text{ nm}$  for the nuclear face and  $13.1 \text{ nm} \pm 8.6 \text{ nm}$  for the cytoplasmic face.

### 5.1.5. Outlook

In the following years, the discovery of the NPC structure and the understanding of the biophysical basis of the nucleocytoplasmic transport is supposed to make further progress. The most frequently used techniques will probably be: (i) AFM to study unstructured components of the NPC like the FG-repeats, which are essential for the function of the NPC, (ii) tomography to refine the structure of the NPC and to gain “snapshots” of nucleocytoplasmic transport, (iii) single particle analysis and X-ray crystallography to analyze the building blocks of the NPC, (iiii) single molecule fluorescence microscopy to analyze single transport cargos in transit through the NPC, (v) systems analysis and simulation of the nucleocytoplasmic transport based on quantitative biochemical data, e.g. the concentration of the different transport receptors in the near field of the NPC, and (vi) advanced biochemical techniques like *in vivo* x-linking to determine the interactions inside the NPC (Suchanek, Radzikowska et al. 2005).

## 5.2. References

- Beck, M., F. Forster, et al. (2004). „Nuclear pore complex structure and dynamics revealed by cryoelectron tomography.“ *Science* 306(5700): 1387-90.
- Beck, M., V. Lucic, et al. (2007). „Snapshots of nuclear pore complexes in action captured by cryo-electron tomography.“ *Nature* 449(7162): 611-5.
- Dabauvalle, M. C., R. Benavente, et al. (1988). „Monoclonal antibodies to a Mr 68,000 pore complex glycoprotein interfere with nuclear protein uptake in *Xenopus* oocytes.“ *Chromosoma* 97(3): 193-7.
- Dargemont, C., M. S. Schmidt-Zachmann, et al. (1995). “Direct interaction of nucleoporin p62 with mRNA during its export from the nucleus.” *J Cell Sci* 108: 257-263.
- Finlay, D. R., E. Meier, et al. (1991). „A complex of nuclear pore proteins required for pore function.“ *J Cell Biol* 114(1): 169-83.
- Franz, C., P. Askjaer, et al. (2005). „Nup155 regulates nuclear envelope and nuclear pore complex formation in nematodes and vertebrates.“ *Embo J* 24(20): 3519-31.
- Grandi, P., T. Dang, et al. (1997). „Nup93, a vertebrate homologue of yeast Nic96p, forms a complex with a novel 205-kDa protein and is required for correct nuclear pore assembly.“ *Mol Biol Cell* 8(10): 2017-38.
- Hawryluk-Gara, L. A., E. K. Shibuya, et al. (2005). „Vertebrate Nup53 interacts with the nuclear lamina and is required for the assembly of a Nup93-containing complex.“ *Mol Biol Cell* 16(5): 2382-94.
- Hu, T., T. Guan, et al. (1996). „Molecular and functional characterization of the p62 complex, an assembly of nuclear pore complex glycoproteins.“ *J Cell Biol* 134(3): 589-601.
- Kubitscheck, U., D. Grunwald, et al. (2005). „Nuclear transport of single molecules: dwell times at the nuclear pore complex.“ *J Cell Biol* 168(2): 233-43.

- Lim, R. Y., B. Fahrenkrog, et al. (2007). „Nanomechanical Basis of Selective Gating by the Nuclear Pore Complex.“ *Science* 318(5850): 640-643.
- Lim, R. Y., J. Koser, et al. (2007). „Nanomechanical interactions of phenylalanine-glycine nucleoporins studied by single molecule force-volume spectroscopy.“ *J Struct Biol* 159(2): 277-289.
- Lutzmann, M., R. Kunze, et al. (2005). „Reconstitution of Nup157 and Nup145N into the Nup84 complex.“ *J Biol Chem* 280(18): 18442-51.
- Mansfeld, J., S. Guttinger, et al. (2006). „The conserved transmembrane nucleoporin NDC1 is required for nuclear pore complex assembly in vertebrate cells.“ *Mol Cell* 22(1): 93-103.
- Melcak, I., A. Hoelz, et al. (2007). “Structure of Nup58/45 suggests flexible nuclear pore diameter by intermolecular sliding.” *Science* 315(5819): 1729-32.
- Miller, B. R., M. Powers, et al. (2000). „Identification of a new vertebrate nucleoporin, Nup188, with the use of a novel organelle trap assay.“ *Mol Biol Cell* 11(10): 3381-96.
- Pante, N. and U. Aebi (1996). „Sequential binding of import ligands to distinct nucleopore regions during their nuclear import.“ *Science* 273(5282): 1729-32.
- Paschal, B. M. and L. Gerace (1995). “Identification of NTF2, a cytosolic factor for nuclear import that interacts with nuclear pore complex protein p62.” *J Cell Biol* 129(4): 925-37.
- Sabri, N., P. Roth, et al. (2007). „Distinct functions of the *Drosophila* Nup153 and Nup214 FG domains in nuclear protein transport.“ *J Cell Biol* 178(4): 557-65.
- Schetter, A., P. Askjaer, et al. (2006). „Nucleoporins NPP-1, NPP-3, NPP-4, NPP-11 and NPP-13 are required for proper spindle orientation in *C. elegans*.“ *Dev Biol* 289(2): 360-71.
- Siniossoglou, S., M. Lutzmann, et al. (2000). „Structure and assembly of the Nup84p complex.“ *J Cell Biol* 149(1): 41-54.

Stochaj, U., P. Banski, et al. (2006). „The N-terminal domain of the mammalian nucleoporin p62 interacts with other nucleoporins of the FXFG family during interphase.“  
Exp Cell Res 312(13): 2490-9.

Stoffler, D., B. Feja, et al. (2003). „Cryo-electron tomography provides novel insights into nuclear pore architecture: implications for nucleocytoplasmic transport.“ J Mol Biol 328(1): 119-30.

Schrader, N., P. Stelter, et al. (2008). “Structural basis of the nic96 subcomplex organization in the nuclear pore channel.” Mol Cell 29(1): 46-55.

Yang, W., J. Gelles, et al. (2004). „Imaging of single-molecule translocation through nuclear pore complexes.“ Proc Natl Acad Sci U S A 101(35): 12887-92.





Name: Kyrill Schwarz-Herion  
Date of birth: August 26th, 1975  
Place of birth: Ettlingen, Germany  
Nationality: German

**Education:**

Aug2003-Feb2008 PhD in Biochemistry, Biozentrum, University of Basel  
2003-2007 University of Hagen, Germany, Master of Science Business Administration  
("Diplom-Wirtschaftschemiker")  
1994-2002 University of Freiburg i. Br., Germany, Master in Chemistry  
(German "Diplom");  
additional studies in economic sciences and modern languages  
1985-1994 Abitur, Eichendorff-Gymnasium Ettlingen (Main courses: Latin, History)

**Research and Professional Experience:**

May 2007- Manager (Marketing and Product Management), greenovation Biotech  
GmbH Freiburg/Heilbronn, Germany  
Responsibilities: Marketing and Sales; patent law; scientific  
communication (conventions; articles); corporate communication;  
quality management  
  
Aug.2003-May 2007 PhD student, M. E. Müller Institute for Structural Biology  
Biozentrum, University of Basel, Switzerland  
Advisor: Prof. Dr. U. Aebi  
Supervisor: PD Dr. B. Fahrenkrog  
Research field: The molecular architecture of the nuclear pore complex;  
characterization of the p62 complex by molecular biology, microscopy,  
and cell biology techniques

- Jan. 2003-Jul. 2003      Biochemist, Institute for Biochemistry and Molecular Biology,  
University Hospital, University of Freiburg i. Br., Germany  
Advisor: Prof. Dr. Roderich Brandsch  
Research fields: Protein purification, Enzymology; Microbiology
- 2002                      Master Student, Institute for Organic Chemistry and Biochemistry,  
Division of Biochemistry, University of Freiburg i. Br., Germany  
Topic of the Master thesis: "Cloning, Purification, Crystallization  
and Structural Characterization by X-Ray of the O-Acetyl-Serine-  
Sulfhydrylase CysM of E. coli"  
Advisor: Prof. Dr. G. E. Schulz
- 1999- 2001              Head of the student association Stusie e.V. and chairman of the residence  
hall "Studentensiedlung am Seepark", Freiburg i. Br., Germany  
(two years full time)

### **Additional practical experience and courses:**

- Structural Biology:      EMBO Course Cryo-EM EMBL, Heidelberg 2004  
Introduction to Protein Structure Bioinformatics, Basel 2004  
Advanced imaging & microscopy course, FMI, Basel 2006
- Cell Biology:              Flow Cytometry, Bern 2005  
Signal Transduction, Bern 2005
- Molecular Biology:      DNA Microarrays, Lausanne 2005  
Phage Display Technology, ETH Zurich 2006
- Summer School:          Participation Onassis Lecture Series "Genomics, Bioinformatics and  
beyonds", Heraklion, Crete 2004
- Pharma business:        SKMB patent law workshop "embracing life", Gwatt 2004  
Good Manufacturing Practice workshop, Pharmacenter Basel 2006  
The Making of a Drug, Biozentrum Basel SS 2005

- Prices/Grants: Full scholarship of the Onassis foundation to visit the Onassis Summer School, Crete 2004  
Travel scholarship SSOM, 2006  
Travel grant of the Swiss Society for Cell Biology, Molecular Biology and Genetics 2006
- Presentations: Cryo-EM course 2004, EMBL, Heidelberg (Chair: Dr. Bettina Böttcher);  
Institute for Organic Chemistry, Basel 2005 (Host: Prof. Dr. Helma Wennemers)
- Posters: Biozentrum Symposium, St. Chrischona 2005  
Structural Biology and Biophysics Meeting, Basel 2006  
ASCB Meeting, San Diego, Dec 9-13 2006
- Conferences: ASCB Meeting San Diego, USA (2006)  
Plant-based Pharmaceuticals and Vaccines, Verona, Italy (2007)  
Protein Expression Europe, Prague, Czech (2007)
- Teaching activities: Biochemistry course for medical students, University of Freiburg (2003);  
Fluorescence Microscopy course Biozentrum Basel (2003, 2004, 2005, 2006)

**Extracurriculum Activities:**

Social activities:

- Member Supervisory Board, Studentenwerk Freiburg 2000-2002  
Member of the Management Board "Studentensiedlung am Seepark" 1997-1999  
Engagement as a soloist for violin concertos of Beethoven, Bruch and Bach (1997, 1998, 2000/2001)  
Member of the orchestra MSG "Alt-Straßburg" 1997-2002  
Member of management board Civil Society FR-Betzenhausen 2003-2005

Languages: German (mother tongue); English; French; Spanish; Chinese (basics)

### **Publications:**

Stoffler, D., Schwarz-Herion, K., Aebi, U. and Fahrenkrog, B.: “Getting across the nuclear pore complex: new insights into nucleocytoplasmic transport”. *Canadian Journal of pharmacology and physiology* (2006);

Lim, R. Y., Huang, N. P., Koeser, J., Deng, J., Lau, K. H., Schwarz-Herion, K., Fahrenkrog, B and Aebi, U.: „Flexible FG-Nucleoporins as Entropic Barriers to Nucleocytoplasmic Transport”. *PNAS* (2006);

Lill, Y., Lill, M.A., Fahrenkrog, B., Schwarz-Herion, K., Paulillo, S., Aebi, U., and Hecht, B. “Single Hepatitis-B virus core capsid binding to individual nuclear pore complexes in HeLa cells”. *Biophysical Journal* (2006);

Schwarz-Herion, K., Guan, T., Sauder, U., Gerace, L. and, Fahrenkrog, B. Novel Insights into the Location of the p62 Complex and Its Role in Nuclear Import. *Abstract Molecular Biology of the Cell* (2006);

Lim, R. Y., J. Koser, Huang, N. P., Schwarz-Herion, K, and Aebi U. „Nanomechanical interactions of phenylalanine-glycine nucleoporins studied by single molecule force-volume spectroscopy.“ *Journal of Structural Biology* (2007);

Schwarz-Herion, K., Maco, B., Sauder, S., and Fahrenkrog B. „Domain Topology of the p62 Complex Within the 3-D Architecture of the Nuclear Pore Complex.“ *Journal of Molecular Biology* (2007)

Lim, R. Y., B. Fahrenkrog, Koeser, J., Schwarz-Herion, K., Deng, J., and Aebi U.: „Nanomechanical Basis of Selective Gating by the Nuclear Pore Complex.“ *Science* (2007);

Schwarz-Herion, K., Guan, T., Sauder, U., Gerace, L. and, Fahrenkrog, B.  
“Impact of p62 complex antibodies on nuclear import”. In preparation

### Acknowledgements

First of all, I would like to thank Birthe Fahrenkrog for the opportunity to take my PhD at the Biozentrum, her great support and supervision during my thesis. Thank you, Birthe, for your understanding for my interest in further education and for supporting my scientific work!

I am deeply indebted to Ueli Aebi for the great opportunity to work at the M.E. Müller Institute, his generous support of my thesis and his feedback in critical situations.

I am also very grateful to all my colleagues in the NPC lab: Sara, Rod, David, Yvonne, Bohus, Jochen and Esther. Thanks to Sara for the funny time with her in the lab and for introducing me into the elementary cell biology techniques. Many thanks to Rod for the great time I spent with him in the lab. I do not only have a fruitful collaboration with him, but I remember especially very well the relaxing evenings with him at the Cargo Bar. Thank you, Rod, for your great advices and your support as a friend during good and bad times in the lab!

I want to thank David and Yvonne for being great colleagues, for their warm companionship, and their support in the lab. Many thanks Bohus for teaching and supporting me and being a nice colleague for many years. I would like to thank also Jochen for helpful scientific discussions and supporting my work for placing me generously a bed when it was necessary. Thanks also to Esther for being my colleague and teaching me immunoprecipitation.

I started my PhD in the Aebi lab together with Uli Schröder. Thank you, Uli, for being my colleague, for helpful discussions, and for your support!

I am also very grateful to my long-term lunch partners Maria, Daniel, Martin, Andreas, Marco, and Riccardo. We did not only enjoy the meals together but also several other activities! Especially I want thank Daniel for his support.

Also many thanks to Liselotte and Rosi, who made my stay at the Biozentrum very comfortable. I would like to thank also Cora for helpful scientific discussions and advices.

The „new“ generation in the NPC lab, Ilona and Therese, I wish all the best for their master theses.

Without the technical support of Ursula Sauder, Vesna Olivieri and MaDü I couldn't successfully finish my thesis. Many thanks to them for their help and (not only technical) support. Thank you very much, Maxime Quebatte, for your patience during teaching me qPCR!

## APPENDIX 2: ACKNOWLEDGEMENTS

---

I want to thank Magrit and Rolli for their great IT support in every aspect.

Many thanks to my colleagues outside the Biozentrum, who helped me: Chantal Feder for teaching me FACS and Per Rigler for teaching me live imaging with the confocal Zeiss microscope. I want to thank Gulio Spagnoli for helpful discussions and the access to the FACS of his group. Thanks also to Daniel Vonwiel for his help and being my colleague. I'm very grateful to Christoph, who helped me a lot with InDesign.

In addition, I want to thank everybody, especially the current and former members of the Aebi lab and friends at the Biozentrum, whom I forgot to mention above.